universität wien

MASTERARBEIT / MASTER'S THESIS

Titel der Masterarbeit / Title of the Master's Thesis

„Synthetic studies toward molecules for protein NMR“

verfasst von / submitted by

Gabriel Kiesenhofer BSc

angestrebter akademischer Grad / in partial fulfilment of the requirements for the degree of

Master of Science (MSc)

Wien, 2020 / Vienna 2020

Studienkennzahl lt. Studienblatt / degree programme code as it appears on the student record sheet:	UA 066 862
Studienrichtung lt. Studienblatt / degree programme as it appears on the student record sheet:	Masterstudium Chemie
Betreut von / Supervisor:	Mag. Dr. Roman Lichtenecker, Privatdoz.

Synthetic studies toward molecules for protein NMR

Gabriel Kiesenhofer

2018/11/07 - 2019/06/28

Lass die Moleküle rasen,
was sie auch zusammenknobeln!
Lass das Tüfteln, lass das Hobeln,
heilig halte die Ekstasen!
C. Morgenstern

Wann immer wir nämlich glauben,
die Lösung eines Problems gefunden zu haben,
sollten wir unsere Lösung nicht verteidigen,
sondern mit allen Mitteln versuchen, sie selbst umzustoßen.
K. Popper

Contents

List of abbreviations

ACN: acetonitrile
APSY: automated projection spectroscopy
aq.: aqueous
Cbz-chloride: benzyl chloroformate
CSA: camphorsulfonic acid, chemical shift anisotropy
dba: dibenzylideneacetone
DBU: 1,8-diazabicyclo[5.4.0]undec-7-ene
DCM: dichloromethane
DD: dipole-dipole relaxation
DFI: 2,2-difluoro-1,3-dimethylimidazolidine
DFT: density fuctional theory
DIBAL: diisobutylaluminium hydride
DMF: dimethyl formamide
dppa: bis(diphenylphosphino)amine
EDC: 1-ethyl-3-(3-dimethylaminopropyl)carbodiimide
F-TEDA: 1-chloromethyl-4-fluoro-1,4-diazoniabicyclo[2.2.2]octane bis(tetrafluoroborate)
HMBC: heteronuclear multiple bond correlation
HOBt: hydroxybenzotriazole
HSQC: heteronuclear single quantum coherence
KO*t*Bu: potassium *tert*-butoxide
LHMDS: lithium bis(trimethylsilyl)amide
NFSI: *N*-fluorobenzenesulfonimide
NFTPT: *N*-fluoro-2,4,6-trimethylpyridinium triflate
NOE: nuclear Overhauser effect
NOESY: nuclear Overhauser enhancement spectroscopy
PCS: pseudo-contact shift
PDB: protein database
PE: petrol ether
PRE: paramagnetic relaxation enhancement
*p*TsOH: *para*-toluenesulfonic acid
RDC: residual dipolar coupling
RMSD: root mean square deviation
RT: room temperature
SAIL: stereo-array isotope labeling
sat.: saturated
TBAI: tetrabutylammonium iodide
THF: tetrahydrofuran
TLC: thin layer chromatography
TMSCl: trimethylsilyl chloride
TROSY: transverse relaxation optimized spectroscopy
UHP: urea hydrogen peroxide

Part I

Protein NMR

1 Motivation

Proteins and polypetides encompass a vast variety of structures in biosystems making them a central column of life itself. Their functions include structural elements such as collagen in skin and bones, keratin as a major component of hair, fingernails and also beaks, as well as central roles in the movement of the body, antibodies as an element of the immune system, defense strategies of animals and plants that use toxic peptides, and also signal molecules such as hormones. Highly important is also their part in cellular chemistry. Ion channels as well as proton pumps for ATP synthesis are composed of membrane proteins. Furthermore, they comprise the "machines" of the body. The machines that build up polypetides as DNA strands and other proteins, machines that perform the processing of virtually any molecule taken up into the body, be it food or toxic substances. There is no doubt that without proteins not a single organism could exist. In order to fulfill their duties proteins need to adopt a certain structure which is caused by the sequence of amino acids. An expressed sequence undergoes folding to minimize its energy by avoiding interactions between hydrophobic and hydrophilic areas and at the same time preferring interactions in which both moieties are either polar or non-polar. In the course of enzymatic reactions the enzyme may be required to change its conformation which in turn leads to the necessity of structural flexibility within the folding. Thus, a finely tuned balance between structural integrity and flexibility at the same time is highly important. When this balance fails, the consequences are severe. Misfolded proteins, so called prions, are responsible for diseases such as Creutzfeld-Jacob or BSE (bovine spongiforme encephalitis) that cause grave damages to the brain. Apart from this, malfunctions or absence of proteins can have serious effects on the biological system. In order to find cures for ailments caused by protein malfunctions or where proteins can be influenced to achieve health improvements, it is crucial to have knowledge about their structure and mode of working. Based on this motivation methods to obtain structural and dynamic information on proteins were and still are much sought after.

2 Structure determination

2.1 General information and X-ray diffraction

The concept of secondary protein structure was introduced by Linderstrøm-Lang in 1952[1] describing the folding of the amino acid sequence. Types of this folding are e.g. α-helix, β-sheet or loops that are caused by different patterns of hydrogen bonds within the protein (Figure 1).

A comprehensive characterization of a protein requires first the determination of its primary structure, i.e. the sequence of amino acids, and second the folding of this sequence. There are methods such as circular dichroism that give access to the ratios of helices, sheets and other secondary structures, yet this is only global information giving no hint to the sequence and structure of the protein. After X-ray diffraction became a reliable tool in crystallography to determine crystal structures on an atomar resolution it was also applied on protein crystals. The first protein structure ever to have been determined in 1958 using X-ray crystallography belonged to the oxygen storing protein myoglobin.[3] While this was still a rather cumbersome endeavor yielding a primitive result compared to modern standards, the technique was evolved dramatically over the next years, making it the nowadays most used tool for structural determination of proteins. Up to this day 157,145 structures have been determined,[4] about 140,000 of them by X-ray diffraction. Information on determined structures are deposited in the Protein Data Bank (PDB). Despite this obvious power crystallography is far from being an allround approach as it comes with certain limits. An inherent precondition for it to work is the possibility to form protein crystals which is especially difficult for proteins with large unfolded regions that are relatively free to move. In turn crystallization requires sufficient solubility in the first place. If crystallization from water fails other solvents can be tried, although this bears the risk of changing the structure of the protein as a reaction to the altered environment. In general there is a chance that the protein loses its natural conformation during

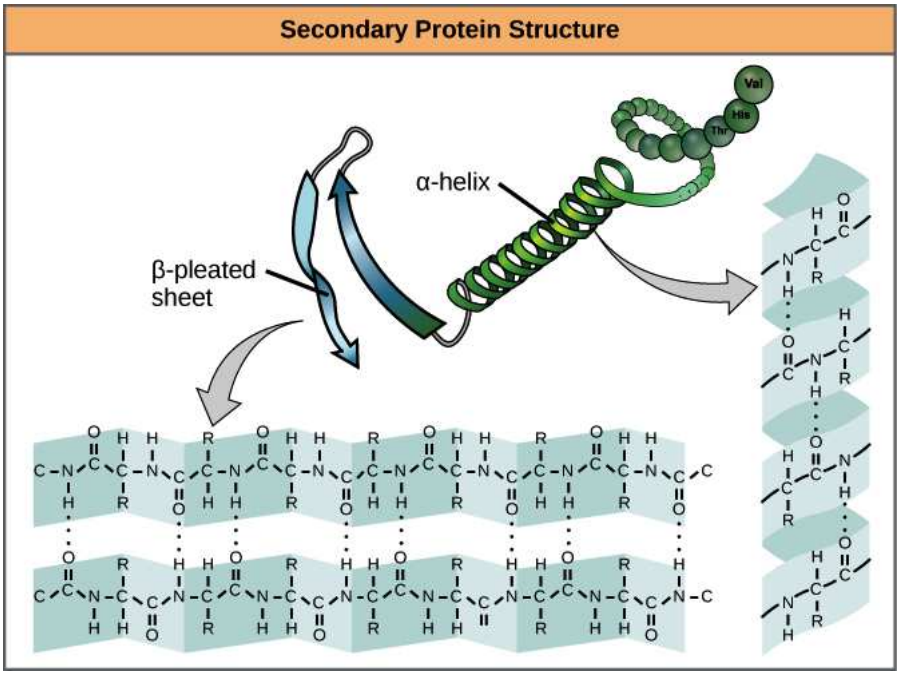

Figure 1: The secondary structure of proteins[2]

the formation of the crystal, leading to diffraction results that do not correspond to the native state of the molecule in its biological context. Moreover, by definition, crystallography yields static data, meaning that any observation of protein movement is precluded. This poses a major obstacle when it comes to the investigation of working principles of enzymes. For all those reasons, it is desirable to have a complementary access to structural data.

2.2 Structure determination by NMR

First steps

NMR as a technique that uses nuclear spins to draw conclusions on atoms and their close environment was first described in 1946. It was only 11 years later that the first proton spectrum of a protein (ribonuclease) was recorded and published.[5] Further improvements enabled NMR to at least distinguish between folded and unfolded proteins.[6] Structure determination, however, was still far away. This was only possible after the hardware had undergone sufficient evolution which resulted in the first structure of a protein being investigated by ^{1}H-NMR.[7]

Working principle

The keyword for the determination of structures is “restraints”, meaning that a close proximity between two structural entities must exist to give rise to a NOE (nuclear Overhauser effect) signal. In turn, a signal restrains the protein to certain foldings. The more restraints can be determined the higher the precision of the determined folding becomes. After successful assignment of 1D proton signals to a certain amino acid in the sequence NOESY spectra are recorded: crosspeaks indicate interactions between the residues, the signal intensity allows conclusions on the distance in a range from 2 Å (about the radius of two hydrogens, the minimal possible distance) to 5 Å.[8] From this restraining information a first structure can be derived (Figure 2).
As already mentioned the starting point is to perform an assignment of signals to amino acids. While the first studies did this by e.g. pH titration, chemical modification and inhibitor binding,[9] progress has been made later to use 2D spectra (COSY, NOESY) to achieve a systematic assignment method without the need for actual

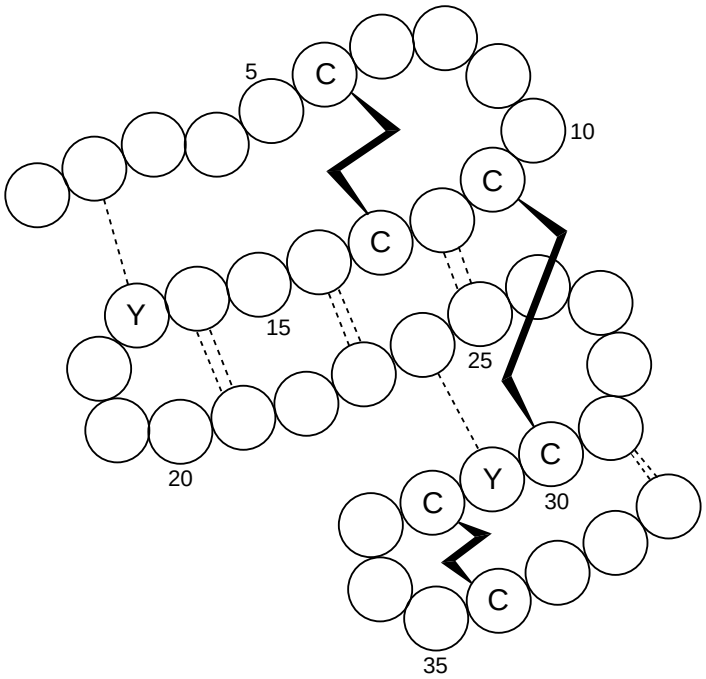

Figure 2: NOE interactions in a peptide sequence

chemical reactions.[10] The assignment is mostly done manually and therefore prone to errors, leading to false structures that do not correspond to the real conformation. To prevent wrong results caused by human errors, software assisted assignment is being developed. As of today several programs are available that use different approaches for assignment: sequence and 3D-NMR (GARANT), ^{13}C shifts and dihedral angles (SEASCAPE) or APSY and NOESY data (UNIO).[11] The structure derived from NOESY data is not yet a high-precision result. Several structures are proposed that are summed up in an ensemble of structures that comply with the measured restraints within a given tolerance. The deviation of the measured structures within this ensemble is then described by an RMSD value. The lower this value, the higher the agreement. In terms of X-ray crystallography, this corresponds to a high resolution.

Apart from NOE, further restraints can be introduced by RDC (residual dipolar coupling). This method is based on the fact that large dipolar interactions between nuclei exist within the protein[6] which lead to a coupling. However, this is strongly dependent on the orientation in the magnetic field. Since the molecules are free to move in solution-NMR, an orientation that leads to an observable signal has too short a lifetime to be actually measured. Nevertheless, it is possible to make use of RDCs by collecting NMR data in an aligning medium that immobilizes molecules in a favorable position long enough for the coupling to be measured. This medium is required to display a highly favored orientation in a magnetic field and must be able to hold the molecule of interest in place. Examples of orienting media are e.g. lipid bicelles,[12] DNA nanotubes[13] and also viruses.[14] While NOE is dependent on distance (to the sixth power) and therefore the provided restraints are in terms of distance also, RDC supports complementary information on the orientation of residues. Not only does this yield data on the secondary structure but also on the orientation of folding motifs in respect to each other, that being the tertiary structure. As the relative orientation within an enzyme may change in the course of an enzymatic reaction, RDC even permits insight in the movements and conformational changes.

A variety of additional approaches exist to further increase the number of restraints and thus make the structure more precise, such as PRE (paramagnetic relaxation enhancement)[15] or PCS (pseudo-contact shift)[16] that provide structural information over a distance of up to 40 Å.

Finally, after a family of structures is generated, it is further refined by performing energy minimization that takes into account the already determined restraints, leading eventually to the final structure which is ready to

be published to PDB.

2.3 NMR techniques and labeling

Structural determination of native proteins using NMR is feasible only up to a certain size of proteins above which problems occur. Increasing protein size also means an increasing number of protons. Since the shift range for hydrogen is rather small, spectra of large molecules tend to become very crowded to the point where overlaps make the assignment of signals to amino acids difficult or even impossible. With increasing size of the protein, another challenge to cope with is line broadening due to a larger system that can accept transverse relaxation energy in the course of spin-spin-relaxation, thus shortening T_2 time which in turn leads to broad lines that are even more likely to overlap. A first simplification step consists in introducing deuterium to the protein to remove proton resonances from the spectrum and to prevent fast relaxation of other excited nuclei, an effect that is caused by the much lower gyromagnetic ratio of ^{2}H, thereby extending the accessible size from 12 kDa to 30 kDa.[6,8] Furthermore, ^{13}C and ^{15}N labeling is a precondition to perform multidimensional resonance spectroscopy which makes signal assignment to residues far easier. This has led to the development of the SAIL labeling strategy to achieve maximum simplification without losing too much information on restraints.
Instrument-based improvements encompass NMR experiments that have been evolved to permit even further line sharpening (TROSY) and investigation of specific connectivities (multidimensional NMR).
By exploiting these strategies, it is possible to greatly extend the size of proteins that are amenable to structural elucidation by NMR (Figure 3).

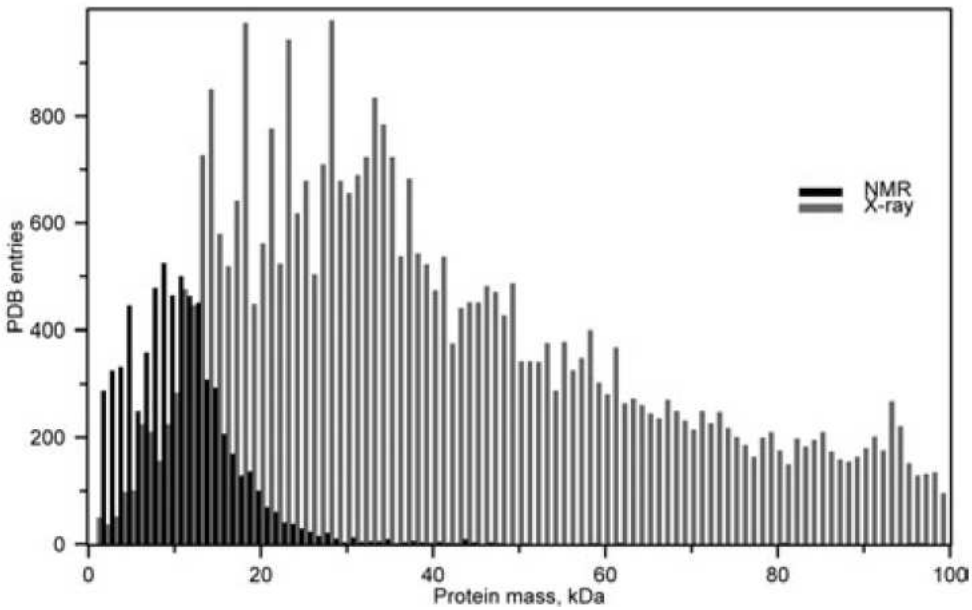

Figure 3: Contribution of NMR to structure determination[17]

Isotopes for labeling

Deuterium Among the multitude of protons in a protein only a fraction has to be used to gain the desired information. As a consequence, all other protons may be replaced by deuterons, thus reducing the NMR spectra to the relevant information. Before proceeding to synthesize a deuterated amino acid, which likely requires costly deuterated building blocks, it has therefore to be decided which protons are deemed necessary for a given purpose. When investigating an active center, it may not be important to retain protons far away

from this site as those residues are not likely to play a role in the process. On the contrary, protonated side chains in an otherwise deuterated background give signals with good intensity while other unwanted signals are suppressed.
In practice, it has turned out that a deuteration level of 50-70% in arbitrary sites leads to an eight times longer T_2 compared to fully protonated proteins.[18] This arbitrary deuteration pattern can be accomplished by expressing the desired protein in *E. coli* in a D_2O environment.[19] Deuteration of amides or, generally speaking, acid protons, can be achieved by solving the protein in D_2O: Because of their acidity and the manifold excess of D^+, protons will be replaced by deuterons in the protein.
When devising ^{13}C-labeled molecules for heteronuclear NMR studies, it may also be necessary to implement deuteration patterns in order to prolong relaxation of the labeled carbons.

^{13}Carbon ^{12}C accounts for about 99% of naturally occurring carbon, only 1% is the other stable isotope ^{13}C. ^{12}C has a nuclear spin of 0, resulting in inactivity in NMR spectroscopy. As only 1% of all carbon atoms is useable for recording spectra, a great number of measuring cycles has to be run to yield acceptable signal to noise ratios. A first advantage of labeling with ^{13}C is the reduction of this number since more active isotopes per run are in a certain position. As will be explained in more detail below, ^{13}C labeling is crucial to perform multidimensional NMR studies for an improved assignment of signal to the corresponding residues.
On the other hand, it can be desirable to leave certain positions unlabeled. For instance couplings between adjacent ^{13}C atoms result in complicated spectra which further exacerbate the problem of assignment. A problem that can be solved by introducing alternating ^{13}C$-^{12}$C$-^{13}$C sequences that reduce ^{1}J to much weaker ^{2}J couplings.[20] Furthermore, T_2 is prolonged in ^{12}C$-^{13}$C pairs compared to ^{13}C$-^{13}$C because ^{12}C cannot accept any magnetization, resulting in sharper lines.

^{15}Nitrogen The by far most abundant isotope of nitrogen is ^{14}N (99.6%), followed by ^{15}N (0.37%).[21] Both nuclei are NMR active, the major drawback of ^{14}N, though, is its nuclear quadrupole moment which makes lines broad due to fast relaxation. As the challenge is to minimize line broadening, this isotope poses a disadvantage. ^{15}N on the other hand has a nuclear dipole moment, accounting for sharp lines. The low gyromagnetic ratio γ of ^{15}N ($-27.126 \cdot 10^6$ rad$\cdot$T$^{-1}\cdot$s^{-1})[21] results in a sensitivity penalty. Therefore, a high level of labeling is desirable when nitrogen is involved in recording NMR spectra. The method of choice is to express proteins in living cells that are supplied by ^{15}N sources only.
Like ^{13}C, Nitrogen is of special interest in the assignment of residues in multidimensional spectroscopy.

TROSY

Transverse relaxation optimized spectroscopy provides a valuable tool to sharpen NMR peaks. In a system of scalar coupled spins two main T_2 relaxation mechanisms are dominant, one being dipole-dipole relaxation (DD), the other being the chemical shift anisotropy mechanism (CSA).[22] Both mechanisms can interfere additively, leading to fast transverse relaxation and broad lines, or subtractively which leads to slow relaxation and sharp lines. Scalar coupled nuclei give rise to two signals in NMR that stem from their different nuclear spins. Differing line widths, corresponding to different T_2, show the influence of either additive or subtractive relaxation interference. In NMR spectroscopy of smaller molecules the separate lines are decoupled to sum them up in one line. The benefit of increased signal intensity, however, comes at the cost of an average line width. While this effect only slightly diminishes the spectral quality in spectra of small molecules, the relaxation rates may differ a lot in large molecules such as proteins due to many relaxation pathways. The TROSY approach relinquishes decoupling and aims at selecting the one signal out of a multiplet representing the slowest relaxation. The loss of signal intensity is less of a disadvantage compared to the advantage of a gain in resolution. Prolonged relaxation time further increases signal intensities when using techniques that require longer pulse sequences or evolution times, such as multidimensional spectroscopy, since less of the magnetization is lost while correlations

evolve throughout the spin system. TROSY is not an experiment on its own to yield information unavailable via other experiments, but rather a variation that improves the spectral quality.
For the reason described in ^{15}N labeling, this positive effect would be in vain when using ^{14}N, as this isotope gives naturally broad lines. Thus, TROSY involving nitrogen only makes sense in ^{15}N labeled proteins.
TROSY is not restricted to ^{1}H$-^{15}$N systems but also results in an improvement of spectral quality of ^{1}H$-^{13}$C moieties. In general, since this approach is based on a dipole-dipole coupling relaxation mechanism, it is applicable in every NMR study involving bonds between nuclei that display a nuclear dipole moment different from 0. Therefore, as a nuclear dipole moment is the most basic precondition for NMR measurements, TROSY is apt for any NMR experiment.

SAIL

SAIL[17] (stero-array isotopic labeling) describes an approach to maximally reduce the number of protons in amino acids without losing information in NOESY experiments. The general idea is to eliminate redundancies that arise from e.g. two protons being present in methylene groups that yield virtually the same information but give slightly different shifts as a consequence of a different magnetic environment, accounting for unnecessary crowding of spectra. At the same time, while retaining the desired information, the relaxation pathways are reduced to give sharper peaks. The SAIL strategy is based on five basic considerations (Figure 4):

1. $-CH_3$ moieties are replaced by $-CD_2H$ moieties
2. $-CH_2-$ moieties are replaced by $-CDH-$ moieties. For this labeling to be effective it is necessary to take into account that in amino acids methylene groups are always prochiral centers, leaving the two protons chemically inequivalent. It is therefore necessary to perform a stereoselective exchange of protons and deuterons.
3. In amino acids with prochiral methyl groups (Val, Leu) one is labeled according to the first rule, the other one is replaced by $-{}^{12}CD_3$. For the same reason as in methylene groups it is necessary to always label the same prochiral methyl group.
4. $-CH-$ moieties in aromatic rings are replaced by alternating ^{12}C$-$D and ^{13}C$-$H moieties in order to prevent complicated ^{13}C$-^{13}$C coupling patterns and slow down T_2 relaxation
5. Otherwise, global labeling with ^{13}C and ^{15}N is performed to enable multidimensional NMR experiments.

The resulting labeling patterns of the amino acids are accessible by chemical and enzymatic reactions using labeled starting material.[17]
Although removal of a great number of signals that can (in theory) be used to establish inter-proton distances leads to a lesser resolution, this is by far compensated by the simplification of the spectra, allowing assignment and structure determination in the first place.

Multidimensional spectroscopy

The first structure determination of a protein relied exclusively on proton spectra.[7] When assignment problems due to overlaps become the limiting factor for the size of protein structures accessible with NMR, another spectral dimension can be added to obtain additional information that can be used for assignment. Standard 2D experiments consist in e.g. HMBC that use up to ^{4}J heteronuclear couplings to determine long range connectivities in a molecule.[23] This technique, however, struggles with low intensities since the coupling over three or four bonds is weak compared to ^{1}J or ^{2}J couplings. Furthermore, both ^{1}H$-^{15}$N and ^{1}H$-^{13}$C 2D spectra only yield intra-residual information, which precludes obtaining information on adjacent residues.

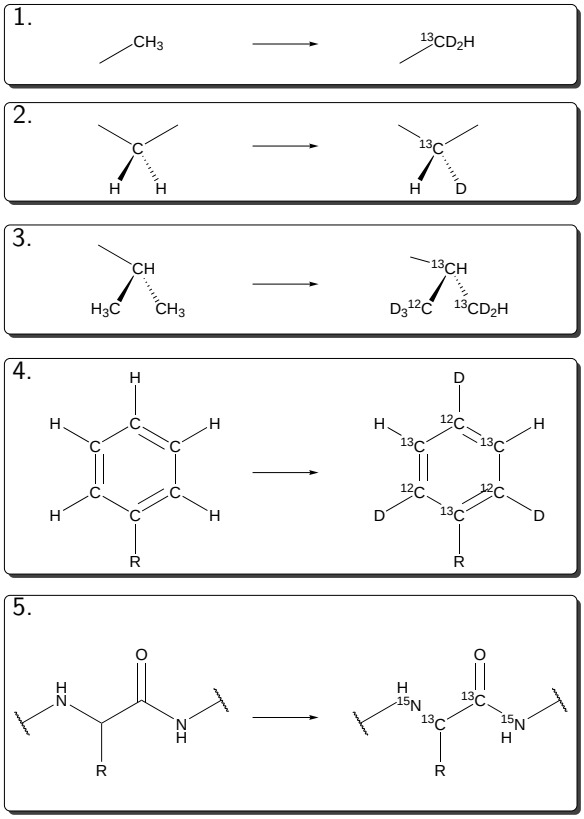

Figure 4: SAIL principles of labeling

A major breakthrough in the signal assignment was the development of triple-resonance spectroscopy. This method extends the range of nuclei addressed in one measurement cycle. While 2D spectroscopy usually involves ^{1}H and ^{13}C **or** ^{15}N, 3D spectra encompass all three atomic species simultaneously. Thus, intra-residual as well as inter-residual correlations can be established, making it a tool not only for signal assignment but for determining connectivities between the residues. It is highly beneficial for signal intensities of 3D spectra that crosspeaks are not based on far-range $^{3}J_{H\text{-}C}$ couplings but that the nuclear magnetization is transferred from one nucleus to the next by effective ^{1}J couplings between H-N, H-C, C-C and C-N.

Measurement cycles are denominated by the sequence of nuclei that are involved. E.g. the HNCACB experiment starts at the amide proton, then the magnetization is transferred to the nitrogen and then passed on to first C_α and then C_β. As ^{1}H is by far the most sensitive nucleus, most experiments start with magnetizing the proton before transferring it to other nuclei. In the same manner the magnetization is finally transferred back to the proton to be measured. This principle, where a signal is sent out and finally recollected, is called "out-and-back".[24]

Up to date, many protocols for 3D measurement exist, the most used for assignment are CBCANH (or HNCACB) and CBCA(CO)NH.[25,26] In the CBCANH experiment magnetization is first transferred from C_β to C_α. Two options exist for the subsequent transfer to amide nitrogen: the amide of the same residue (i+1), or via a ^{2}J coupling to the nitrogen of the following amino acid (i+2). This means, that every amide proton couples to two residues, providing the information on connectivity. To establish exact boundaries and unequivocal assignment of residues to backbone, a CBCA(CO)NH experiment is performed. This experiment correlates the i+1 amide protons with the C_α and C_β of the i residue and does not give signals for the i+1 sidechain correlating with the i+1 amide proton (Figure 5).

It is easy to identify the amino acid by the $^{13}C_\alpha$ and $^{13}C_\beta$ shifts of the side chain. Furthermore, an overlay of both experiments yields a pattern that allows the determination of a sequence and the assignment of the

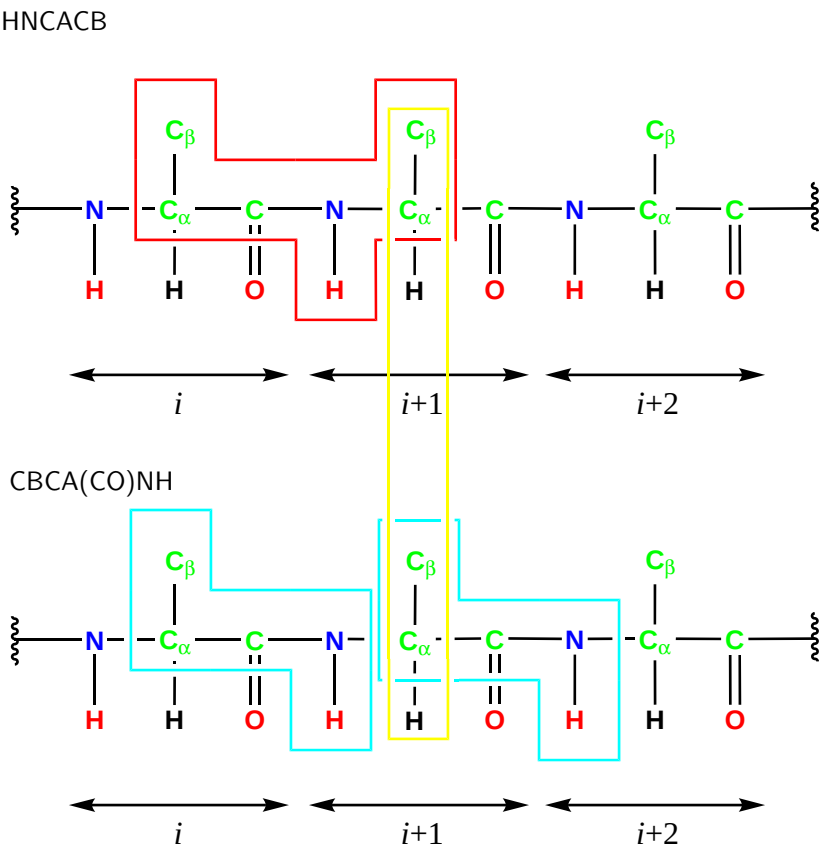

Figure 5: Magnetization pathways in the HNCACB and CBCA(CO)NH experiments

corresponding ^{1}H, ^{13}C and ^{15}N peaks. For this purpose the results of both experiments for one amide are displayed next to each other as stripes (Figure 6) where CBCA(CO)NH gives signals only from the i side chain and HNCACB from both i and i+1.

While the chemical shifts for ^{1}H and ^{13}C can be read on the axes, the ^{15}N-shift, representing the amide that is involved in both experiments, is given above the stripes since they are different for each of them. In Figure 6 the different peak colors highlight the fact that peaks from C_α (black) can be made to appear in the opposite phase from C_β (red) and can therefore easily be distinguished.[27]

The power of this technique is that only protons in a position where a given transfer sequence can occur, give a signal. The spectra are therefore simplified to a large extent.

The need for labeling in multidimensional experiments is obvious since only ^{13}C nuclei can accept and transfer magnetization and only ^{15}N will result in sharp lines. Uniform labeling with these isotopes is therefore required. On the other hand, in a protein that has been deuterated for reasons of simplification or slowed relaxation, "reverse" labeling with protons is required for any experiment that uses ^{1}H at any point in the magnetization transfer sequence. This is why synthetic approaches that allow for specifically designed labeling patterns are of great use in protein NMR studies.

Labeling methods

As demonstrated above, labeling plays a significant role in the structure determination of proteins with NMR. Since those labels do not naturally occur they have to be introduced by biological or chemical methods. The most straightforward approach is expressing desired proteins in cell systems that are fed with labeled nutrients. Bacteria can use e.g. glucose, acetate or pyruvate as sole carbon sources and NH_4^+ as sole nitrogen source to build up all amino acids.[19] Uniformly labeled proteins will hence result from uniformly labeled substrates while

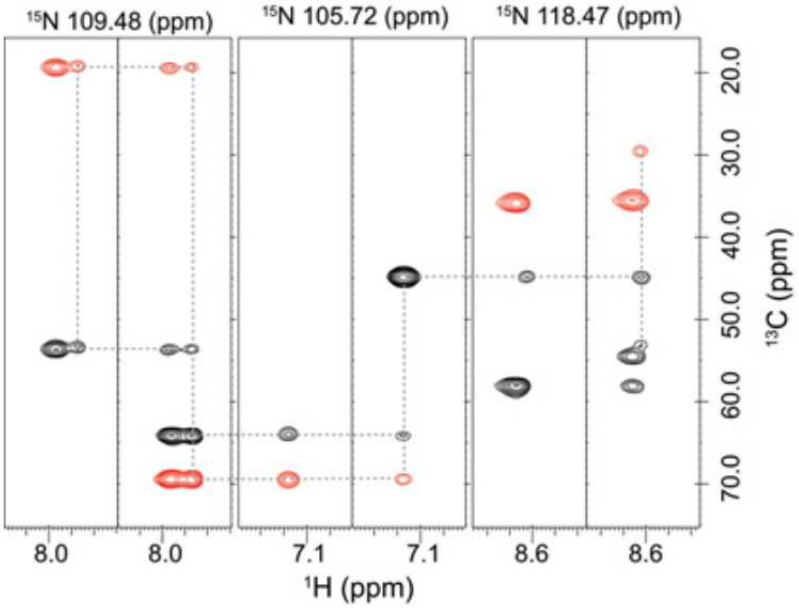

Figure 6: Stripes of CBCA(CO)NH (left) and CBCANH (right) and correlations indicating the sequence[27]

randomly labeled substrates give random global labeling. Regarding perdeuteration, problems can arise since D_2O is often toxic for cells, resulting in a reduced expression yield or even failure. This stems from the fact that in protium/deuterium the isotope effect is more influential than in any other element, causing reactions involving H^+ to slow down significantly.

When more specific labeling patterns are needed, a substrate further down the metabolic pathway has to be chosen. For example, anthranilic acid is the compound of choice when aiming exclusively for labeled tryptophan.[28]

When biosynthesis of labeled amino acids fails, it can be a viable option to perform a chemical synthesis of the labeled compounds and use them as nutrients for cell systems to express proteins. Chemical synthesis is ultimately required for unnatural amino acids also used for structure determination, such as fluorinated derivatives (Part III). Additionally, it provides the possibility to selectively label specific sites within a protein without any cross-labeling due to biosynthetic pathways shared by two or more different amino acids. Hence, synthetic strategies that allow for different labeling patterns of amino acids are most valuable since structure determination, especially of large proteins, is highly dependent on labeled compounds.

Chemical synthesis of whole proteins, on the other hand, comes with the disadvantage that only proteins up to a certain size are accessible due to solubility problems.

Chemical ligation reactions are useful tools to combine two protein fragments to a larger one. An N-terminal fragment with a thioester on its C-terminal can be reacted in a native chemical reaction with another fragment bearing a cystein on its N-terminal.[29]

The splicing method is an autocatalytic process that links two extein fragments by excising an inbetween intein sequence.[30] Like the native chemical ligation this process uses the N,S - acyl shift (and vice versa) in combination with transesterification of cysteins to connect protein segments. Apart from a cystein in the N-terminus of both the carboxyl extein and the intein, an asparagine residue is required at the C-terminus of the intein for this method to work.

A modification of the splicing process is trans-splicing. The major difference is that part of the intein is synthesized on the terminus of each extein. After mixing both sequences the separate intein fragments refold to form a functional intein that subsequently cleaves and rearranges the protein.[31]

Ligation and splicing methods give access to segmentally labeled proteins when a labeled sequence is combined with unlabeled segments. When no elucidation of the complete structure is needed and the focus is on protein

dynamics in a specific site, it is desirable to perform deuteration labeling in remote parts so as to simplify ^{1}H spectra, and at the same time incorporate uniform ^{13}C and ^{15}N labeling in the area of interest to allow for multidimensional spectroscopy. In total, this makes for an approach to investigate only specific parts of the protein without a large interfering background.

2.4 Summary

Isotope labeling with ^{2}H, ^{13}C and ^{15}N and new NMR measurement approaches such as TROSY and multidimensional spectra have more and more extended the size of proteins amenable to structure elucidation. This has led to large proteins, such as a 900 kDa chaperone protein complex,[32] to be investigated by NMR spectrosopy. Although NMR has advantages over X-ray analysis there are also major drawbacks compared to diffraction analysis, the most prominent being time. Even though 1D proton spectra may be recorded in a very short time, this is not necessarily the case for other nuclei, let alone experiments of higher dimensions that require measuring times of several months.[33] Since proteins are not constrained in a rigid crystal in an NMR analysis, they retain a higher degree of freedom of motion. This lowers the resolution, especially of regions that do not display a distinct secondary structure as helices or sheets but rather adopt random coil structures. On the contrary, it opens a window for the investigation of protein dynamics, a field that is inaccessible to X-ray diffraction as a matter of principle. Furthermore, NMR does not require the crystallization of the sample. This is interesting since many membrane situated proteins are prone to fail crystallization.[34]

When performing NMR spectroscopy, the choice of solvent is of central importance as this may affect solubility and folding of the protein. An aqueous environment is most similar to the natural surrounding in biological context. Therefore, a protein is most likely to retain its native folding when water is used as a solvent. The high abundance of H_2O in aqueous samples requires a suppression of the solvent peak. Alternatively D_2O can be used, which is precluded in some multidimensional measurements since they rely on $^{15}N-^{1}H$ moieties that are acidic enough to be transformed to $^{15}N-D$ amides.

In total, neither of the two major structure determination techniques can fulfill all demands of structural biology. While X-ray is the more precise and quick approach that does not have size limitations, NMR gives insight into dynamics. The choice of method thus depends on the exact research goal.

Part II

Synthethic approaches towards the unnatural amino acid 3,4-dihydro-2*H*-pyrrole-2-carboxylic acid

1 Proline

The non-essential proteinogenic amino acid stands out against other amino acids because of some unique properties, the most obvious being the five-membered ring that connects its backbone with the side chain. This induces extensive consequences. In respect to other amino acids lacking this ring structure, proline's accessible conformations are restricted. This may lead to the conclusion that proline renders proteins more rigid. Yet the opposite is the case. In normal peptide bonds the *trans* conformations is favoured over *cis* by a factor of 10^3.[35] The bond between proline and the preceding amino acid (N→C), however, occurs up to 60% in the *cis* conformation, this also depending on the preceding[36] and subsequent[37] residues.

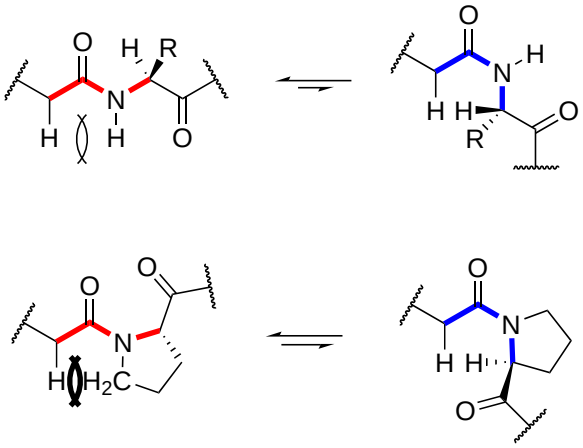

Figure 7: *cis* and *trans* conformation in Xaa and Pro

This can be explained by steric reasons (Figure 7). In every other amino acid the *cis* conformation poses a much greater steric strain than the *trans* conformation because the α-hydrogen of both residues point towards each other. The same is true for proline, yet in proline there is also an increased steric hindrance in the *trans* conformation because of the δ-hydrogens. This means that in proline *cis* is **not** more favored but that *trans* is more disfavored compared to other non-cyclic amino acids.
The fact that *cis* is not disfavored so much causes the peptide bond between proline and the preceding amino acid to readily isomerize, making the protein less rigid. Therefore proline is of central importance concerning conformational changes of the protein during enzymatic reactions or receptor peptides which pass on signals by changing their shape.

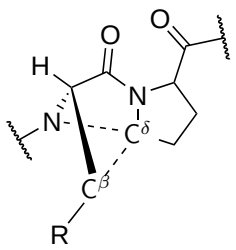

Figure 8: Steric hindrance between Pro and preceding amino acid

Not only does proline play a major role in changes of the structure but in the structure itself. Because of the space occupied by the ring, especially the $-C^{\delta}H_2-$ moiety, proline also affects the ϕ and ψ angles of the preceding amino acid. Said $-CH_2-$ moiety interferes with the $-C^{\beta}H_2-$ group of the previous amino acid rendering otherwise easily accessible conformations energetically unfavorable (Figure 8). Secondary structures

such as helices and sheets require certain ϕ and ψ angles in the partaking residues, visualized in a Ramachandran plot. The steric hindrance between proline and the previous amino acid especially disfavors the conformation needed for α-helices.[38]

Another effect of the backbone being linked to the side chain via the nitrogen is the missing amide hydrogen in the peptide bond between proline and its preceding residue. As described above, hydrogen bonding patterns account for the secondary structure by connecting certain parts of the sequence. Due to this lacking of hydrogens available for bonds proline is not suitable for regular α-helices and β-sheets. Still, proline can be found in these structures under certain circumstances. Statistic distribution of proline[39] shows that proline is most abundant directly before and after the helix, acting as a helix breaker and initiator. Within the helix, it is necessary that hydrogen bonds can maintain the residue before proline in the disfavored α-conformation. Due to different demands regarding conformational angles β-sheets are less affected by proline, but as in α-helices firm hydrogen bondings between other residues are mandatory to compensate for the lacking hydrogen of proline's amide nitrogen.

A further quality of proline is its ability to build up structures on its own. Polyproline stretches may adopt left- or right-handed helix structures[40] that play a role in protein interactions and signal transduction.[41]

1.1 This work

As demonstrated above, proline is a central factor in protein structures and dynamics. Investigation on proline, therefore, provides deeper understanding of how and when conformational changes occur during enzyme catalyzed reactions and signal transduction by proteins. Since C^{δ} is the main target of interest regarding proximity to other moieties, special emphasis should be put on this region. Considering the need for labeled amino acids explained in the introduction, it is desirable to have a generally applicable method to synthesize proline that can be varied so as to gain access to diverse labeling patterns including deuteration of less important locations. When it comes to synthesis with labeled building blocks, it should be kept in mind that reagents become more expensive as they contain more complicated labeling patterns. A strategy that involves $K^{13}CN$ (273.00 €/g, SigmaAldrich[42]) would therefore be preferred over one applying glucose labeled with ^{13}C in position 1 and 2 (945.00 €/g, SigmaAldrich[43]).

2 Synthetic approaches

2.1 Starting from diethyl malonate

The first step in this approach was to introduce an oxime in α-position of the malonate. According to Antina et al.,[44] this can be achieved by treating diethyl malonate **1** with $NaNO_2$ in acetic acid, yielding diethyl 2-(hydroxyimino)malonate **2** (Scheme 1).

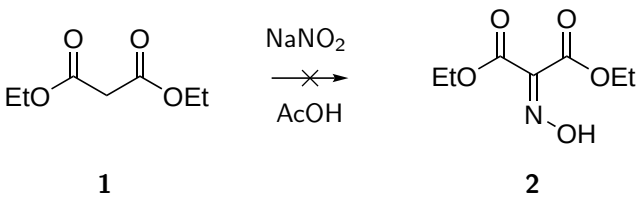

1 **2**

Scheme 1: Introduction of an oxime group to diethyl malonate

NMR proved that only starting material had been recovered after the workup. Comparison with other papers that reported the same transformation indicated that this reaction requires the presence of NaOH[45] in order to activate the malonate by deprotonating it. This procedure gave 77% yield. An NMR spectrum was recorded

and the integration of the peak originating from the remaining hydrogens in the α-position was compared to the integrals of $-CH_2-$ and $-CH_3$ groups to determine the purity of the product (21%). To increase the purity of the yielded material a chromatography was done. NMR confirmed high purity afterwards. By increasing the reaction temperature from RT to 55°C a yield of 72% pure product could be generated.

Table 1: Conditions for the introduction of an oxime to diethyl malonate

Reaction number	Solvent	Reagents	Temperature	Time	Yield
GKM001	AcOH	$NaNO_2$	RT	20h	0%
GKM005	AcOH	$NaNO_2$, NaOH	RT	18h	16%
GKM011	AcOH	$NaNO_2$, NaOH	RT	20h	17%
GKM015	AcOH	$NaNO_2$, NaOH, argon	RT	18h	13%
GKM017	AcOH	$NaNO_2$, NaOH	55°C	20h	72%

A subsequent hydrogenation using the H-Cube reactor and a Pd^0 catalyst cartridge (CatCart® 10% Pd/C) gave good yields with high purity (GKM014[1]).

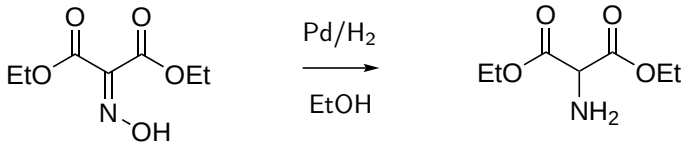

2 **3**

Scheme 2: Reduction of the oxime to the amine

The next step consisted in introducing an acetyl group in order to prevent the amino moiety from interfering in another upcoming step (Scheme 3). For this introduction several methods were tried (Table 2).

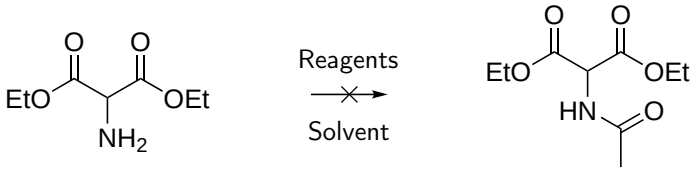

3 **4**

Scheme 3: Acylation of diethylamino malonate with various reagents and solvents

All results had in common that no $-CH-$ peak could be detected in the NMR spectra. As this proton is still activated by the adjacent carboxylic moieties it is possible that this reactive center interferes with the acylation.

Table 2: Attempts to introduce an acyl group

Reaction number	Solvent	Reagents	Yield
GKM021[46]	CH_2Cl_2	AcCl, NEt_3	0%
GKM023	CH_2Cl_2	HOBt, EDC, AcOH	0%
GKM030[47]	CH_2Cl_2	Ac_2O, NEt_3	0%

[1] All reaction numbers that are not mentioned in this text refer either to repetitions of prior identical reactions in order to synthesize more substance for further reactions or to unsuccessful reactions that were discarded. For detailed information see the experimental part (Part IV).

As an alternative to the stepwise synthesis of the acetamidomalonate **4**, there are reports of a one-pot procedure. While the reaction of diethyl malonate **1** with acetic anhydride, sodium nitrite, acetic acide and Pd on activated charcoal in diethyl ether[48] (Scheme 4, GKM031) resulted in no product, the synthesis was successful when the solvent was changed to water and zinc dust was added as a reducing agent for the intermediate oxime[49] (Scheme 5, GKM035).

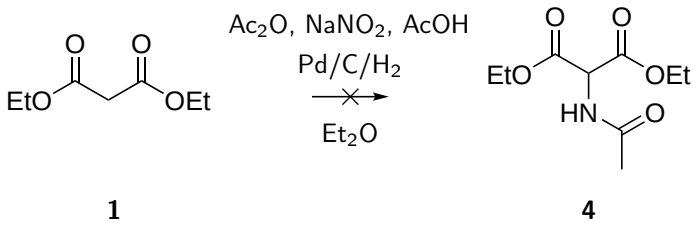

Scheme 4: First attempt of a one-pot synthesis of diethyl 2-acetamidomalonate

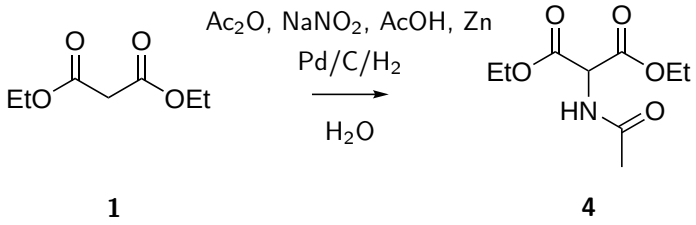

Scheme 5: Second, successful attempt of a one-pot synthesis of diethyl 2-acetamidomalonate

This reaction gave an acceptable yield of 46% in good purity so that no additional purification was necessary after the workup. With this compound available it was possible to address the next step. For the introduction of the three carbon atoms of the final ring structure a possibility is to perform an addition reaction of the acetamidomalonate **4** to acrolein **5** (Scheme 6),[50] yet, because of the high polarity of the carbonyl, an addition is more likely to take place there instead of at the alkene.

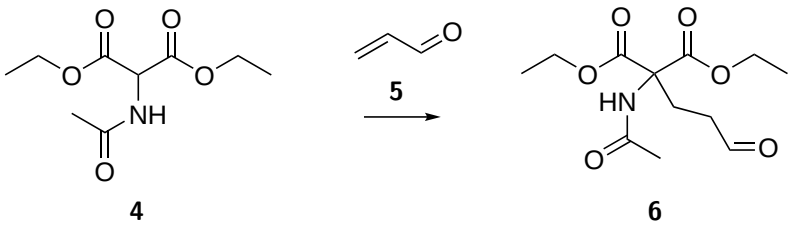

Scheme 6: Original idea: addition to acrolein

To circumvent this unwanted side reaction acrolein was replaced by 3-bromo-1,1-dimethoxypropane **7** (Scheme 7). With this, some attempts were made to yield the desired product (Table 3).
However, by none of this methods product could be obtained that was consistent with literature NMR spectra.

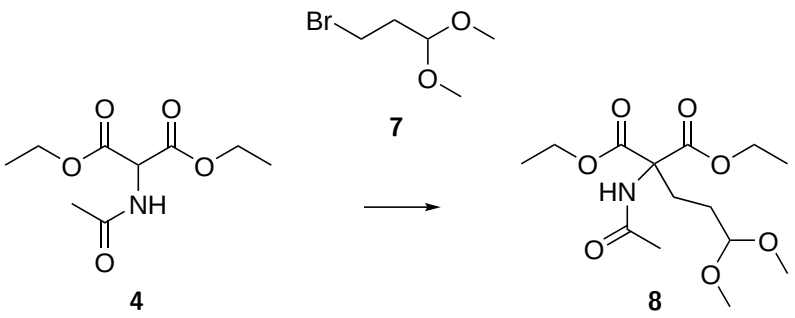

Scheme 7: S_N2 reaction with 3-bromo-1,1-dimethoxypropane **7**

Table 3: Conditions for the introduction of the acetal

Reaction number	Solvent	Reagents	Temperature	Time	Yield
GKM037[51]	DMF	NaH, TBAI	60°C	92 h	0%
GKM040[52]	DMF	KO*t*Bu, argon	80°C	16 h	0%
GKM038[53]	ACN	Cs_2CO_3, NaI	130°C, MW	20 min	0%
GKM041	ACN	Cs_2CO_3, NaI	60°C, MW	40 min	0%
GKM043	ACN	Cs_2CO_3, NaI	90°C, MW, 30 min and 90 Watt MW, 10 min		0%
GKM045	ACN	Cs_2CO_3, NaI	130°C, MW	90 min	0%

If this introduction of the acetal had been successful, the further planned steps would have consisted in the hydrolysis of the acetal, the amide and the malonic ester, resulting in the cyclization of the aldehyde with the now free amine and the decarboxylation of the malonic acid to yield the desired final product *rac*-4,5-dehydro-proline **9** (Scheme 8). As the educt of this transformation **8** has a prochiral quaternary carbon atom which becomes a chiral center after the decarboxylation, this results in a racemate since there is no preference as to which carboxylic functionality will undergo the decarboxylation. Reports exist for the hydrolysis of the amide and ester functionalities and the subsequent cyclization by refluxing the aldehyde **6** in 6N HCl[54] or by submitting the compound to microwave irradiation for 10 minutes at 90°C in 6N HCl.[53] Although the hydrolysis of the acetal moiety is not mentioned in the latter paper, it is likely to happen as the standard protocol for it consists in subjecting it to acidic aqueous conditions.[55]

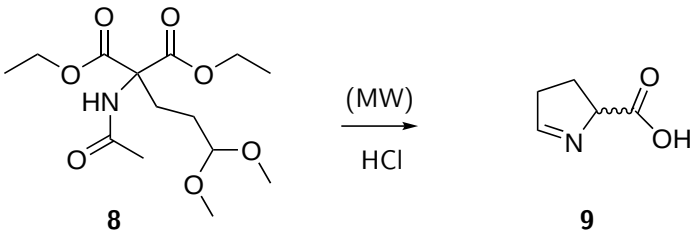

Scheme 8: Final hydrolysis and cyclization

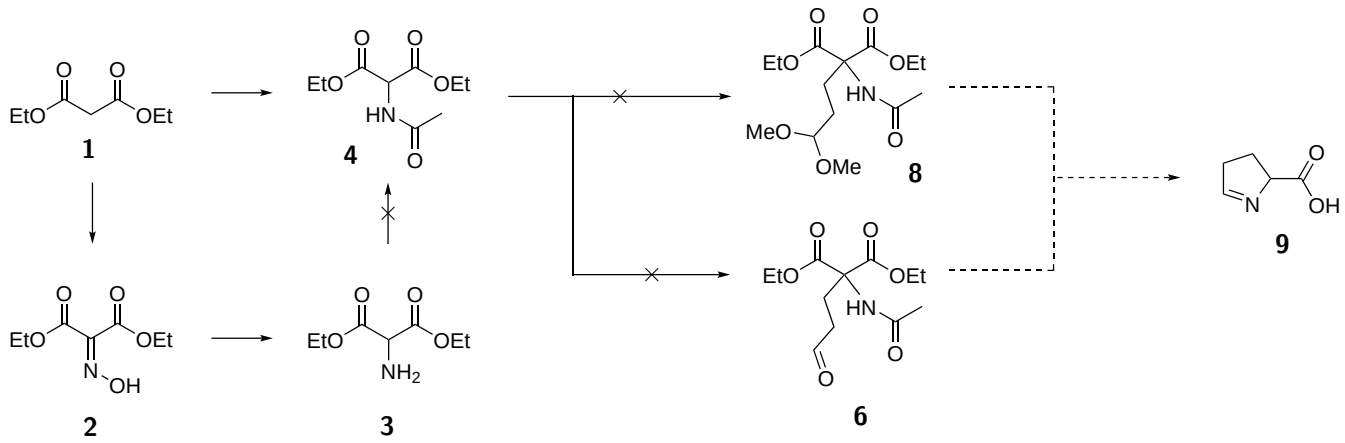

Scheme 9: Overview of the synthesis

2.2 Starting from glutamic acid

Another synthetic approach started from glutamic acid **10**. In a first step this amino acid was equipped with a Cbz protection group[56] (GKM054) followed by the ring closure with formaldehyde[57,58] (Scheme 10, GKM060). The reason for this was to enable specific reactions with the γ-COOH moiety while leaving the α-carboxylic group untouched. According to the NMR data this worked decently and with acceptable yields of 83% and 63%.

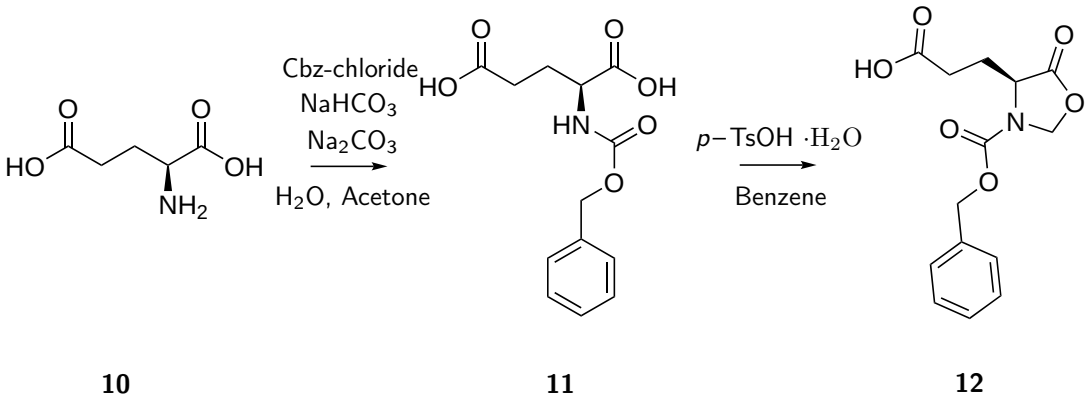

Scheme 10: Protection and cyclization of glutamtic acid

To avoid benzene as a solvent this was also tried in toluene (GKM061) using a Dean-Stark apparatus to remove the originating water from the solvent. Aside from switching to a less toxic solvent, this also increased the yield as it allowed higher reaction temperatures.
In order to activate the γ-COOH it was transformed to the acid chloride **13** using PCl_5 in benzene[59] (Scheme 11, GKM064).

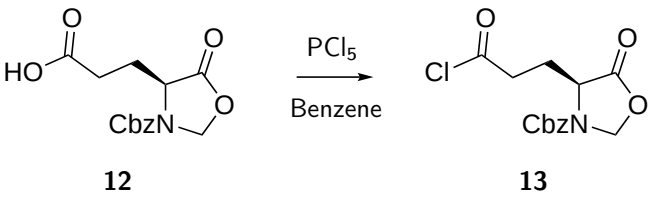

Scheme 11: Transforming the acid **12** to its chloride **13**

An NMR analysis is not the appropriate method to confirm the success of acid chloride formation as there is no proton that would undergo a significant change of its chemical shift and also the ^{13}C shifts of carboxylic acids and its corresponding chlorides do not differ very much. To prevent any decay caused by moisture, a yield of 100% was assumed and the material was instantly used for the next step. This consisted in the coupling of two acid chlorides **13** to form the peroxo anhydride **14**. Regarding its structure, hydrogen peroxide appears to be ideal for the formation of this peroxide: each –OH will react with an acid chloride resulting in the desired product and two equivalents of HCl. However, in order to exclude the moisture induced decay of the acid chloride it is necessary to perform this in a water free environment. Hydrogen peroxide is mostly handled in aqueous solutions with a concentration up to 30%. This is due to the fact that higher concentrated solutions or even pure hydrogen peroxide are unstable and prone to spontaneous explosion.[60] The compromise of using hydrogen peroxide and the need for dry conditions led to the idea to use urea hydrogen peroxide (UHP), which is an adduct of urea and H_2O_2, thus making the peroxide available as a dry (though hygroscopic) and stable solid. The reaction itself was then performed in dry Et_2O and pyridine as a scavenger for the emerging HCl[61] (Scheme 12, GKM065).

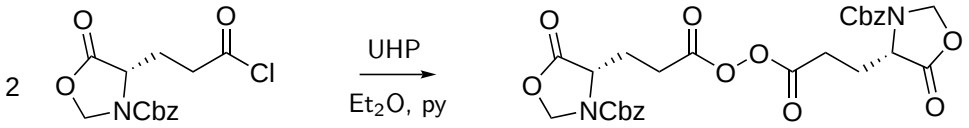

13 **14**

Scheme 12: Formation of the peroxide **14**

Again NMR is not suitable to produce revealing information as no protons are in close proximity to the transformed area. Instead a MS was made. Because of its homonuclear oxygen bond it is probably an unstable compound requiring mild ionisation. The MS result in positive ion mode showed a peak at m/z 607 which would fit the Na^+ peak of the compound. Again assuming that the reaction worked, the material was used in the following step. In this, the peroxide is cleaved again, causing a chain reduction by one carbon and transforming it to an alkyl bromide **15**[61] (Scheme 13, GKM067).

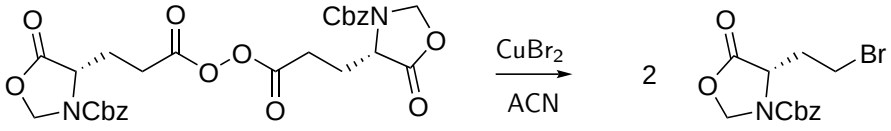

14 **15**

Scheme 13: Cleavage of the peroxo anhydride, formation of the bromide

This synthesis was not further pursued. In case the synthesis of **15** had been successful, the next step would have consisted in a S_N2 reaction to replace Br with a nitrile functionality. This is the central step as it provides the relatively inexpensive opportunity to introduce a ^{13}C label by using $K^{13}CN$ (Scheme 14).[62]
For the subsequent selective reduction of the nitrile **16** to the aldehyde **17** (Scheme 15) several options exist: Either to first reduce it to the alcohol and then perform a mild oxidation that stops at the aldehyde stage (e.g. Swern oxidation) or to choose a reduction that also stops at the aldehyde. Examples for this include the use of DIBAL or of metal catalysts and a hydrogen source as $NaBH_4$[63] or HCl.[64]
Eventually, the ring opening can be done by $NaHCO_3$ in an alcohol that gives the ester and the Cbz protected amine **18**[65] (Scheme 16) followed by removing the Cbz group.

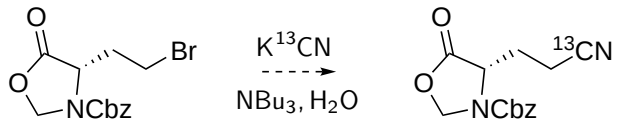

15 **16**

Scheme 14: Introduction of the cyanide

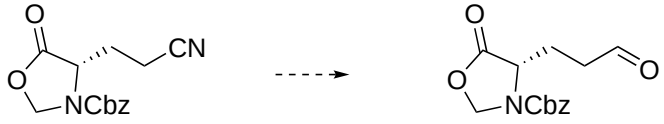

16 **17**

Scheme 15: Reduction of the cyanide **16** to the aldehyde **17**

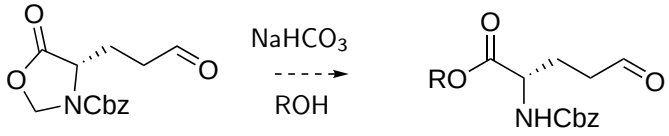

17 **18**

Scheme 16: Ring opening of the oxazolidinone

The standard protocol for removing Cbz protecting groups consists in Pd-catalysed hydrogenation which in this case, though, would probably make an alcohol out of the aldehyde. Another way to remove benzyl protection groups is provided by treatment with HBr in AcOH[66] (Scheme 17). The aldehyde **19** will readily undergo cyclization with the amine producing the target compound **20**. Since the starting material was the enantiopure glutamic acid, this synthetic approach yields also enantiopure dehydroproline.

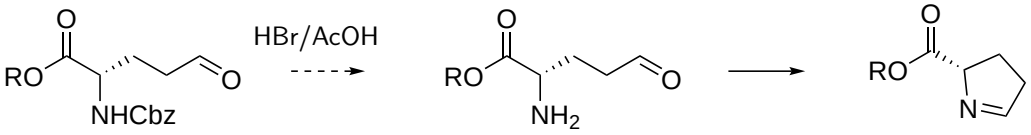

18 **19** **20**

Scheme 17: Removal of the protecting group and cyclization

2.3 Starting from glycin (hydrochloride)

This approach aimed for the construction of the oxazolidinone ring first and then the addition of the desired side chain. Starting from glycine methyl ester hydrochloride **21** the first two steps were identical with the previous synthesis: to introduce a Cbz protection group (GKM055)[67] and close the ring (GKM057)[68] (Scheme 18). Further alkylation with bromoalkanes **7** (GKM072) and allyl bromide (GKM073) can be achieved by LHMDS in THF at -78°C[69] (Scheme 19).

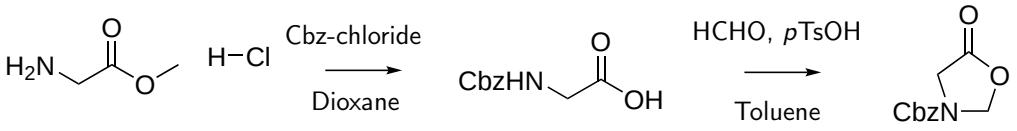

21 **22** **23**

Scheme 18: Protection and ring closure of glycine

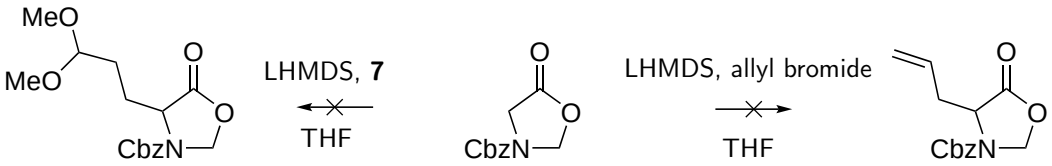

24 **23** **25**

Scheme 19: Alkylation of the glycin derivative

Compound **24** can be further processed as compound **17** after hydrolysis of the acetal,[70] even though this leads to a racemic product. Compound **25** can be transformed either to the aldehyde **17** after hydroboration and subsequent oxidation, or it can be subjected to ozonolysis resulting in an alcohol after workup with $NaBH_4$ and $BH_3 \cdot Me_2S$.[71] Converting the alcohol to a good leaving group and performing an S_N2 reaction with KCN leads again to compound **16** which can then be processed analogously to the previous synthesis.

3 Further ideas

3.1 Synthesis via glycine imine

A further possibility to yield the desired product might also start from glycin methyl ester **26** which can be transformed to its imine **27** by treating it with benzophenone in toluene[72] (Scheme 20).

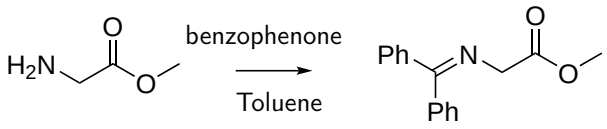

26 **27**

Scheme 20: Formation of the imine from glycin methyl ester

Allylic side chains can then be introduced by using $Pd_2(dba)_3$ and dppa in THF with allyl acetate **28** as the allyl source[73] (Scheme 21).

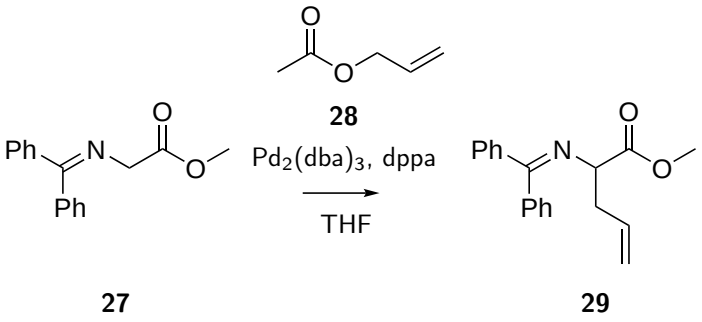

Scheme 21: Addition of the side chain

When the methyl ester is replaced by Oppolzer's camphor sultame this step can also be done enantioselectively. The same method as mentioned above can be applied for the introduction of a nitrile and the conversion to the aldehyde. Ensuing hydrolysis of the imine results in an amine again that will undergo an intramolecular cyclization to the proline derivative.

3.2 Synthesis via a binaphthyl PTC reaction

An innovative approach is to use phase transfer catalysis (PTC)[74] (Scheme 22). The substrate **30** is deprotonated by KOH and then alkylated by allyl bromide. The reaction takes place in toluene, the base, however, is not soluble in this solvent. This is circumvented by using a phase transfer catalyst **31**. This compound is soluble in organic solvents as well as in aqueous systems and acts as an ion ferry. The bromide is exchanged for the hydroxide which is then transported into the organic phase to deprotonate the glycin there. The emerging water will join the aqueous phase. The catalyst displays axial chirality and this causes the reaction to be stereoselective. The reaction of allyl bromide with 1 mol% (*S,S*)-catalyst produces 84% yield of the *R* enantiomer **32** in 94% *ee*.

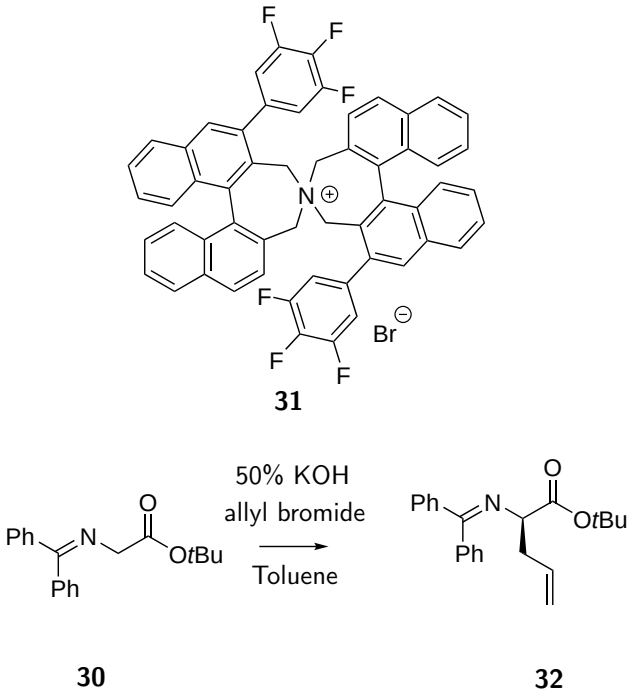

Scheme 22: Phase transfer catalysis reaction

Part III

Synthesis and application of the fluorination agents “PhenoFluor” and “PhenoFluorMix”

1 On Fluorine

Although rather common on earth, fluorine is rare in the body. Due to its high reactivity fluorine can only be found in the form of fluorides. Naturally occurring fluorides display a low bioavailability which accounts for the equally low occurrence in the human body apart from teeth and bones. The almost total absence of organic fluorine compounds in biological samples is beneficial since it allows for analyses without the need for background elimination. A trait that has been used for *in vivo* NMR analyses in many cases.[75–77]

2 ^{19}F NMR spectroscopy

The ^{19}F nucleus has a nuclear spin number of 1/2 and a gyromagnetic ratio of 251.6233 rad·s^{-1}·μT^{-1}.[78] With a sensitivity of 0.83 relative to ^{1}H[79] the ^{19}F nucleus is well suitable for NMR analysis. Since other nuclei do not give a signal in the fluorine experiment, any background from other non-fluorinated compounds is invisible. Thus, it is possible to analyze fluorine compounds in a highly complex matrix, such as living cells, without the problem of spectra becoming very crowded. Its high sensitivity also allows the analysis of low sample concentrations.[80] This is helped additionally by the fact that fluorine is a pure element, consisting naturally only of the isotope ^{19}F. Therefore, every fluorine in the molecule will give a signal, unlike carbon where only about one in 100 atoms is active in NMR. Worth mentioning is also the large chemical shift scale of the ^{19}F nucleus of 1313 ppm,[81] the usable area of which spans about 400 ppm.[82] This is an important feature as it makes signal overlaps less probable compared to the 15 ppm range of ^{1}H and allows for great shift differences caused by small changes in the chemical environment of a fluorine brought about by cleavage of bonds, variations of the pH, ion concentrations and oxygen levels.[83,84] Also a change of orientation relative to another molecule or functional group can prompt changes of the chemical shift, making fluorine NMR applicable to study conformational changes, ligand binding and interactions with proteins, small molecules or membranes.[85]

When ^{19}F NMR emerged as a tool in structural biology it was found that despite its benefits there are also major drawbacks which hamper its application. First and foremost the dependence of T_2 on the applied magnetic field. In high fields the fast CSA relaxation pathway leads to a quick loss of magnetization[86] producing broad signals. Since scalar coupling of fluorine with other nuclei results in two peaks, representing positive and negative overlay of CSA and DD, it is evident that a mutual cancellation of the relaxation pathways is likely to improve the spectral quality a lot. In fact, applying this principle in ^{19}F$-^{13}$C 2D TROSY experiments on aromatic systems gives line widths for ^{13}C that are even narrower than those of ^{1}H$-^{13}$C peaks of the same experiment. This experiment makes use of the high magnetization sensitivity of ^{19}F in combination with the slow relaxation of ^{13}C. The power of ^{19}F$-^{13}$C 2D experiments consists in the enormous simplification of spectra as only those carbons will be detected that are in close proximity of magnetized fluorines, and in the fact that they do not require deuteration, rendering the syntheses of sample compounds less challenging and expensive.
Another benefit of ^{19}F NMR is the amount of time it takes to record spectra. While the standard protocol for assessing protein folding processes consists in ^{15}N$-^{1}$H HSQC that requires measuring times of at least 1 h, fluorine spectra that allow dynamic and structural properties of proteins to be evaluated can be recorded within minutes.[87] Thus, a time resolution for folding processes of 5 s could be achieved.[88,89] Although optical spectroscopy techniques such as circular dichroism easily surpass this resolution, only NMR also gives detailed information on specific positions within the protein. Correct folding of a protein is essential for its appropriate function and inherently misfolding is the cause of malfunctions that result in severe prion diseases such as BSE or the Creutzfeld-Jakob disease. Therefore, detailed insights on folding mechanisms are crucial for the development of new curing strategies.
To mention only shortly, asymmetric fluorination of the aromatic ring systems of Phe and Tyr in proteins have been used to detect ring flips, making use of different shifts corresponding to each position.[90] Finally, line

shape analysis of ^{19}F spectra can be used to study interactions between proteins and membranes.[91]

3 Effects of fluorine on protein structures

A large set of fluorinated amino acid analogues has so far been synthesized[92–95] and applied.[96] While synthesizing analogues of aromatic or branched aliphatic side chains is rather straightforward, problems appear with alanine that is prone to eliminate hydrogen flouride, or with serine and cysteine that are unstable unless protected.[97] When foreign atoms such as fluorine are incorporated into proteins, it is to be expected that this affects steric and/or electronic properties of the protein. In order to keep this effect minimal only certain changes can be made. With fluorine's van der Waal's radius of 1.47 Å instead of 1.2 Å for hydrogen[80,98] it makes for a perfect surrogate for hydrogen as it can be considered isostere. However, this isosteric properties are lost when more than one fluorine is introduced to a molecule. For instance, the $-CF_3$ moiety occupies twice the van der Waals volume of a $-CH_3$ group, resembling much more an isopropyl functionality in terms of steric demands.[99] The shape of proteins is, among other factors, caused by hydrophobic interactions between uncharged, aliphatic residues. When expanding the space occupied by the side chains it is to be expected that this will alter the protein shape which in turn can affect its function. Thus, it is advisable to minimize the extent of fluorination to a minimal degree in order to retain the original shape and mode of working. When hydrogen is replaced with fluorine it also has to be taken into account that, in contrast to hydrogen, fluorine can act as a hydrogen bond acceptor. Therefore, in the context of proteins, e.g. 4-Fluorophenylalanine may be used as a replacement for Phe but also for its hydroxylated analogue Tyr.

Further effects can be caused by one of fluorine's most prominent features: its high electronegativity. In a C–H bond the negative polarization lies with the carbon, the dipole moment, however, is reversed in a C–F bond. In the case of aromatic rings an increasing substitution with F will gradually turn the ring polarization inside out.[100] Clearly, this affects structural interactions such as π-π stacking and cation-π interactions. Moreover, the loss of electron density has an effect on acidity/basicity of both carboxylic and amino functionalities, rendering them more acidic. Changes in enzymatic transformations that include proton shuttles as well as in hydrogen bonding behavior and thus the secondary structure and its stability may ensue.

Highly fluorinated compounds such as perfluorooctane tend to be immiscible with aqueous *and* organic phases. Not only can an alteration of hydrophilicity and -phobicity provoke problems concerning the correct folding of a protein and its stability but may also interfere with the placement of membrane bound proteins.[101]

Having all those mechanisms in mind how a substitution with fluorine might impede the functionality of a protein or deteriorate its structural integrity it is surprising that no such general effect can be observed. While in many cases the fluorinated analogues lead to lower activity, thermal resistance against denaturation or reduced stability towards degradation, there are also numerous examples of the contrary effect.[96] It turns out that no general claim can be made on what impact a certain change in the substitution pattern will have.

4 Fluorination of organic structures and proteins

To incorporate fluorine into organic molecules a large variety of approaches can be exploited, encompassing nucleophilic as well as electrophilic approaches, radical reactions and fluorinated tags. While in general fluorination of aromatic or aliphatic moieties does not pose a great challenge, the exact circumstances have to be taken care of. As much as it is desirable to afford good yields in any organic synthesis, this aspect is even more emphasized when it comes to isotopically labeled compounds since their syntheses rely on costly labeled starting material. Thus, in the planning of a fluorination approach, it is advisable to avoid long detours and aim for a straightforward method instead. Likewise, it is important to maintain reaction conditions that will not lead to the decomposition of the molecule or product isomerization. Lastly, it has to be decided whether the

fluorination is performed before or after the protein is formed. Fluorinating after peptide synthesis comes with the benefit that the "default" machinery of cells can be used for peptide biosynthesis, the reaction conditions required for the fluorination, however, although acceptable for a single amino acid, may turn out to be too harsh for the protein to remain in a functional condition. On the other hand, incorporation of modified amino acids is prone to require e.g. a modified set of tRNA and its corresponding synthetase[102] or the use of an auxotrophic expression organism if not a complete laboratory synthesis. For reasons of practicability, fluorination methods that use F_2 or XeF_2 have obvious limitations.

Fluorine containing tags

This approach can be considered the easiest way to incorporate labels into proteins. Several tags exist, such as fluoroacetyl groups[103] or linkage via disulfide bridges.[104] While tagging can be performed on the readily expressed protein and therefore does not require great (bio)synthetic effort, there is a realistic chance that the tag will affect the structure since in stead of a single atom a comparatively large group is introduced. Additionally, a site specific tagging to investigate a defined position in the protein is hard to achieve.

Radical mechanisms

As of today, radical mechanisms are limited to aliphatic systems.[105] Although modern approaches do not further rely on elementary fluorine or XeF_2 but on electrophilic fluorination agents such as *N*-Fluorobenzenesulfonimide (NFSI)[106] or Selectfluor (1-Chloromethyl-4-fluoro-1,4-diazoniabicyclo[2.2.2]octane bis(tetrafluoroborate), F-TEDA)[107] they still suffer from low yields, especially with complex substrates and, as already mentioned, are not apt for fluorination of aromatic systems.

Nucleophilic substitution on aromatic systems

Prefunctionalized molecules

The most well-known method for substituting aromatic systems with fluorine is the Balz-Schiemann reaction which starts from a primary aromatic amine. After conversion to the diazonium tetrafluoroborate as an intermediate, the final steps consist in the release of N_2, leaving a positive charge on the aromate, and the subsequent nucleophilic attack of the BF_4^- counterion that leads to the fluorinated aromate (Scheme 23).

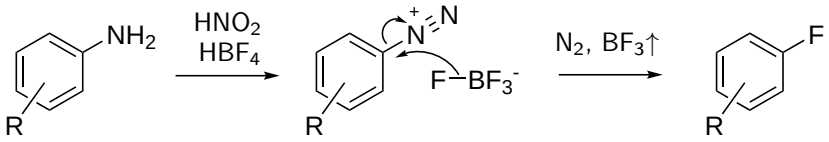

Scheme 23: Nucleophilic substitution via the Balz-Schiemann reaction

This reaction works on substrates that tolerate the acidic environment as well as the heat applied in the second step. In order for this reaction to work decently it is necessary to isolate the intermediate diazonium salt that is - depending on its exact nature - potentially explosive.[108] Due to the harsh reaction conditions a fluorination after protein synthesis is likely to damage the peptide. Furthermore, to produce a fluorinated phenylalanine analogue the synthesis requires an unnatural amino acid as a starting point which precludes the exploitation of biochemical pathways or at least requires additional synthetic steps.

Further nucleophilic fluorination approaches exist that start from a range of functional groups such as halogenated or nitrated aromates,[109] or boron containing substrates.[110] Apart from being also dependent on functional groups that do not occur in natural amino acids, the latter approach is limited to modest yields and

relies on 4 eq. of a copper catalyst, while halogen exchange as well as fluorodenitration work exclusively on electron deficient aromates.

Direct substitution

Additionally, synthetic methods have been developed that work without prefunctionalization, in principle enabling the application of the naturally occurring amino acid Phe. Ag and Cu complexes have been shown to achieve fluorination on aromatics in good yields,[111,112] yet they need a directing group, thus confining the resulting products to *ortho*-substituted molecules. On the other hand, hypervalent iodine complexes achieve a fluorination in *para*-position.[113] However, this comes at the cost of a very limited scope that includes solely alkyl or alkyloxy substituents on the aromate.

The reagents used for nucleophilic substitution reactions in general consist of F^- with an assortment of counterions such as tetrabutylammonium, tetramethylammonium or the metals Cs, K and Ag.[105]

Electrophilic substitution on aromatic systems

Like in nucleophilic approaches, direct electrophilic methods have to be distinguished from those that make use of already present functional groups, including their respective limitations. Direct fluorination reactions using Pd catalysts or Mg reagents display either poor regioselectivity regarding *ortho* and *para* or rely on directing groups such as amides,[114] benzothiazoles[115] or oxazolines[116] to selectively achieve a substitution in *ortho*-position. Any problem with regioselectivity is cleared when using prefunctionalized molecules. Examples exist starting from phenylboronic acids, its pinacol esters, tin or silicon substituents that are converted to the corresponding fluorocompound.[105] Again, to make use of naturally occurring substrates in those approaches, it is necessary to perform additional synthetic transformations.
Generally speaking, the nucleophilicity of an aromatic system is increased in electron rich systems compared to electron deficient aromatics. Complementary, it is desirable to generate a fluorine species that chemically behaves as F^+. To achieve this, the residue bonded to F has to have a strong electron pulling effect. Oxygen has the second highest electronegativity after fluorine, rendering compounds containing an O-F bond promising reagents for electrophilic substitution. However, since compounds as hypofluorous acid or trifluoromethyl hypofluorite are difficult to handle, other more stable reagents have been developed. In most cases they consist of a central nitrogen - ranking 4$^{\text{th}}$ in electronegativity - which is bonded to fluorine and two or even three other substituents capable of accepting electrons (Figure 9). The nature of the residues allows a fine tuning of the reagents' properties.

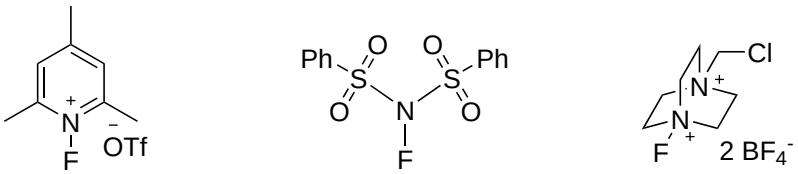

NFTPT NFSI Selectfluor

Figure 9: Some electrophilic fluorination agents

Deoxyfluorination using PhenoFluor

Deoxyfluorination uses a previously existing hydroxy moiety to install a fluorine in the selfsame position. Even though a large variety of fluorination agents for aliphatic alcohols exists, the analogous reaction for phenol

derivatives remained unknown until DFI (2,2-Difluoro-1,3-dimethylimidazolidine) was developed.[117] Although this reagent produces good yields it does not distinguish between aliphatic or aromatic hydroxy functionalities or even enols in a keto-enol tautomerism. PhenoFluor **33**,[118,119] however, selectively addresses phenolic groups, tolerating a broad scope of electron-rich and electron-deficient aromates with almost any other substituent. In other words: no matter which synthesis strategy for a labeled phenol is chosen, as long as there is an aromatic hydroxy group present, it can be easily converted to the corresponding fluorocompound. It combines some beneficial traits that make it an ideally suitable agent in protein chemistry: starting off from a naturally occurring functionality in amino acids, it produces the desired product in a one-step reaction without any intermediate workup in high yields and perfect regioselectivity.

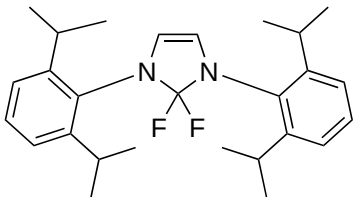

33

Figure 10: PhenoFluor

Due to its moisture sensitivity which significantly diminishes its practicability this agent has been evolved to PhenoFluorMix,[120] a mixture of its penultimate intermediate product **34** during synthesis and CsF. This mixture, though still hygroscopic, can be dried without afflicting damage to the fluorination reagent.

5 The aim of this work

Various synthetic approaches towards isotopically labeled aromatic amino acids have been published,[121,122] respectively their precursors, in order to apply them in the elucidation of protein structures. In addition to deuterium and ^{13}C, fluorine labels provide further information on the behavior of proteins. Knowledge that can ultimately be used to develop strategies against malfunctions of said proteins. The possibility to introduce a fluorine label at a late stage of synthesis without endangering already existing labels gives access to multiply labeled compounds to be used in NMR analyses that include a large set of experiments on just one sample, lowering both costs and synthetic effort. The aim of this thesis's practical work was to perform the synthesis of this fluorination agent and to explore the range of substrates amenable to substitution.

6 Synthesis

The synthesis of this compound[118] started from the easily available precursors glyoxal **35** and 2,6-diisopropylaniline **36**. The reaction of glyoxal with two equivalents of 2,6-diisopropylaniline yielded the Schiff base (1*E*,2*E*)-N^1,N^2-bis(2,6-diisopropylphenyl)ethane-1,2-diimine **37** (GKM002, Scheme 24).
Ring closure was then achieved by TMSCl and formaldehyde **38**, giving 1,3-bis(2,6-diisopropylphenyl)-1*H*-imidazol-3-ium chloride **39** (GKM003, Scheme 25). The oxygen from the formaldehyde in this reaction is converted into hydroxide ions which are scavenged by TMSCl, providing chloride as counterions. For reasons of convenience (formaldehyde as a monomer is gaseous, an aqueous solution would interfere with TMSCl) paraformaldehyde was used, which is cracked into monomers when exposed to heat.
Before fluorine can be introduced in position 2, the hydrogen has to be replaced by the better leaving group chlorine. This can be achieved by deprotonation with the strong base KO*t*Bu and then treatment with hexachloroethane as a chlorine source, resulting in 2-chloro-1,3-bis(2,6-diisopropylphenyl)-1*H*-imidazol-3-ium chloride **34** (Scheme 26).

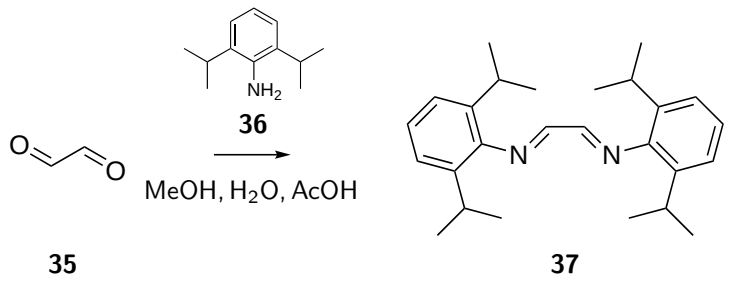

Scheme 24: Formation of the glyoxal diimine

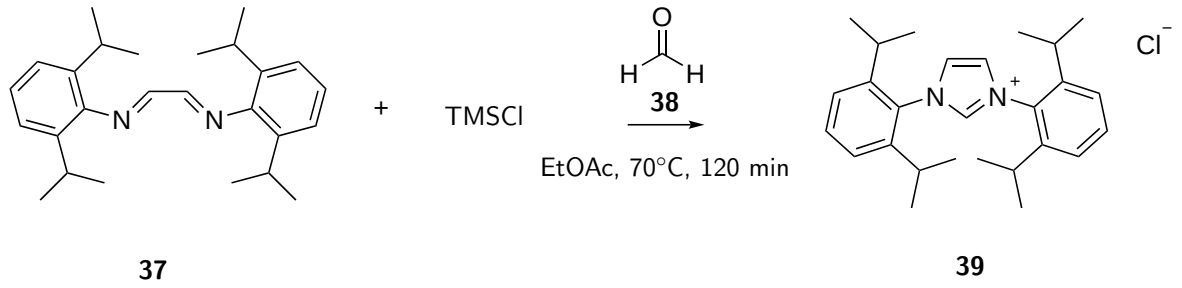

Scheme 25: Ring closure to the imidazolium chloride **39**

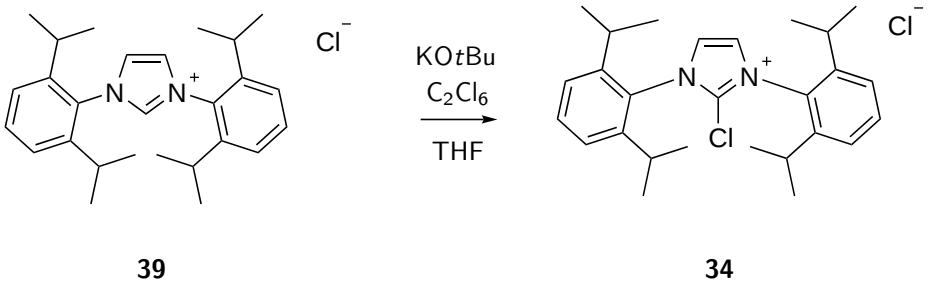

Scheme 26: Substitution with chlorine

Although this experiment was conducted according to literature, the yield of 12% was significantly lower than the literature value of 81%. Reaction conditions were varied to improve the yield (Table 4).

Table 4: Conditions for the substitution with chlorine

Reaction number	Temperature	Rinsing	Time	Yield
GKM006	RT	THF (-20°C), Toluene (20°C)	24h	12%
GKM029	RT	Toluene (20°C)	39h	34%
GKM032	RT	THF (-78°C)	36h	16%
GKM034	50°C	Toluene (-78°C)	20h	0%
GKM048	RT	Toluene (-78°C)	42h	50%
GKM053	RT	Toluene (-78°C)	120h	68%

To finally yield PhenoFluor (1,3-bis(2,6-diisopropylphenyl)-2,2-difluoro-2,3-dihydro-1*H*-imidazole) **33** fluorine is introduced with CsF (Scheme 27).

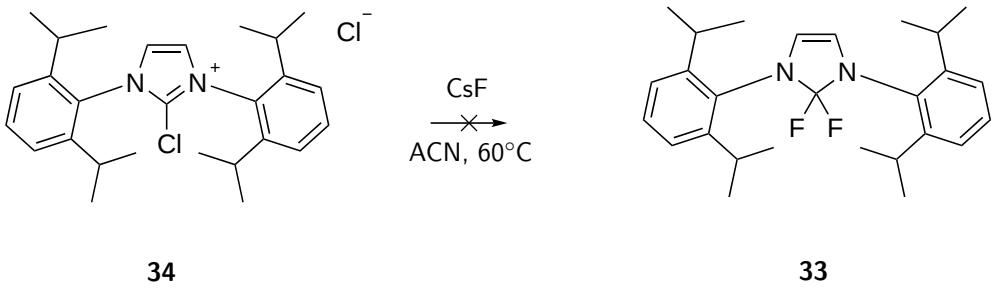

34 **33**

Scheme 27: Substitution with fluorine to the final product

Satisfyingly, the reaction gave 72% yield and good ^{1}H and ^{13}C NMR spectra which were in accordance with the literature values. Also the MS spectra corresponded to the expectations. The ^{19}F NMR spectrum, however, gave no peaks but broad curves representing the baseline, indicating that there was no fluorine present to give any peaks.

A general problem with this fluorination compound is its propensity to hydrolysis. Upon contact with water the difluoromethylene moiety is converted to an oxo group releasing two equivalents of HF (Scheme 28). This irreversible reaction results in the urea derivative **40** which is not applicable in a fluorination reaction. Since no protons are in close proximity to the site of hydrolysis, ^{1}H NMR spectra do not give a hint whether the product has hydrolyzed. The C^{2} shift differed from the reported literature values, yet literature values were not always completely consistent regarding the exact shift. MS showed a peak at m/z 427.3 which is about where the H^{+} peak would be expected. However, the hydrolyzed product with a weight of 404.6 would have a Na^{+} peak in the same region. Additionally, a peak at 405.3 was visible, corresponding to the protonated molecule **40**. On first glance the synthesis was thought to have worked due to the MS peak in the expected area and the fitting ^{1}H spectrum. The ^{19}F spectrum, however, proved the absence of fluorine and therefore the failure of the synthesis. Once hydrolysis was recognized as the cause, measures were taken to avoid water induced decay. Especially in the case of CsF drying is of the utmost importance as this substance is highly hygroscopic.

Drying of CsF in the furnace at 200°C for 65 hours proved to be insufficient. It was then switched to a heating mantle at full power (according to data sheets[123] heating mantles can reach temperatures of 450°C and more) combined with an oil pump that reached 0.18 Torr. 24 hours of drying with this method baked the CsF to a hard brick difficult to break up.
To ensure dry conditions the reaction vessel was prepared in an argon filled glovebox. In preparation all nec-

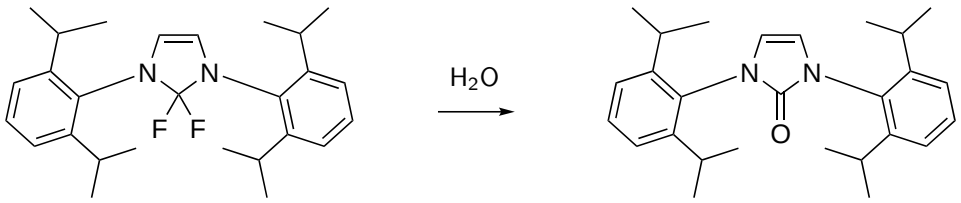

Scheme 28: Hydrolysis of PhenoFluor

essary tools were dried in the furnace at 100°C for 72 hours. In the glovebox CsF was ground and weighed in, along with the substrate dried *in vacuo*. The flask was sealed with a septum before removing it from the box. Dry toluene was injected via a syringe. ^{19}F NMR again showed no peaks. The possibility of the NMR solvent $CDCl_3$ being wet and thereby destroying the molecule during the NMR spectroscopy was excluded by drying $CDCl_3$ over an alox (activity level I) column twice and adding new 4Å molsieve.

An alternative for fluorination with PhenoFluor was published by the same group[120] which described the very same fluorination reaction but with the penultimate intermediate product in stead of the last (Scheme 29).

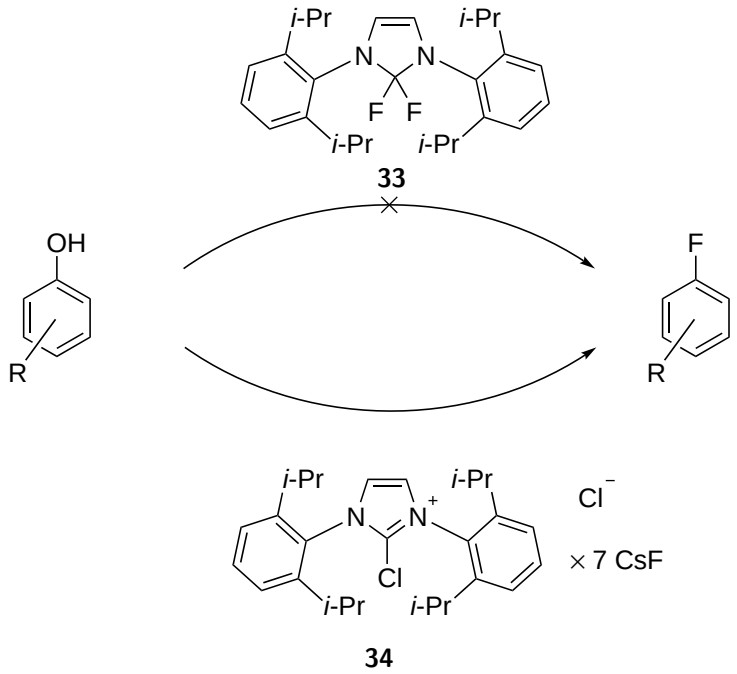

Scheme 29: Alternative with PhenoFluorMix

The major advantage of this strategy is its insensitivity to water. While the original fluorination agent is destroyed irreversibly by water the new one may become wet and can still be dehydrated without loss of the compound. The denomination "PhenoFluorMix" results from a readily useable mixture of the imidazolium salt **34** and CsF. Precisely, the mixture consists of 1 eq. PhenoFluorMix and 7 eq. CsF. The two components were combined, thoroughly mixed and dried for 2 hours at 140°C and 0.18 Torr. Subsequently this mixture was applied for the fluorination of *p*-aminophenol **41a** and *p*-nitrophenol **41b**.
As expected the ^{1}H NMR spectra of the products showed peaks of both benzene derivatives and PhenoFluor. ^{19}F NMR was again used to check for fluorinated product. While in the case of the amino-substituted phenol no product could be obtained, there was a small peak in the case of the nitro-substituted compound. To exclude

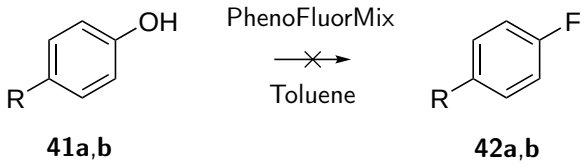

41a,**b** **42a**,**b**

41a, **42a**: R = NH_2; **41b**, **42b**: R = NO_2

Scheme 30: Fluorination with PhenoFluorMix

the possibility of the product getting lost during evaporation of the solvent (although the boiling points of 180-200°C are actually too high to make this seem plausible) a reaction vessel was left open for two days in the fume hood after the reaction in order to allow the solvent to evaporate without reduced pressure. The peak for the nitro-compound became slightly taller but there was still none for the amino-compound.

7 Mechanism of the fluorination

In general nucleophilic substitution reactions in aromatic systems take place via two main pathways: either an elimination-addition sequence with an aryne intermediate or an addition-elimination route.[124] The most characteristic feature of a substitution with an aryne intermediate is the loss of regiospecificity, leading to either substitution in the *ipso* or in the *ortho* position (Figure 11).

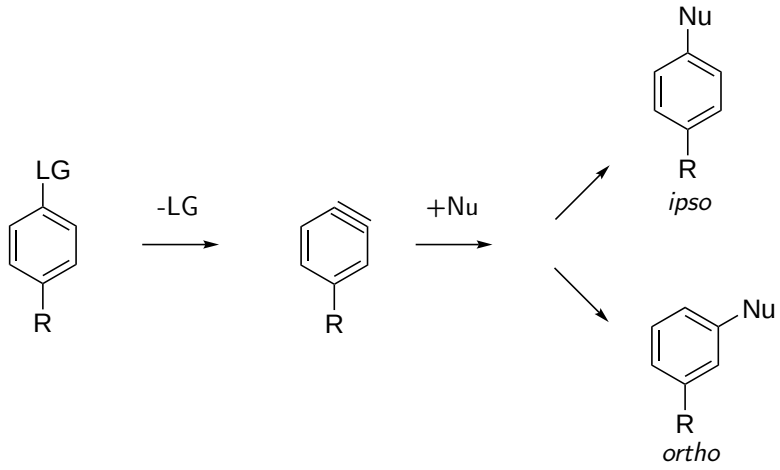

Figure 11: Loss of regiospecificity via arynes

As fluorination reactions with PhenoFluor and PhenoFluorMix do not result in product mixtures the aryne pathway is discarded as a plausible mechanism. Addition-elimination pathways can be further distinguished in two-step processes with a Meisenheimer's complex intermediate (Figure 12) and a concerted one-step mechanism (Figure 13).

In both pathways the electron density is increased in the ring system which accounts for nucleophilic reactions to work better with electron poor systems. This effect is more pronounced in the two-step mechanism since there is an actual negative charge that is distributed throughout the system while a concerted process only gives rise to a partial charge δ-. DFT calculations[125] further support the one-step mechanism for this reaction. The overall substitution consists of two separate reactions that can be done in a one-pot onset or with intermediate workup. First comes the linkage between the phenolic compound and the fluorination agent, resulting in an uronium salt (Figure 14), followed by the actual substitution.

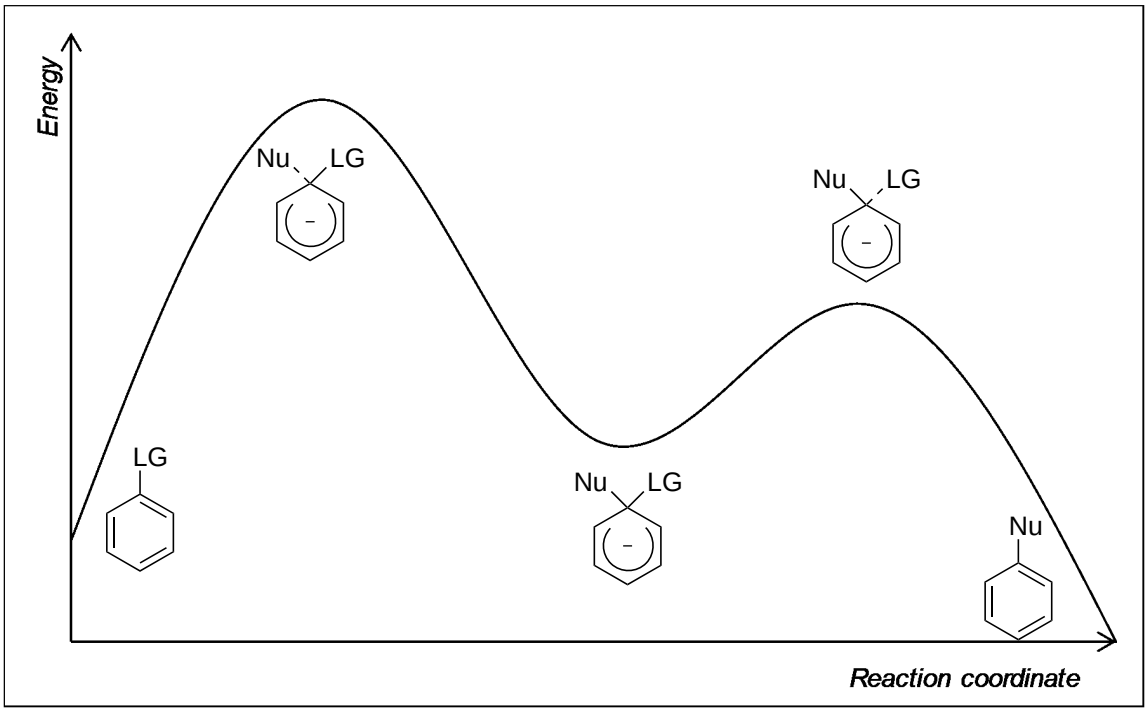

Figure 12: Two-step mechanism of S_NAr reactions

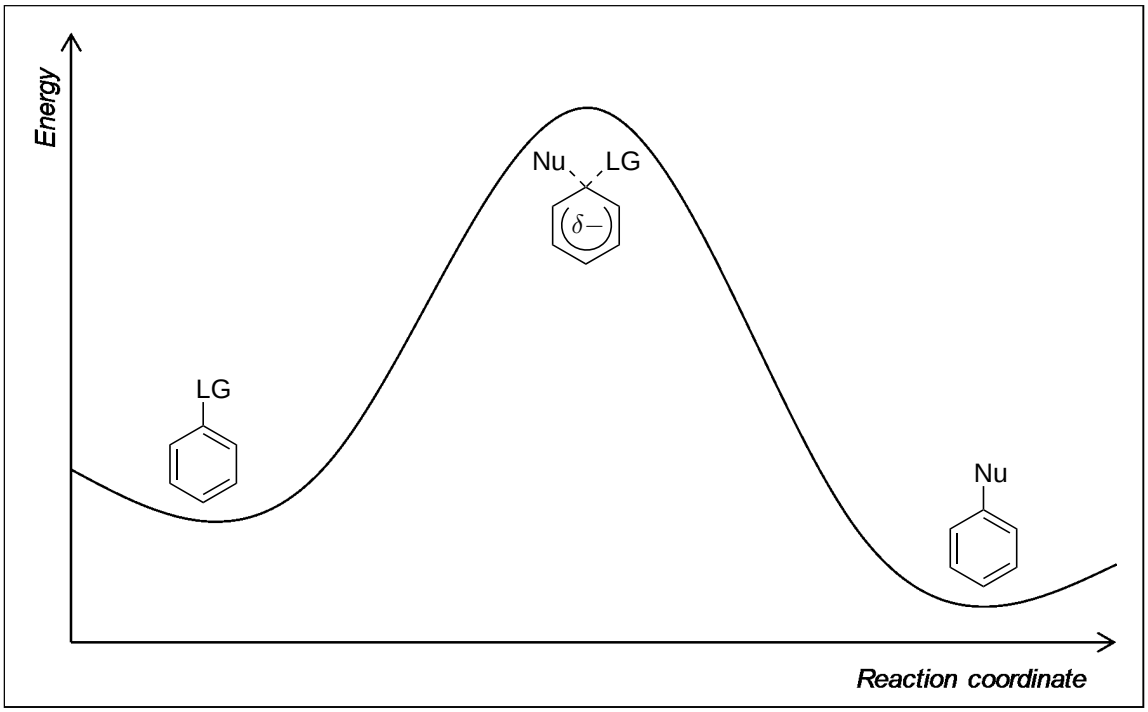

Figure 13: One-step mechanism of S_NAr reactions

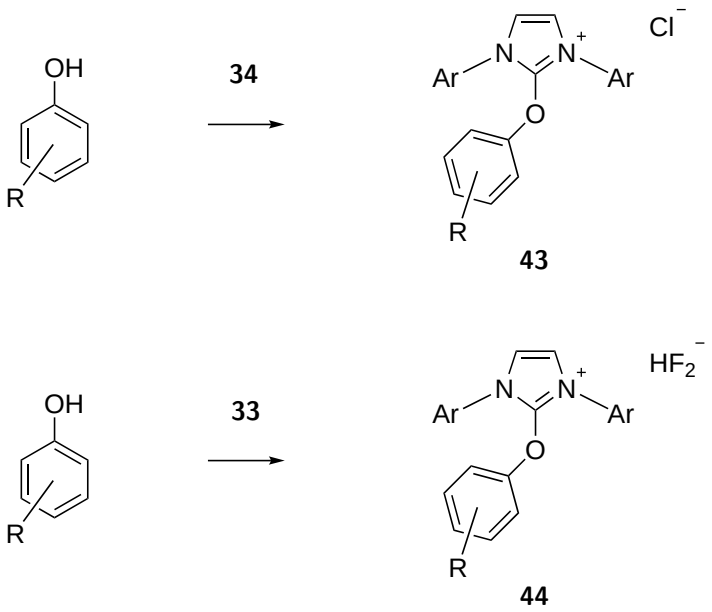

Figure 14: Formation of the uronium salts

Although Fujimoto and Ritter state that the subsequent fluorination using PhenoFluorMix does not proceed via *in situ* formation of PhenoFluor **33** prior to the actual fluorination since they did not find any evidence for the presence of PhenoFluor, I do not go along with this opinion. The reason for this lies in the results obtained for attempted incorporation of ^{18}F. After separate synthesis of the uronium chloride **43** they tried to convert it to the final flourinated compound using external fluoride sources, yet without success. Also with other counterions like OTf, PF_6 and even $H^{19}F_2^-$ no labeling with ^{18}F could be achieved. They explained this by the "lack of anion exchange" between the counterions and ^{18}F in solution. Only after treatment with an ion-exchange cartridge yield could be obtained (Figure 15). Therefore, the *in situ* formation of PhenoFluor from PhenoFluorMix is necessary since a direct reaction between PhenoFluorMix **34** would result in a chloride counterion, a salt that has been proven to be unreactive when synthesized separately.

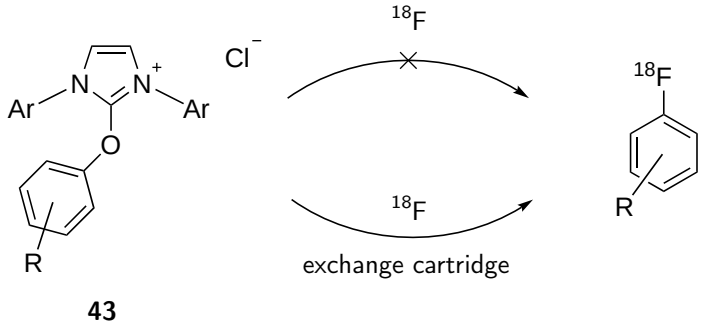

Figure 15: An anion exchange cartridge is necessary to obtain products

Uronium bifluoride **44** is in equilibrium with its corresponding dihydroimidazole **45**, the latter being the actual fluorination agent (Figure 16) in a 4-membered transition state (Figure 17).
The question whether the fluoride in the product stems from PhenoFluor or from CsF can be answered by using labeled fluorides. When ^{19}F PhenoFluor is used with $^{18}F^-$ no radiolabeled products are observed. Thus, the incorporated fluoride's source is PhenoFluor. To achieve labeling with ^{18}F an ion exchange must be accomplished. As already mentioned, this requires an ion exchange cartridge loaded with the desired counterion. After a successful ion exchange fluorination proceeds as described above. Yet the cation plays also a role.

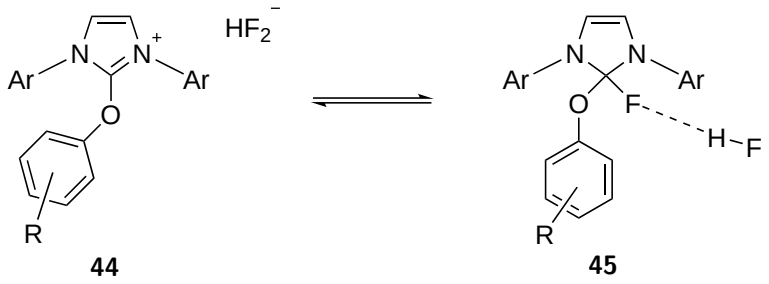

Figure 16: Equilibrium between uronium bifluoride **44** and its corresponding imidazole **45**

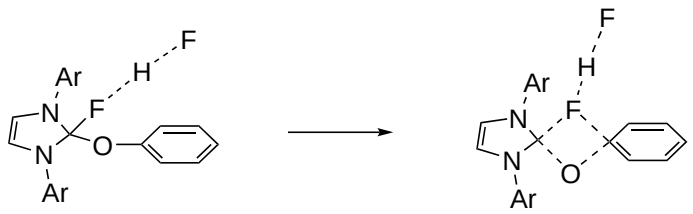

Figure 17: Transition state of the fluorination

Other fluorides ($KF, Lif, AgF, ZnF_2, NMe_4F, Bu_4N\,Ph_3SiF_2$) showed a maximum of 9% yield in the fluorination of 4-methoxyphenol while CsF yielded 82%. "The role of added CsF likely consists in abstracting HF from the bifluoride counteranion of the uronium intermediate to facilitate the formation of the tetrahedral adduct **45**."[125]

8 Conclusion

The synthesis of the fluorination agent worked decently save for the final fluorination step. The most apparent reason would be the presence of moisture despite the described measures to keep the reaction environment as dry as possible. As explained above, an in-situ formation of PhenoFluor **33** is likely even when using PhenoFluorMix which makes both varieties sensitive for moisture. Apart from the fluorinating agent another source of error are the substrates for the fluorination. However, NMR spectra of the phenol derivatives **41a**,**b** were in accordance with the literature. Therefore no evident reason for the failure of this reaction can be presented. In the case of separate synthesis of uronium chlorides **43**, products only would have been possible when using an ion exchange chromatography. As this was not available no products were to be expected from this approach.

Part IV

Experimental section

GKM001 - Diethyl 2-(hydroxyimino)malonate 2

8.4 mL diethyl malonate (1 eq., 0.05 mol, 8 g) were added dropwise to 10 mL glacial acetic acid while stirring. 6,9 g (2 eq., 0.1 mol) $NaNO_2$ were dissolved in water and added via a dropping funnel. Formation of brown fumes was observed. After stirring overnight the color had changed from yellow to almost colorless. The solution was diluted with the same volume of Et_2O and washed with saturated aqueous solutions of $NaHCO_3$/NaCl 1:1 until the aqueous phase reached a pH of 8, whereupon the solution acquired a yellowish hue. After drying with $MgSO_4$ and filtration through organic cotton the solvent was removed by rotary evaporation, followed by final drying *in vacuo*.
Colorless oil
NMR: 4Nov2018 470
No product was obtained. In the used literature no base was mentioned, this reaction, however, seems to require alkaline conditions.

GKM002 - (1*E*,2*E*)-N^1,N^2-bis(2,6-diisopropylphenyl)ethane-1,2-diimine 37

0.2 mL glacial acetic acid were diluted with 1.8 mL water. Thereof 0.4 mL were mixed with 10 mL methanol and 7.54 mL (2 eq., 40 mmol, 7.09 g) 2,6-diisopropylanilin (which displayed a dark brown color) and heated to 50°C. 1.4 g glyoxal (as trimer × 2 H_2O, 1 eq., 20 mmol) were taken up in 10 mL methanol and added to the reaction mixture. The solution was stirred at 50°C for 15 minutes (turns orange) and at RT overnight. Seemingly, the amount of solvent was too little which caused the solution to turn into an inhomogeneous ocher/yellow solid. A small amount of methanol was added and stirring was continued for another 2.5 hours. TLC (PE/EtOAc 1:1) indicated completion of the reaction. After filtration through a P2 glass frit and rinsing with methanol the residue was transferred to a flask and dried *in vacuo*.
Yield: 4.93 g (66%)
Fine yellow powder
NMR: 4Nov2018 491
^{1}H NMR (400 MHz, $CDCl_3$): δ 8.1 (2H, s), 7.22-7.12 (6H, m), 2.94 (4H, sept, J=6.9 Hz), 1.21 (24H, d, J=6.9 Hz)

GKM003 - 1,3-bis(2,6-diisopropylphenyl)-1*H*-imidazol-3-ium chloride 39

1.16 g (1 eq., 3.1 mmol) (1*E*,2*E*)-N^1,N^2-bis(2,6-diisopropylphenyl)ethane-1,2-diimine (product of GKM002) and 0.22 g (2.48 eq., 7.42 mmol) paraformaldehyde were dissolved in 30 mL EtOAc and heated to 70°C. Under vigorous stirring a solution of 0.4 mL (1 eq,. 3.1 mmol, 0.34 g) TMSCl in 1 mL EtOAc was added in portions using a syringe. After stirring at 70°C for 2 hours the reaction mixture was cooled in a waterbath and left to stand overnight. It was filtered through a P2 glass frit. The residue was rinsed three times with EtOAc, transferred to a flask and dried *in vacuo*.
Yield: 1.16 g (91%)
Off-white powder
NMR: 4Nov2118 660, see GKM052

GKM004 - Diethyl 2-aminomalonate 3

0.1 g diethyl 2-(hydroxyimino)malonate were dissolved in 10 mL ethanol and hydrogenated with H-Cube (CatCart™ Pd(II)EnCat_30 (Product ID: THS 05111), 10 bar, 1 mL/min). Comparison by TLC (PE/EtOAc 1:1) with the educt showed no reaction. Apparently this catalyst, handed out by a colleague, is not suitable for

hydrogenation reactions.

GKM005 - Diethyl 2-(hydroxyimino)malonate 2

0.8 g (0.66 eq., 0.02 mol) NaOH were dissolved in 6 mL glacial acetic acid under stirring and cooled to 0°C. A solution of 4.6 mL (1 eq., 0.03 mol, 4.81 g) diethyl malonate in 2 mL glacial acetic acid was added dropwise within 3 minutes. 4.35 g (2.1 eq., 0.063 mol) $NaNO_2$ were dissolved in 35 mL water, cooled to 0°C and added dropwise over the course of 1 hour. Afterwards the flask was fitted with a septum and an empty balloon. The reaction mixture was stirred at RT for 18 hours. When septum and balloon were removed, formation of brown fumes was observed. The solution was saturated with NaCl and extracted three times with approximately the same volume of EtOAc. The united organic phases were washed with saturated aqueous solutions of $NaHCO_3$ sat./brine 1:1 until the aqueous phase reached a pH of 7-8. After drying with $MgSO_4$ and filtration through organic cotton the solvent was removed by rotary evaporation, followed by final drying *in vacuo*.
Slightly yellow oil
NMR: 4Nov2218 570
By comparing peak integrations of the ^{1}H NMR a yield of 21% was calculated.
The crude product was purified by column chromatography with silica gel and PE/EtOAc 3:1 as a mobile phase (R_f: 0.56 in PE/EtOAc 1:1).
Yield: 1.108 g (20%)
NMR: 4Nov2718 340
^{1}H NMR (400 MHz, $CDCl_3$): δ 9.63 (1H, br s), 4,38 (4H, dq, J=18.5 Hz, 7.14 Hz), 1.36 (6H, dt, J=7.1 Hz, 7.1 Hz)

GKM006 - 2-chloro-1,3-bis(2,6-diisopropylphenyl)-1*H*-imidazol-3-ium chloride 34

1.16 g (1 eq., 2.7 mmol) 1,3-bis(2,6-diisopropylphenyl)-1*H*-imidazol-3-ium chloride was suspended in 6 mL THF. 0.37 g (1.2 eq., 3.25 mmol) KO*t*Bu were added whereupon the solution turned orange. After stirring at RT for 4 hours the reaction mixture was cooled to -40°C with dry ice in acetone. 0.85 g (1.33 eq., 3.6 mmol) hexachloroethane were added and stirring was continued for 24 hours at RT. The now yellow solution was again cooled to -40°C and filtered through a P2 glass frit. The residue was rinsed with -20°C cold THF and toluene before suspending it in DCM and filtering it once more. The solvent was removed by rotary evaporation and the product was dried *in vacuo*.
Yield: 0.16 g (12%)
NMR: 4Nov2618 140, see GKM029

GKM007 - Diethyl 2-aminomalonate 3

The reaction was performed as in GKM004. Comparison by TLC (PE/EtOAc 2:1) with the educt showed no reaction.

GKM008 - Diethyl 2-aminomalonate 3

1 g diethyl 2-(hydroxyimino)malonate were dissolved in 100 mL ethanol. The reaction was performed as in GKM004. Comparison by TLC (PE/EtOAc 2:1) with the educt showed no reaction.

NMR: 4Nov2818 630

GKM009 - Diethyl 2-acetamidomalonate 4

0.94 g (1 eq., 5.34 mmol) diethyl 2-aminomalonate were provided in 80 mL DCM. 2.22 mL (3 eq., 16 mmol, 1.62 g) NEt_3 were added, the mixture was cooled to 0°C and 0.4 mL (1 eq., 5.34 mmol, 0.42 g) acetyl chloride were added. The ice bath was removed and stirring was continued for 18 hours. The reaction mixture was diluted with DCM and washed with HCl 1M. The aqueous phase was reextracted with DCM once. The combined organic phases were dried with $MgSO_4$ which was then removed by filtration. After removal of the solvent the product was dried *in vacuo*.
The reaction was discarded as no educt was present.

GKM010 - Diethyl 2-acetamido-2-(3-oxopropyl)malonate 6

1.13 g (1 eq., 5.2 mmol) diethyl 2-acetamidomalonate were dissolved in 100 mL dry DCM and stirred. 0.8 mL (1 eq., 5.2 mmol) 1,8-diazabicyclo[5.4.0]undec-7-ene (DBU) and 0.52 mL (1.5 eq., 7.8 mmol, 0.44 g) acrolein were added and stirring was continued for 24 hours. Afterwards the solution was stripped of the solvent and dried *in vacuo*.
Brown, very viscous liquid
NMR:
4Dec0418 310 ^{1}H
4Dec0418 311 ^{13}C
Peaks do not match literature values

GKM011 - Diethyl 2-(hydroxyimino)malonate 2

The reaction was performed as in GKM005 except for grinding the NaOH before dissolving.
Colorless liquid.
According to NMR a yield of 21% was calculated. The crude product was purified by column chromatography with silica gel and PE/EtOAc 3:1 as a mobile phase.
Yield: 1.16 g (20%)
NMR: 4Dec0618 280, see GKM005

GKM012 - Diethyl 2-aminomalonate 3

1.16 g diethyl 2-(hydroxyimino)malonate were dissolved in 100 mL ethanol. The reaction was performed as in GKM004. NMR and MS data did not comply with literature values of the desired product but rather with the educt.
NMR: 4Dec1018 210
Mass Spectrometry: ESI-ion trap (*m/z*): Calcd for $[C_7H_{13}NO_4+H]^+$, 176.08. Found: -.
D:\DATA\MS_Service_MSC\61283_GKM012_hct.d
For further hydrogenations the catalyst was changed.
Product was used as educt for GKM014.

GKM013 - Diethyl 2-acetamidomalonate 4

0.53 g (1 eq., 3 mmol) diethyl 2-aminomalonate were dissolved in 130 mL dry THF and cooled to 0°C. 0.7 mL (4 eq., 12 mmol, 0.72 g) glacial acetic acid and 2.48 g (4 eq., 12 mmol) *N,N'*-dicyclohexylcarbodiimide (DCC) in portions were added and warmed to RT.
The reaction was discarded as no educt was present.

GKM014 - Diethyl 2-aminomalonate 3

0.44 g (2.35 mmol) diethyl 2-(hydroxyimino)malonate were dissolved in 50 mL ethanol and hydrogenated with H-Cube (CatCart® 10% Pd/C (Product ID: THS 01111), 20 bar, 1 mL/min). The solvent was then removed and the product was dried *in vacuo*.
Yield: 0.36 g (88%)
Colorless, slightly viscous liquid
NMR: 4Dec1218 360
^{1}H NMR (400 MHz, $CDCl_3$): δ 4.25 (4H, q, J=7.1 Hz), 4.17 (1H, s), 1.97 (2H, s br), 1.29 (6H, t, J=7.1 Hz)

GKM015 - Diethyl 2-(hydroxyimino)malonate 2

The reaction was performed as in GKM005 except for replacing NaOH by NaOAc and using argon atmosphere, resulting in 4.32 g of crude product.
NMR indicated a yield of 13%.
The product was used as educt for GKM017 without prior purification.
NMR: 4Dec1218 480, see GKM005

GKM016 - Diethyl 2-acetamidomalonate 4

0.36 g (1 eq., 2 mmol) diethyl 2-aminomalonate
0.83 mL (3 eq., 6 mmol, 0,61 g) triethylamine
0.16 mL (1.1 eq., 2,2 mmol, 0.17 g) acetyl chloride
30 mL DCM
The reaction was performed as in GKM009.
Yield: 0.34 g (73%)
Ocher solid
NMR: 4Dec1318 690, see GKM035
Used in GKM018 without purification

GKM017 - Diethyl 2-(hydroxyimino)malonate 2

0.6 g (0.66 eq., 15 mmol) NaOH in 4.5 mL glacial acetic acid
3.5 mL (1 eq., 22.4 mmol) diethyl malonate in 2 mL glacial acetic acid
3.1 g (2 eq., 44.8 mmol) $NaNO_2$ in 25 mL water
The reaction was performed as in GKM011 except for stirring at 55°C and using an argon atmosphere, resulting in 3.98 g of a slightly yellow, viscous oil.
NMR: 4Dec1718 150, see GKM005
NMR indicated a purity of 77%, thus resulting in a yield of 72%.

The crude product, combined with the product of GKM019, was purified twice with column chromatography (silica gel and PE/EtOAc 3:1) to give pure product (according to TLC). The combined yield was not determined.

GKM018 - Diethyl 2-acetamido-2-(3-oxopropyl)malonate 6

Preparation of sodium ethanolate A three-necked flask was evacuated, baked out and filled with argon. This was done three times in a row. To a small amount of PE were given 0.17 g (7.3 mmol) sodium. The PE was removed through a septum and the piece of sodium was rinsed five times with 5 mL PE before 5 mL ethanol were added.

Addition to acrolein 0.34 g (1 eq., 1.6 mmol) diethyl 2-acetamidomalonate were dissolved in 2.8 mL EtOH which was then evaporated again almost completely. 0.08 mL of the 2M NaOEt solution were added and the mixture was cooled to 0°C. 0.13 mL acrolein (1.2 eq, 1.92 mmol, 0.11 g) were added dropwise over 1 minute, giving a yellow solution. This mixture was stirred overnight and subsequently quenched with 0.15 mL AcOH. It was extracted with H_2O and the aqueous phase was reextracted with EtOAc. The combined organic phases were tried to dry with $MgSO_4$ which resulted in wet lumps regardless of the amount of added $MgSO_4$. The solution was filtered and the solvent was evaporated before the product was dried *in vacuo* resulting in 0.43 g of a yellow, viscous liquid.
NMR:
4Dec1818 130 ^{1}H
4Dec1818 131 ^{13}C
In the ^{1}H NMR hardly any aldehyde could be seen.

GKM019 - Diethyl 2-(hydroxyimino)malonate 2

The reaction was performed as in GKM011 except for stirring at 55°C and using an argon atmosphere, resulting in 3.2 g crude product.
NMR: 4Dec1818 170, see GKM005
NMR indicated a purity of 46%, resulting in a total yield of 26%.
The product was combined with GKM017 and subjected to chromatography twice (silica gel and PE/EtOAc 3:1) to give pure product (according to TLC). The combined yield was not determined.

GKM020 - Diethyl 2-aminomalonate 3

The combined products of GKM017 and GKM019 (not weighed) were taken up in 120 mL ethanol. The hydrogenation was performed as in GKM014.
Yield: 4.27 g
Viscous, yellow liquid

GKM021 - Diethyl 2-acetamidomalonate 4

2.1 g (1 eq., 12 mmol) diethyl 2-aminomalonate
5 mL (3 eq., 36 mmol) NEt_3
0.94 mL (1.1 eq., 13.2 mmol) AcCl

180 mL DCM
The reaction was performed as in GKM009.
NMR: 4Jan0819 380
TLC (PE/EtOAc 4:1) indicated a product mixture. A chromatography was done (silica gel and PE/EtOAc 4:1) which resulted in a very poor separation of two spots. It was then tried to protonate the alleged educt with HCl 0.1 mM at pH 4 and extract the unprotonated product with DCM which turned out not the be successful. It was then tried at pH 2 with HCl 10 mM to the same result. To separate the two spots another chromatography was performed with a column twice as long. Separation was bad again, however at least four pure fractions could be obtained which were freed of the solvent by rotary evaporation and dried *in vacuo*.
The yield was not determined as there was hardly any product.
NMR: 4Jan1019 240
Mass Spectrometry: ESI-ion trap (*m/z*): Calcd for $[C_9H_{15}NO_5+H]^+$, 218.10. Found: -.
D:\Data\MS_MessService\61628_GK11021_amazon.d
No product peak.

GKM022 - 1,3-bis(2,6-diisopropylphenyl)-2,2-difluoro-2,3-dihydro-1*H*-imidazole - PhenoFluor 33

0.16 g (1 eq., 0.34 mmol) 2-chloro-1,3-bis(2,6-diisopropylphenyl)-1*H*-imidazol-3-ium chloride were dissolved in 9 mL anhydrous ACN. 0.2 g (4 eq., 1.35 mmol) CsF were added and the mixture was heated to 60°C. After 22 hours it had become a light brown solution which was cooled after completing 24 hours reaction time and freed of the solvent by rotary evaporation. The residue was taken up in toluene, filtered through a P3 glass frit and rinsed with toluene. The solvent was evaporated and the product dried *in vacuo*. After recording the NMR spectra the product was dissolved in 6 mL toluene (0.04 M) and stored under argon atmosphere in the fridge.
Light brown solid
NMR:
6Jan1419 50 ^{1}H
6Jan1419 51 ^{13}C
6Jan1419 52 ^{19}F
According to ^{19}F NMR no fluorocompounds were present in the product.

GKM023 - Diethyl 2-acetamidomalonate 4

0.5 g (1 eq., 2.8 mmol) diethyl 2-aminomalonate were dissolved in 20 mL DCM and 0.16 mL (1 eq., 2. mmol) AcOH. The flask was flushed with argon. 0.52 g (1.2 eq., 3.36 mmol) benzotriazol-1-ol (HOBt) and 0.65 g (1.2 eq., 3.36 mmol) 3-(ethyliminomethyleneamino)-*N*,*N*-dimethylpropan-1-amine (EDC) were added slowly. The flask was again flushed with argon before stirring the mixture for 25 hours. 10 mL EtOAc were added and the mixture was washed with 20 mL H_2O, $NaHCO_3$ aq. sat. and brine. The organic phase was dried with $MgSO_4$. The solvent was removed and the product was dried *in vacuo*.
NMR:
4Jan1519 730 ^{1}H
4Jan1519 731 ^{13}C
TLC (PE/EtOAc 2:1) indicated that there was still educt present.

A chromatography was done with silica gel and PE/EtOAc 6:1 as an eluent. No yield could be obtained.

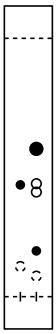

Figure 18: TLC of the crude product of GKM023, left: educt, right: product

GKM024 - 4-fluorobenzaldehyde

8.5 mg (1 eq., 0.07 mmol) *p*-hydroxybenzaldehyde was provided in a flask. 2 mL of the 0.04 M solution (1.1 eq., 0.08 mmol) of 1,3-bis(2,6-diisopropylphenyl)-2,2-difluoro-2,3-dihydro-1*H*-imidazole in toluene as well as 33 mg (3 eq., 2 mmol) CsF were added and stirred vigorously for 30 minutes. It was then heated to 80°C and stirred for another 3.5 hours. NMR was not possible due to the solvent not being deuterated. As the product is rather volatile, evaporation of the solvent was not an option. The experiment was discarded.

GKM025 - 4-fluoroaniline 42a

8 mg (1 eq., 0.07 mmol) *p*-hydroxyaniline was provided in a flask. 2 mL of the 0.04 M solution (1.1 eq., 0.08 mmol) of 1,3-bis(2,6-diisopropylphenyl)-2,2-difluoro-2,3-dihydro-1*H*-imidazole in toluene as well as 0.04 g (3 eq., 2 mmol) CsF were added and stirred vigorously for 30 minutes. It was then heated to 110°C and stirred for another 20 hours. NMR was not possible due to the solvent not being deuterated. As the product is rather volatile, evaporation of the solvent was not an option. The experiment was discarded.

GKM026 - 1-fluoro-4-nitrobenzene 42b

10 mg (1 eq., 0.07 mmol) *p*-nitrophenol were provided in a flask. 2 mL of the 0.04 M solution (1.1 eq., 0.08 mmol) of 1,3-bis(2,6-diisopropylphenyl)-2,2-difluoro-2,3-dihydro-1*H*-imidazole as well as 0.04 g (3 eq., 2 mmol) CsF were added and stirred vigorously for 30 minutes. It was then heated to 80°C and stirred for another 5 hours. It was then filtered through a frit and rinsed twice with 2 mL DCM before removing the solvent. The very small amount of product was not weighed. ^{19}F NMR indicated that no fluorine compounds were present.
NMR:
6Jan1819 80 ^{1}H
6Jan1819 81 ^{13}C
6Jan1819 82 ^{19}F

GKM027 - Diethyl 2-acetamidomalonate 4

Reaction setup as in GKM023 without argon atmosphere and with 1.5 eq. of HOBt and EDC. After 96 hours H_2O was added whereupon a white jelly formed. EtOAc was added and the phases were separated. The jelly remained in the aqueous phase. The organic phase was washed with $NaHCO_3$ aq. sat. and brine. TLC (PE/EtOAc 2:1) showed no product spot.

GKM028 - 1,3-bis(2,6-diisopropylphenyl)-1*H*-imidazol-3-ium chloride 39

2 g (1 eq., 5.3 mmol) (1*E*,2*E*)-N^1,N^2-bis(2,6-diisopropylphenyl)ethane-1,2-diimine
0.23 g (1.5 eq., 7.7 mmol) paraformaldehyde
0.7 mL (1.03 eq., 5.5 mmol) TMSCl
60 mL EtOAc
The reaction was performed as in GKM003.
Yield: 2.07 g (93%)
Fine beige powder
NMR: 4Jan2119 110, see GKM052

GKM029 - 2-chloro-1,3-bis(2,6-diisopropylphenyl)-1*H*-imidazol-3-ium chloride 34

0.5 g (1 eq., 1.2 mmol) 1,3-bis(2,6-diisopropylphenyl)-1*H*-imidazol-3-ium
0.16 g (1.2 eq., 1.4 mmol) KO*t*Bu
0.33 g (1.2 eq., 1.4 mmol) hexachloroethane
The reaction was performed as in GKM006 except for stirring for 195 minutes at RT before adding hexachloroethane and for 39 hours thereafter, and rinsing with 7 mL toluene.
Yield: 0.19 g (34%)
NMR: 4Jan2319 470
^{1}H NMR (400 MHz, DMSO-d_6): δ 8.85 (2H, s), 7.75 (2H, t, J=7.8 Hz), 7.60 (4H, d, J=7.8 Hz), 2.28 (4H, sept, J=6.7 Hz), 1.23 (24H, dd, J=28.4 Hz, J=6.8 Hz)

GKM030 - Diethyl 2-acetamidomalonate 4

0.56 g (1 eq., 3.2 mmol) diethyl 2-aminomalonate were dissolved in 10 mL DCM and cooled to 0°C. 1.33 mL (3 eq., 9.6 mmol) NEt_3 and 0.33 mL (1.1 eq., 3.5 mmol) Ac_2O were added. The mixture was stirred overnight at RT. TLC (PE/EtOAc 2:1) still indicated educt. 0.5 mL Ac_2O were added and stirred for further 2 hours. The solution was washed twice with 10 mL brine and dried with $MgSO_4$ before removing the solvent and drying the residue *in vacuo*.
NMR: 4Jan2319 90
No signal for a −CH− group could be detected.

GKM031 - Diethyl 2-acetamidomalonate 4

3.86 mL (1 eq., 25 mmol) diethyl malonate were provided in a flask. 7.2 mL (3 eq., 76 mmol) acetic anhydride and 2.3 g (1.3 eq., 33 mmol) $NaNO_2$ were added and the solution was cooled to -40°C. 2.55 mL (1.8 eq., 45 mmol) AcOH were added dropwise. The reaction mixture was warmed to 50°C and stirred for 4 hours. After cooling to RT a white jelly had formed. The suspension was filtered twice through a glass frit and rinsed twice respectively with 8 mL Et_2O. The filtrate was subjected to hydrogenation in the H-Cube but no sufficient pressure could be reached. The hydrogenation was then done with a Parr apparatus. 0.35 g Pd/C 10% were added and hydrogenated at 4.5 bar at RT for 4.5 hours. The catalyst was removed by filtration through celite before evaporating the solvent resulting in 4.68 g of a yellow oil.
NMR: 4Feb0119 420
No signal for a −CH− group could be detected.

GKM032 - 2-chloro-1,3-bis(2,6-diisopropylphenyl)-1*H*-imidazol-3-ium chloride 34

The reaction was performed as in GKM029 except for stirring for 255 minutes at RT before adding 1.5 eq. hexachloroethane at 0°C and for 36 hours thereafter, cooling to -78°C before rinsing with the mother liquor and 7 mL cold (-78°C) THF.
Yield: 0.09 g (16%)
NMR: 4Jan2519 320, see GKM029

GKM033 - Diethyl 2-aminomalonate 3

0.73 g (0.66 eq., 18 mmol) NaOH in 4.5 mL AcOH
4.21 mL (1 eq., 28 mmol) diethyl malonate in 2 mL AcOH
3.9 g (2 eq., 55 mmol) $NaNO_2$ in 30 mL H_2O
The reaction was performed as in GKM019 resulting in 3.87 g crude product. NMR indicated a purity of 71%. The crude product was dissolved in PE/EtOAc 3:1 and a few drops of DCM and subjected to chromatography with silica gel and PE/EtOAc 3:1 as a solvent.
Diethyl 2-(hydroxyimino)malonate: 2.41 g (46%)
NMR: 4Jan2919 461, see GKM005
The product was dissolved in 130 mL ethanol and subsequently hydrogenated as in GKM014.
Yield: 2.2 g (45%)
NMR: 4Jan2919 470, see GKM014

GKM034 - 2-chloro-1,3-bis(2,6-diisopropylphenyl)-1*H*-imidazol-3-ium chloride 34

The reaction was performed as in GKM029. It was stirred for 4 hours at RT before adding 2 eq. hexachloroethane at RT. Thereafter it was stirred 2 hours at RT before stirring it at 50°C overnight. Cooling to -78°C, rinsing with cold (-78°C) toluene. No product was obtained, the experiment was discarded.

GKM035 - Diethyl 2-acetamidomalonate 4

4.76 mL (1 eq., 30 mmol) diethyl malonate and 5.1 mL (3 eq., 91 mmol) AcOH were stirred with 8.3 mL H_2O at 0°C for 2 hours during which 10.32 g (5 eq., 149 mmol) $NaNO_2$ were added in portions, at RT for 1 hour and at 45°C overnight. The mixture was extracted twice with EtOAc. To the combined organic phases were added 7.86 mL (2 eq., 83.2 mmol) Ac_2O dropwise before heating the mixture to 50°C. 7.38 g (3.8 eq., 113 mmol) zinc powder were added in portions and stirring was continued for 18 hours. During the night pressure seemed to have been built up which had flung away the stopper. The reaction however had not run dry. The mixture was filtered through a glass frit and rinsed with 5 mL EtOAc and 2 × 5 mL AcOH. The solvent was removed and the product crystallized upon cooling.
Yield: 2.96 g (46%)
Yellow powder
NMR: 4Jan3019 900
^{1}H NMR (400 MHz, $CDCl_3$): δ 6.48 (1H, s br), 5.16 (1H, d, J=7.0 Hz), 4.27 (4H, m), 2.08 (3H, s), 1.30 (6H, t, J=7.2 Hz)

GKM036 - 2-chloro-1,3-bis(2,6-diisopropylphenyl)-1*H*-imidazol-3-ium chloride 34

The reaction was set up as in GKM029. After adding hexachloroethane stirring was continued overnight. Due to pressure the stopper was flung away and the reaction ran dry. 5 mL THF were added and stirring was continued for a total of 48 hours. The mixture was cooled to -78°C and filtered through a glass frit. The residue was rinsed with very little toluene at -78°C before it was transferred to a flask and dried *in vacuo*.
Yield: 0.23 g (41%)
NMR: 4Feb0119 430, see GKM029

GKM037 - Diethyl 2-acetamido-2-(3,3-dimethoxypropyl)malonate 8

0.11 g (1.03 eq., 2.4 mmol) of a 60% dispersion of NaH were washed with PE and taken up in 5 mL DMF. 0.5 g (1 eq., 2.3 mmol) diethyl 2-acetamidomalonate were dissolved in 5 mL DMF and added dropwise to the NaH solution. After foam formation subsided a septum equipped with a balloon was put on the flask. The reaction was stirred for 105 minutes at RT. 25 mg (0.03 eq., 0.069 mmol) tetrabutylammonium iodide (TBAI) and 0.42 g (1 eq., 2.3 mmo) 3-bromo-1,1-dimethoxypropane were added. Stirring continued for 92 hours after which the solution was diluted with 80 mL EtOAc. The organic phase was washed twice with each 8 mL H_2O and with 16 mL brine. Separation of the aqueous and organic phase was very slow. The organic phase was dried with $MgSO_4$. After removing the solvent the product was dried *in vacuo*.
NMR: 4Feb0519 80
NMR was not in accordance with literature values.

GKM038 - Diethyl 2-acetamido-2-(3,3-dimethoxypropyl)malonate 8

0.1 g (1 eq., 0.45 mmol) diethyl 2-acetamidomalonate, 0.11 mL (1.7 eq., 0.76 mmol) 3-bromo-1,1-dimethoxypropane, 0.3 g (2.03 eq., 0.91 mmol) Cs_2CO_3 and 0.03 g (0.4 eq., 0.18 mmol) NaI were suspended in 5 mL ACN and treated 2 ×10 minutes in the microwave at 130°C. After that the solution was filtered through a glass frit. The solvent was removed and the crude product dried *in vacuo*.
NMR: 4Feb0619 230
Oily brown liquid with a solid residue smelling like the acetal
The crude product was taken up in 5 mL EtOAc, filtered through a glass frit again and freed of the solvent by rotary evaporation followed by drying *in vacuo* .
NMR: 4Feb0619 520
TLC (PE/EtOAc 2:1) showed only 2 spots: one at the baseline, the other at the same R_f value as the educt. Since this R_f value is not plausible for the expected product the experiment was discarded.

GKM039 - 1,3-bis(2,6-diisopropylphenyl)-2,2-difluoro-2,3-dihydro-1*H*-imidazole - PhenoFluor 33

0.56 g (1 eq., 1.22 mmol) 2-chloro-1,3-bis(2,6-diisopropylphenyl)-1*H*-imidazol-3-ium chloride
9.5 mL anhydrous ACN
0.74 g (4 eq., 4.88 mmol) CsF
The reaction was performed as in GKM022. The product was stored in the fridge as a solution in 20 mL toluene.
NMR:
6Feb0819 60 ^{1}H
6Feb0819 61 ^{19}F

According to ^{19}F NMR no fluorinated compound is present.

GKM040 - Diethyl 2-acetamido-2-(3,3-dimethoxypropyl)malonate 8

0.5 g (1 eq., 2.3 mmol) diethyl 2-acetamidomalonate were provided in a flask flushed with argon. 1.6 mL anhydrous DMF and 0.26 g (1 eq., 2.3 mmol) KO*t*Bu in 0.85 mL were added. The mixture was heated to 80°C. 0.26 mL (0.83 eq., 1.91 mmol) 3-bromo-1,1-dimethoxypropane in 0.24 mL DMF were added. When the addition was done too quickly the solution started to fume. The reaction mixture was stirred overnight. After cooling to RT the solvent was removed. 4 mL each of EtOAc and H_2O were added. After separating the phases the organic phase was washed thrice with 3.3 mL NaCl aq. 10%. The organic solvent was evaporated, giving the crude product which was recrystallized from Et_2O and Et_2O/EtOAc.
NMR peaks do not match structure.

GKM041 - Diethyl 2-acetamido-2-(3,3-dimethoxypropyl)malonate 8

The reaction was performed as in GKM038 except for using the microwave apparatus for 40 minutes at 60°C.
NMR:
4Feb0719 360 (oily brown liquid)
4Feb0719 370 (light brown powdery residue)
NMR peaks do not match structure.

GKM042 - 3,4-dihydro-2*H*-pyrrole-2-carboxylic acid 9

0.13 g diethyl 2-acetamido-2-(3,3-dimethoxypropyl)malonate from GKM038 were suspended in 5 mL HCl 6N and heated in the microwave apparatus for 10 minutes at 90°C which resulted in a highly viscous dark brown lump. The experiment was discarded.

GKM043 - Diethyl 2-acetamido-2-(3,3-dimethoxypropyl)malonate 8

0.1 g (1 eq., 0.45 mmol) diethyl 2-acetamidomalonate, 0,06 mL (1 eq., 0.45 mmol) 3-bromo-1,1-dimethoxypropane, 0,29 g (2 eq., 0.9 mmol) Cs_2CO_3 and 0.7 g (1 eq., 0.45 mmol) NaI were suspended in 5 mL ACN and subsequently tried to microwave at 150°C which turned out not to be possible due to the pressure rising above the allowed limit. It was then heated in the microwave apparatus at 90°C for 30 minutes and at 90 W for 10 minutes. The mixture was then filtered through a glass frit and partially freed of the solvent by rotary evaporation. The precipitating residue was taken up in EtOAc and again filtered through a glass frit. After rinsing once with EtOAc the solvent was evaporated completely by rotary evaporation.
Oily brown substance
NMR: 4Feb0819 740
The TLC (DCM/MeOH 40:1) indicated a mixture of substances. A silica gel chromatography with the same eluent resulted in good separation yet the recovered material was not enough to be weighed.
NMR:
4Feb1419 640 (red spot)
4Feb0409 650 (blue spots)

Figure 19: TLC of the crude product of GKM043

GKM044 - 1-fluoro-4-nitrobenzene 42b

0.04 g (1 eq., 0.25 mmol) *p*-nitrophenol
6.6 mL solution of GKM039 (1.2 eq., 0.3 mmol)
0.11 g (3 eq., 0.75 mmol) CsF
The reaction was performed as in GKM026 except for using an argon atmosphere.
No product could be obtained.

GKM045 - Diethyl 2-acetamido-2-(3,3-dimethoxypropyl)malonate 8

The reaction was set up as in GKM041 and heated in the microwave apparatus at 130°C for 90 minutes. The mixture was then filtered through a glass frit and partially freed of the solvent by rotary evaporation. The precipitating residue was taken up in EtOAc and again filtered through a glass frit. After rinsing once with EtOAc the solvent was evaporated completely. Hardly any product could be obtained.
NMR: 4Feb1119 340

GKM046 - 3,4-dihydro-2*H*-pyrrole-2-carboxylic acid 9

Diethyl 2-acetamido-2-(3,3-dimethoxypropyl)malonate (product of GKM045, not weighed) was dissolved in 5 mL HCl 6N and refluxed for 25 minutes. After cooling to RT the solution was diluted with 32 mL $NaHCO_3$ aq. sat. and washed twice with EtOAc. The volume of the aqueous solution was reduced by evaporation on the magnetic stirrer. The precipitated solid was isolated by filtration and taken up in water. Absence of carbonate was checked by adding a drop of HCl 6N. The solution was transferred in a flask and freed of the solvent by rotary evaporation.
NMR: 4Feb1319 550
Peaks do not correspond to literature values.

GKM047 - 1,3-bis(2,6-diisopropylphenyl)-1*H*-imidazol-3-ium chloride 39

1.7 g (1 eq., 4.5 mmol) (1*E*,2*E*)-N^1,N^2-bis(2,6-diisopropylphenyl)ethane-1,2-diimine
0.14 mg (1.03 eq., 4.6 mmol) paraformaldehyde
0.59 mL (1.03 eq., 4.6 mmol) TMSCl
50 mL EtOAc
The reaction was performed as in GKM003, except that it was done under argon atmosphere and with cooling before filtration.

Yield: 1.65 g (86%)
Off-white powder
NMR: 4Feb2519 280, see GKM052

GKM048 - 2-chloro-1,3-bis(2,6-diisopropylphenyl)-1*H*-imidazol-3-ium chloride 34

The experiment was set up as in GKM036. After a total stirring time of 42 hours it was worked up and rinsed with cold (-78°C) toluene, transferred to a flask and dried on the rotary evaporator.
Yield: 0.9 g (50%)
Beige powder
NMR: 4Feb2819 340, see GKM029

GKM049 - ((Benzyloxy)carbonyl)glutamic acid 11

3 g (1 eq., 20.4 mmol) glutamic acid were suspended in 20 mL of a 4:6 mixture of NEt_3 and MeOH. The flask was flushed with argon and equipped with a septum and an argon balloon. 4 mL (1.4 eq., 28.5 mmol) Cbz-chloride were added dropwise. The pressure rose quickly enough to fling away the septum. Because a small amount of Cbz-chloride was spilt another 0.5 mL were added. After 3 hours of stirring the solvent was partly removed and the mixture was diluted with water. The solution was washed with Et_2O and saturated with NaCl before extracting it twice with EtOAc. The combined organic phases were dried with $MgSO_4$ and freed of the solvent by rotary evaporation. The crude product was purified by chromatography with silica gel and DCM/MeOH 20:1 as an eluent.
Yield: 2.38 g (41%)
NMR: 4Mar0819 870, see GKM054

GKM050 - 1,3-bis(2,6-diisopropylphenyl)-2,2-difluoro-2,3-dihydro-1*H*-imidazole - PhenoFluor 33

0.9 g (1 eq., 1.97 mmol) 2-chloro-1,3-bis(2,6-diisopropylphenyl)-1*H*-imidazol-3-ium chloride (product from GKM048)
1.2 g (4 eq., 7.88 mmol) CsF (dried for 24 hours at 0.18 Torr using a heating cap at full power).
15 mL anhydrous ACN
The reaction was performed as in GKM022 except for using an argon atmosphere.
NMR:
7Mar1319 60 ^{1}H
7Mar1319 61 ^{13}C
7Mar1319 62 ^{19}F
According to ^{19}F NMR no fluorinated compounds are present.

GKM051 - (1*E*,2*E*)-N^1,N^2-bis(2,6-diisopropylphenyl)ethane-1,2-diimine 37

7.54 mL (2 eq., 40 mmol) 2,6-diisopropylanilin and 0.4 mL (0.035 eq., 0.7 mmol) AcOH were provided in 10 mL MeOH. After heating to 50°C 1.4 g (1 eq., 20 mmol) glyoxal in 10 mL MeOH were added (the containing Erlenmeyer flask was flushed with addidtional 10 mL MeOH). The solution was stirred at 50°C for 20 minutes and for 20 hours at RT. Afterwards the mixture was filtered through a glass frit. The residue was rinsed with MeOH, transferred to a flask and dried on the rotary evaporator.

Yield: 5.55 g (74%)
Bright yellow powder
NMR: 4Mar1919 70, see GKM002

GKM052 - 1,3-bis(2,6-diisopropylphenyl)-1*H*-imidazol-3-ium chloride 39

5.55 g (1 eq., 14.7 mmol) (1*E*,2*E*)-N^1,N^2-bis(2,6-diisopropylphenyl)ethane-1,2-diimine
0.46 g (1.03 eq., 15.2 mmol) paraformaldehyde
1.94 mL (1.03 eq., 15.2 mmol) TMSCl
140 mL EtOAc
The reaction was performed as in GKM047.
Yield: 6 g (96%)
Off-white powder
NMR: 4Mar1919 560
^{1}H NMR (400 MHz, DMSO-d_6): δ 10.18 (1H, s), 8.56 (2H, s), 7.69 (2H, t, 7.8 Hz), 7.53 (4H, d, 7.8 Hz), 2.36 (4H, sept, J=6 Hz), 1.21 (24H, dd, J=40.3 Hz, J=6.8 Hz)

GKM053 - 2-chloro-1,3-bis(2,6-diisopropylphenyl)-1*H*-imidazol-3-ium chloride 34

The experiment was performed as in GKM048 with a total stirring time of 120 hours.
Yield: 4.38 g (68%)
NMR:
4Mar2519 580
4Jun1719 80, see GKM029

GKM054 - ((Benzyloxy)carbonyl)glutamic acid 11

3 g (1 eq., 20.4 mmol) glutamic acid were dissolved in 30 mL distilled water and cooled to 0°C. 6.5 g (3 eq., 61 mmol) Na_2CO_3 and 1.71 g (1 eq., 20.4 mmol) $NaHCO_3$ were added, followed by 3 mL acetone and then 6.4 mL (2.2 eq., 45 mmol) Cbz-chloride. The flask was equipped with a septum and an empty balloon and the mixture was stirred for 96 hours. After that the pH was lowered to 1-2 with HCl. The solution was extracted thrice with each 100 mL EtOAc. The combined organic phases were dried with $MgSO_4$. The solvent was evaporated to give colorless oil.
NMR: 4Mar2519 500
The crude product was purified by chromatography with silica gel and DCM/MeOH 20:1 as an eluent.
Yield: 3.78 g (66%)
Highly viscous oil crystallizing overnight in the fridge
NMR: 4Mar2619 530
^{1}H NMR (400 MHz, DMSO-d_6): δ 12.36 (2H, s br), 7.36 (5H, m), 5.03 (2H, s), 4.0 (1H, m), 2.3 (2H, m), 1.96 (1H, m), 1.76 (1H, m)

GKM055 - ((Benzyloxy)carbonyl)glycine 22

0.88 g (2.75 eq., 22 mmol) NaOH were dissolved in 20 mL distilled water and cooled to 0°C. 1 g (1 eq., 8 mmol) glycine methyl ester hydrochloride and 1.5 mL (1.3 eq., 10.5 mmol) Cbz-chloride in 10 mL dry dioxane were added. The solution was then stirred for 96 hours at RT. The pH was brought to 1 with HCl 3M before

extracting thrice with each 30 mL Et_2O. The combined organic phases were washed with brine and dried with $MgSO_4$. The solvent was removed by rotary evaporation. 26 mL MeOH and 14 mL THF were added and the solution was stirred for 1 hour at RT. The solvent was almost completely removed and 60 mL HCl 3M were added. The solution was extracte thrice with Et_2O. The combined organic phases were washed with brine and and dried with $MgSO_4$. The solvent was then removed again by rotary evaporation.
NMR: 4Mar2619 370
Colorless crystallizing oil
As the NMR indicated impurities the crude product was taken up in 5 mL ACN, heated to 70°C and filtered through a glass frit before removing the solvent.
Yield: 1.38 g (82%)
White solid
NMR: 4Mar2619 600, see GKM070

GKM056 - 3-(3-((benzyloxy)carbonyl)-5-oxooxazolidin-4-yl)propanoic acid 12

3.78 g (1 eq., 13.4 mmol) Z-Glu were suspended in 100 mL toluene. 0.81 g (2 eq., 26.9 mmol) paraformaldehyde and 0.15 g (0.06 eq., 0.8 mmol) *p*TsOH·H_2O were added and the reaction mixture was reluxed for 5 hours at 130°C bath temperature. After that 50 mL EtOAc were added. The solution was washed with brine and dried with $MgSO_4$ before the solvent was evaporated. TLC (PE/EtOAc 7:3) indicated impurities which were tried to remove by chromatography with silica gel and PE/EtOAc 7:3 as an eluent.
NMR: 4Apr0819 430
NMR data do not fit literature values.

GKM057 - benzyl 5-oxooxazolidine-3-carboxylate 23

1.38 g (1 eq., 6.6 mmol) Z-Gly (product from GKM055) were suspended in 15 mL toluene. 1 g (5 eq., 33 mmol) paraformaldehyde and 75 mg (0.06 eq., 0.4 mmol) *p*TsOH·H_2O were added. The reaction mixture was refluxed for 5 hours at 130°C bath temperature. The solvent was then evaporated.
NMR: 4Apr0819 420, see GKM071

GKM058 - ((Benzyloxy)carbonyl)glutamic acid 11

The reaction was performed as in GKM054.
Yield: 4.74 (83%)
Light brown ighly viscous oil crystallizing overnight
NMR: 4Apr0819 440, see GKM054

GKM059 - 1,3-bis(2,6-diisopropylphenyl)-2,2-difluoro-2,3-dihydro-1*H*-imidazole - PhenoFluor 33

2-chloro-1,3-bis(2,6-diisopropylphenyl)-1*H*-imidazol-3-ium chloride and dried CsF were brought into a glovebox filled with argon, alongside with a reaction flask, a spatula and a mortar which were all dried at 100°C for 72 hours in the oven. 1 g (1 eq., 2.2 mmol) 2-chloro-1,3-bis(2,6-diisopropylphenyl)-1*H*-imidazol-3-ium chloride and 3.3 g (10 eq., 22 mmol) finely ground CsF were put in the flask which was then sealed with a septum before it was removed from the glovebox. 8 mL dry toluene were added and the mixture was subjected to ultrasound for

40 minutes before stirring it at 100°C for 95 hours. After 75 hours another 3 mL toluene had been added. The product was separated by filtration through a glass frit and rinsed with dry toluene.
NMR:
6Apr1219 110 ^{1}H
6Apr1219 111 ^{13}C
6Apr1219 112 ^{19}F
According to ^{19}F NMR no fluorinated compounds were present. As the NMR solvent ($CDCl_3$) did not seem dry the molecular sieve (4Å) was exchanged and the chloroform was dried by passing it through a 25 cm long column filled with alox (activity level I). Still, thereafter no satisfying ^{19}F NMR could be recorded.

GKM060 - 3-(3-((benzyloxy)carbonyl)-5-oxooxazolidin-4-yl)propanoic acid 12

1 g (1 eq., 3.56 mmol) Z-Glu was suspended in 28 mL dry benzene. 0.23 g (2.1 eq., 7.48 mmol) paraformaldehyde and 40 mg (0.06 eq., 0.21 mmol) *p*TsOH·H_2O were added. The reaction mixture was stirred at 85°C bath temperature for 150 minutes.The solvent was evaporated and the crude product was dissolved in PE/EtOAc 7:3 and a few drops of DCM. The product was purified by chromatography with silica gel and PE/EtOAc as an eluent.
Yield: 0.66 g (63 %)
Colorless oil
NMR: 4Apr1119 100, see GKM061

GKM061 - 3-(3-((benzyloxy)carbonyl)-5-oxooxazolidin-4-yl)propanoic acid 12

1 g (1 eq., 3.56 mmol) Z-Glu was suspended in 50 mL toluene. 0.16 g (1.5 eq., 5.4 mmol) paraformaldehyde and 10 mg (1% w/w) *p*TsOH·H_2O were added. The flask was equipped with a Dean-Stark-apparatus filled with toluene. The reaction mixture was then heated for 3 hours to 110°C (bath temperature) which was apparently too cold for the vapor to reach the cooler. After standing on the bench for 5 days the crude product was purified by passing the solution through a short column (silica gel, 5 cm). The column had been packed with toluene, the product was then eluted with EtOAc.
Yield: 0.95 g (91%)
NMR: 4Apr2419 180
^{1}H NMR (400 MHz, $CDCl_3$): δ 7.40-7.34 (5H, m), 5.54 (1H, s br), 5.23 (1H, d, J=4.6 Hz), 5.19 (2H, s), 4.4 (1H, t, J=5.9 Hz), 2.51 (2H, s br), 2.32 (1H, m), 2.20 (2H, m)

GKM062 - 4-fluoroaniline 42a

PhenoFluorMix 3.3 g (1 eq., 7.2 mmol) 2-chloro-1,3-bis(2,6-diisopropylphenyl)-1*H*-imidazol-3-ium chloride (product of GKM053) were thoroughly mixed with 7.7 g (7 eq., 50.7 mmol) CsF and dried at 140°C and 0.18 Torr for 2 hours.

Fluorination 1 g (1.5 eq., 0.68 mmol) PhenoFluorMix was weighed into a three-necked flask equipped with a septum and two adapters with a valve and again dried at 140°C and 0.18 Torr. The flask was backfilled with argon before opening it and quickly adding 50 mg (1 eq., 0.45 mmol) *p*-aminophenol. The flask was evacuated and backfilled with argon again. 5 mL dry toluene were added through the septum and the reaction mixture was stirred at RT for 1 hour and at 110°C for 24 hours after which a black substance had formed. The product

was separated by filtration through a glass frit. The residue was rinsed thrice with each 4 mL DCM, transferred to a flask (flushing with 10 mL DCM) and dried on the rotary evaporator.
Brown crystals
NMR:
6Apr3019 40 ^{1}H
6Apr3019 41 ^{19}F
According to ^{19}F NMR no fluorinated compounds were present.

GKM063 - 1-fluoro-4-nitrobenzene 42b

1 g (1.5 eq., 0.68 mmol) PhenoFluorMix was weighed into a three-nekced flask equipped with a septum and two adapters with a valve and dried for 1 hour at 140°C and 0.18 Torr. The flask was backfilled with argon before openening it and quickly adding 63 mg (1 eq., 0.45 mmol) *p*-nitrophenol. The flask was evacuated and backfilled with argon again. 5 mL dry toluene were added through the septum and the reaction mixture was stirred at RT for 1 hour and at 110°C for 24 hours after which a yellow mass had formed sticking on the flask's inside. The yellow residue could be flushed out with 3 × 4 mL DCM, was then separated by filtration through a glass frit, transferred to a flask and dried on the rotary evaporator.
Yellow crystals
NMR:
6Apr3019 50 ^{1}H
6Apr3019 51 ^{19}F, see GKM066

GKM064 - Benzyl 4-(3-chloro-3-oxopropyl)-5-oxooxazolidine-3-carboxylate 13

0.95 g (1 eq., 3.2 mmol) Z-Glu (product of GKM061) were dissolved in 10 mL dry benzene with the aid of the ultrasound bath. The solution was then cooled in an ice bath. As this resulted in the benzene turning solid the ice bath was replaced by a water bath at 6°C. 0.76 g (1.1 eq., 3.7 mmol) PCl_5 were added and the reaction mixture was stirred for 20 minutes. The solvent was subsequently evaporated by rotary evaporation. The residue was then taken up in 10 mL dry toluene which was again evaporated. This was repeated twice. When backfilling the flask it was always done with argon to prevent contact of the product with air moisture. For weighing the product the flask was filled with air and immediately evacuated again afterwards.
Yield: 0.98 g (98%) Yellow oil with a sweet smell

GKM065 - 3-(3-((benzyloxy)carbonyl)-5-oxooxazolidin-4-yl)propanoic peroxyanhydride 14

0.98 g (1 eq., 3.1 mmol) benzyl (*S*)-4-(3-chloro-3-oxopropyl)-5-oxooxazolidine-3-carboxylate were suspended in 10 mL dry Et_2O and 0.5 mL dry pyridin resulting in the mixture turning solid. It was cooled to 0°C before 0.5 g (0.6 eq., 1.9 mmol) UHP (containig 35% w/w of H_2O_2) were added. The reaction mixture was stirred for 4 hours at 0°C during which it turned from yellow to white and sticking to the flask's inside. 15 mL EtOAc and 10 mL H_2SO_4 (made from 9 mL H_2O and 1 mL H_2SO_4 conc.) were added which dissolved the residue. The phases were separated and the organic phase was washed twice with each 5 mL $NaHCO_3$ aq. sat. and once with 5 mL H_2O. It was then dried with $MgSO_4$ and after 48 hours standing in the fridge the solvent was removed at 25°C bath temperature.
Yield: 0.23 g (25%)

Turbid white oil
NMR:
4May0619 10 ^{1}H
4May0619 11 ^{13}C
Mass Spectrometry: ESI-ion trap (m/z): Calcd for $[C_{28}H_{28}N_2O_{12}+H]^+$, 585.16. Found: -.
D:\Data\MS_MessService\63817_GKM065_amazon.d

GKM066 - 1-fluoro-4-nitrobenzene 42b

The reaction was performed as in GKM063 except for using a glass tube with a NS14 ground joint and using a nitrogen atmosphere.
Yellow crystals
NMR:
6May0819 10 ^{1}H
6May0819 11 ^{19}F
^{19}F NMR (565 MHz, $CDCl_3$): δ -102.0 (1F, m)

GKM067 - Benzyl 4-(2-bromoethyl)-5-oxooxazolidine-3-carboxylate 15

51 mg (0.6 eq., 0.23 mmol) $CuBr_2$ were dissolved in 3.3 mL dry ACN and heated to 50°C. 0.23 g (1 eq., 0.4 mmol) (*S*)-3-(3-((benzyloxy)carbonyl)-5-oxooxazolidin-4-yl)propanoic peroxyanhydride (product of GKM065) were dissolved in 1 mL dry ACN and added dropwise. The reaction mixture was stirred 5.5 hours at 50°C and 18 hours at RT. Thereafter the solvent was evaporated and the residue was taken up in 7 mL EtOAc. The solution was washed once with 5 mL HCl 0.25M and twice with each 1 mL H_2O. The organic phase was dried with $MgSO_4$ before removing the solvent by rotary evaporation.
NMR: 4May1319 70
NMR indicated no product. The experiment was discarded.

GKM068 - 1-fluoro-4-nitrobenzene 42b

The reaction was performed as in GKM066 except for leaving the vessel open in the hood for the solvent to evaporate.
Orange crystals
NMR:
6May1319 50 ^{1}H
6May1319 51 ^{19}F, see GKM066

GKM069 - 4-fluoroaniline 42a

1 g (1.5 eq., 0.68 mmol) PhenoFluorMix were weighed into a glass tube with a NS14 ground joint and dried for 1 hour at 130°C and 0.18 Torr after which it was backfilled with N_2. 50 mg (1 eq., 0.45 mmol) *p*-aminophenol were added quickly after which the reaction vessel was again evacuated and backfilled with N_2. 5 mL dry toluene were added and the reaction mixture was stirred at RT for 1 hour and at 110°C for 24 hours. After further 24 hours standing on the bench a small volume of Et_2O was added. The solution was extracted thrice with each 20 mL HCl 3M. The combined aqueous phases were adjusted to pH 14 with NaOH 3M and extracted 5 times

with each 50 mL Et_2O. The combined organic phases from the extraction were dried with $MgSO_4$. The major part of the solvent was removed carefully at RT and reduced pressure before the product was left open to dry in the hood.
NMR:
6May1619 20 ^{1}H
6May1619 21 ^{19}F
According to ^{19}F NMR no fluorinated compounds were present.

GKM070 - ((Benzyloxy)carbonyl)glycine 22

3 g (1 eq., 40 mmol) glycin and 6.71 g (2 eq., 80 mmol) $NaHCO_3$ were dissolved in 100 ml distilled water and subsequently cooled to 0°C. 8.56 mL (2 eq., 80 mmol) Cbz-chloride were dissolved in 25 mL dioxane and added dropwise. The reaction mixture was stirred overnight at RT and then washed twice with each 50 mL EtOAc. The pH was adjusted to 1 with HCl 3M before the solution was extracted thrice with each 50 mL EtOAc. The combined organic phases from the extraction were dried with $MgSO_4$. After removing the solvent the product was left to crystallize in the fridge.
Yield: 5.14 g (61%)
White solid
NMR: 4May1519 230
^{1}H NMR (400 MHz, MeOD): δ 7.39-7.26 (5H, m), 5.13 (2H, s), 3.85 (2H, s)

GKM071 - Benzyl 5-oxooxazolidine-3-carboxylate 23

5.14 g (1 eq., 20.6 mmol) Z-Gly (product of GKM070) were suspended in 180 mL toluene (with aid of the ultrasound bath and gentle warming). 0.43 g (0.09 eq., 1.87 mmol) CSA and 6.51 g (1.05 eq., 21.7 mmol) paraformaldehyde were added. The reaction vessel was equipped with a glass adapter with an argon balloon. The reaction mixture was stirred at 115°C for 90 minutes and left standing on the bench overnight. Afterwards the residue was separated by filtration through a glass frit and rinsed with toluene. The filtrate was freed of the solventby rotary evaporation.
Yield: 3.95 g (87%)
White resin
NMR: 4May1719 440
^{1}H NMR (400 MHz, $CDCl_3$): δ 7.42-7.36 (5H, m), 5.45 (2H, s), 5.22 (2H, s), 4.10 (2H, s)

GKM072 - Benzyl 4-(3,3-dimethoxypropyl)-5-oxooxazolidine-3-carboxylate 24

0.57 g (1 eq., 2.6 mmol) benzyl 5-oxooxazolidine-3-carboxylate were dissolved 10 mL dry THF, put under argon atmosphere and cooled to -78°C. 6.2 mL of a 0.5M solution in THF of LHMDS were added dropwise in portions. The reaction mixture was stirred for 10 minutes at -78°C before 0.4 mL (2 eq., 5.2 mmol) 3-bromo-1,1-dimethoxypropane were also added dropwise. It was stirred for 3 hours at -78°C. Then 20 mL of a 10% w/w $KHSO_4$ aq. and 10 mL EtOAc were added and the mixture was brought to RT. After separating the phases the organic phase was washed with 10% w/w $KHSO_4$ aq., $NaHCO_3$ aq. sat. and brine and left standing on the bench for 36 hours, covered with parafilm. Some EtOAc was added resulting in a white solid precipitating. 10 mL were added to check solubility of the solid which went again in solution. The solvent was evaporated.
Brown viscous liquid

NMR:
4Jun0319 70 ^{1}H
4Jun0319 71 ^{13}C
TLC (PE/EtOAc 7:3) gave only one spot on the baseline

GKM073 - Benzyl 4-allyl-5-oxooxazolidine-3-carboxylate 25

0.59 g (1 eq., 2.7 mmol) benzyl 5-oxooxazolidine-3-carboxylate were dissolved in 10 mL dry THF with the aid of gentle warming and the ultrasound bath. The reaction vessel was flushed with argon and cooled to -78°C. 6.4 mL of a 0.5M solution in THF of LHMDS were added dropwise in portions. The reaction mixture was stirred for 20 minutes at -78°C. Then 0.46 mL (2 eq., 5.3 mmol) allylbromide (from an almost empty and apparently old bottle, also containig little black particles) were added. It was stirred at -78°C for another 4 hours before bringing the reaction mixture to RT and adding 20 mL of a 10% w/w $KHSO_4$ aq. and 20 mL EtOAc. After separating the phases the organic phase was washed with 10% w/w $KHSO_4$ aq., $NaHCO_3$ aq. sat. and brine. The solution was dried with $MgSO_4$ before the solvent was removed.
Yield: 0.24 g (36%)
NMR:
4Jun0319 80 ^{1}H
4Jun0319 81 ^{13}C

GKM074 - 3-(3-((benzyloxy)carbonyl)-5-oxooxazolidin-4-yl)propanoic acid 12

2.02 g (1 eq., 7.18 mmol) Z-Glu
100 mL toluene
0.33 g (1.5 eq., 11 mmol) paraformaldehyde
33 mg (1 % w/w) *p*TsOH·H_2O
The reaction was performed as in GKM061 at 120°C bath temperature. Purification was done on a 10 cm column first and a second time on a 5 cm column.
Yield: 1.95 g (93%)
Brown oil
NMR: 4Jun1919 480, see GKM061

GKM075 - Benzyl 4-(3-chloro-3-oxopropyl)-5-oxooxazolidine-3-carboxylate 13

1.95 g (1 eq., 6.66 mmol) (*S*)-3-(3-((benzyloxy)carbonyl)-5-oxooxazolidin-4-yl)propanoic acid were dissolved in 7 mL DCM with the aid of the ultrasound bath. 0.9 mL (1.5 eq., 10.12 mmol) oxalyl chloride and a few drops of DMF were added. The reaction mixture was stirred for 1 hour. The volatile components were removed by rotary evaporation and subsequently by drying at 0.18 Torr.
Yield: 1.73 g (83%)
Red-brown oil
NMR: 4Jun2619 190

Part V

Spectra

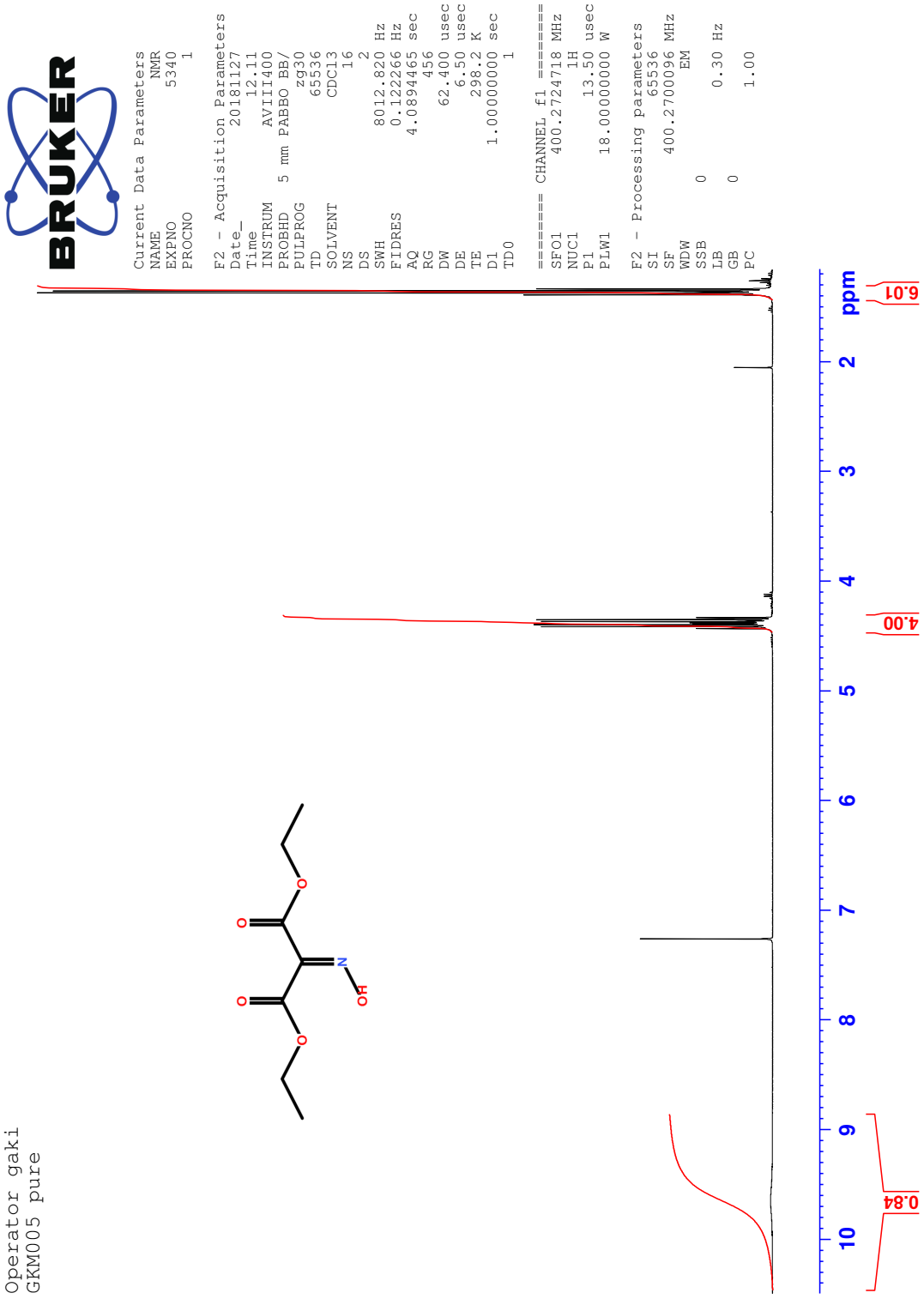

Figure 20: NMR of diethyl 2-(hydroxyimino)malonate **2**

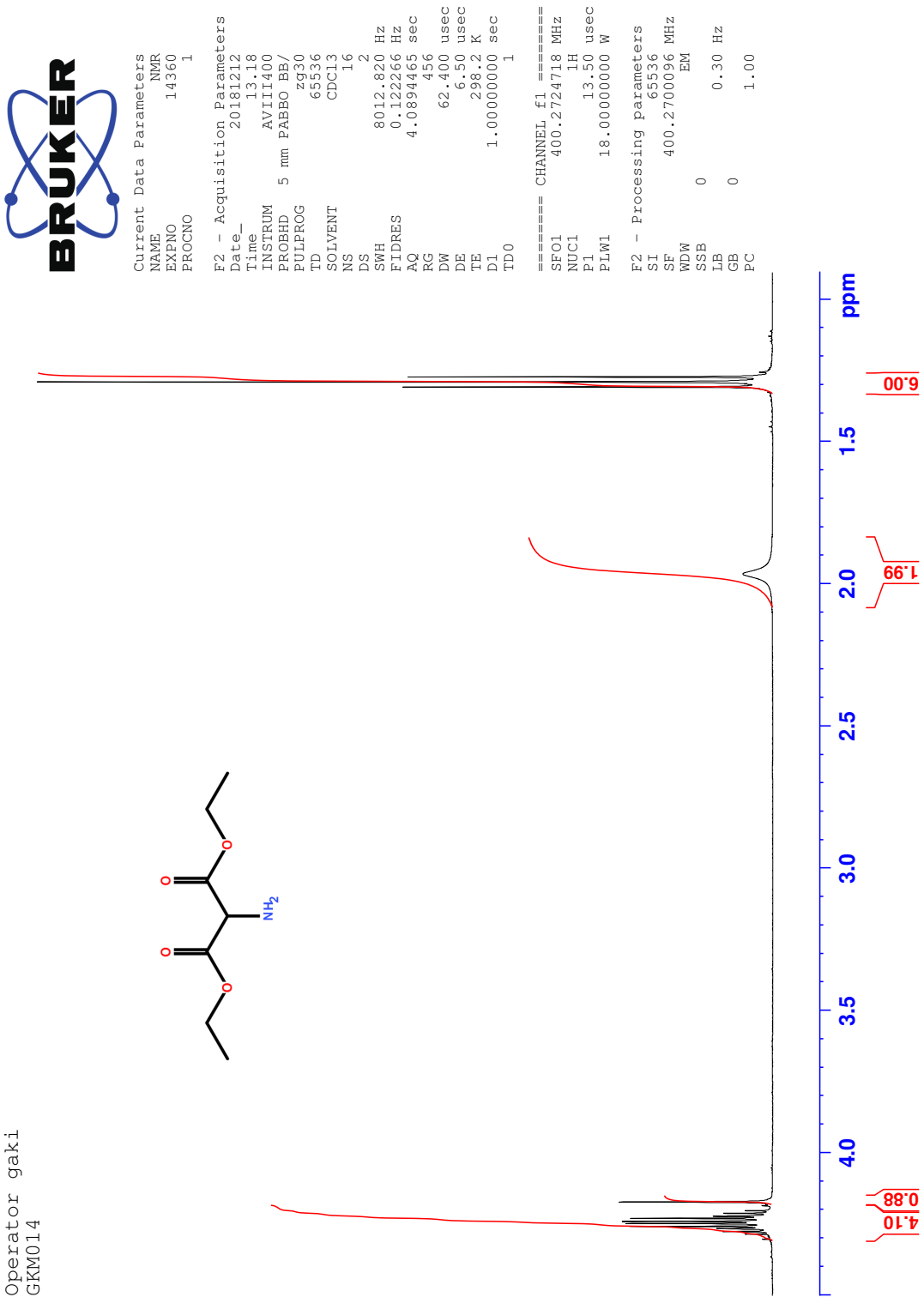

Figure 21: NMR of diethyl 2-aminomalonate **3**

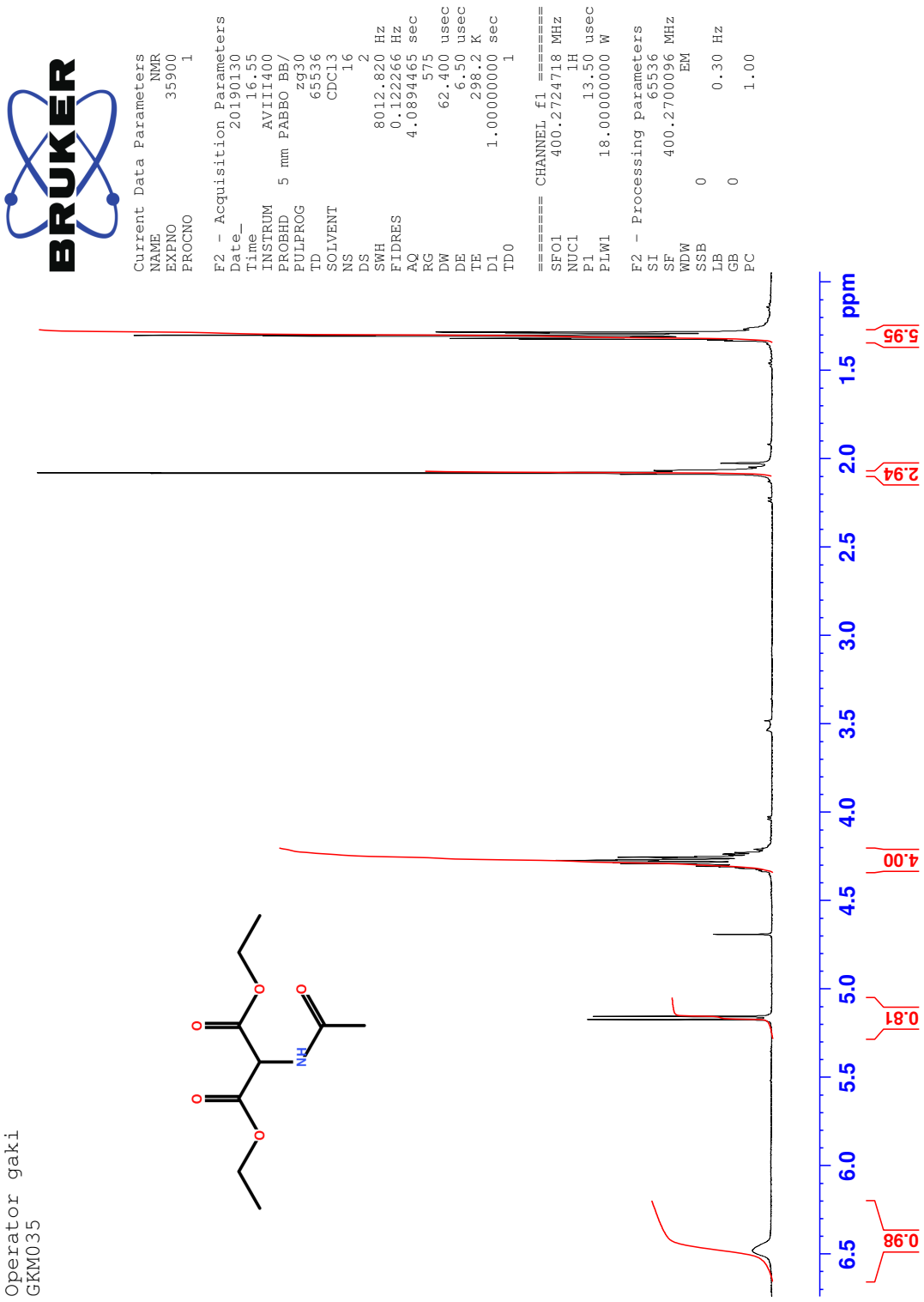

Figure 22: NMR of diethyl 2-acetamidomalonate **4**

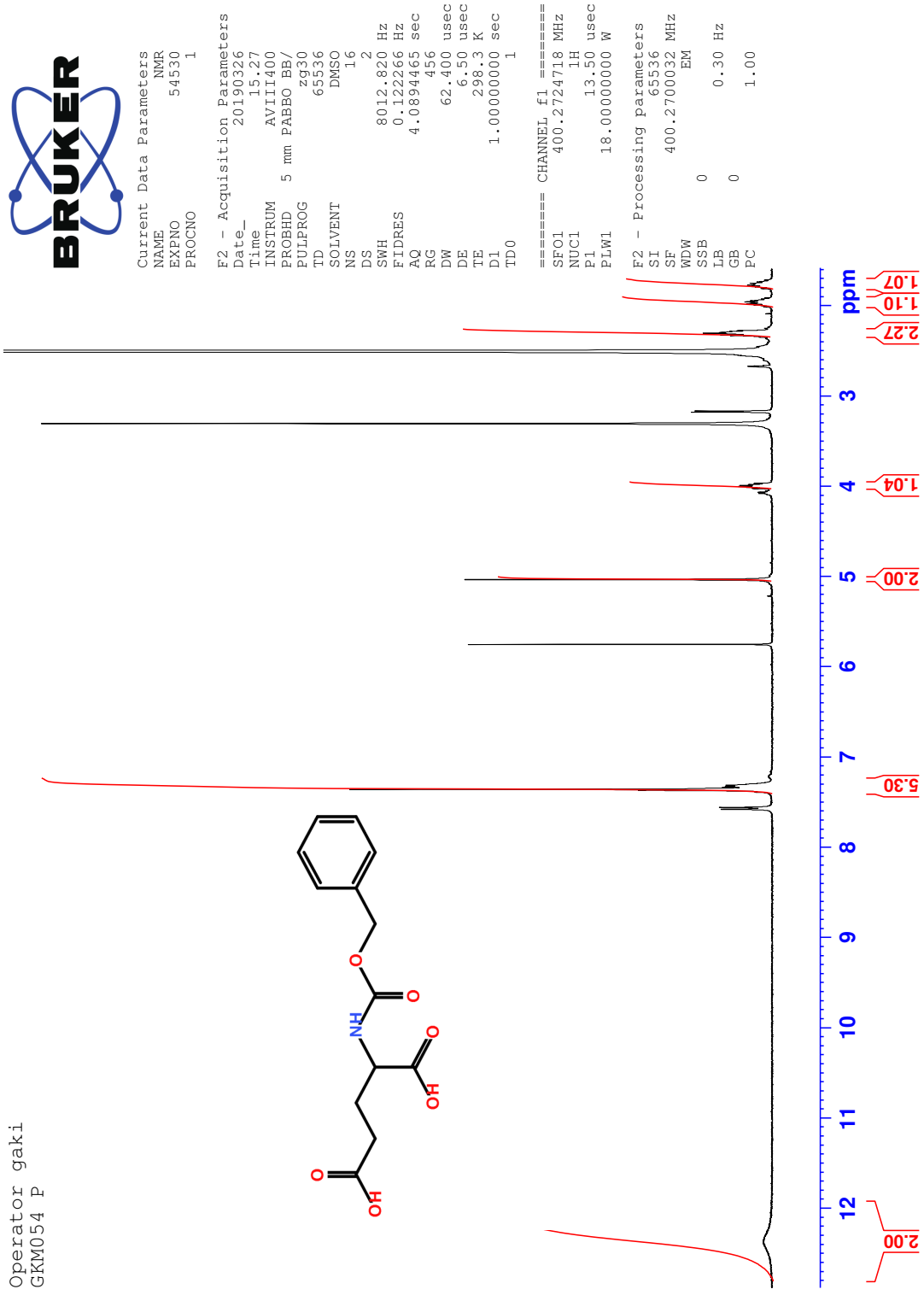

Figure 23: NMR of ((benzyloxy)carbonyl)glutamic acid **11**

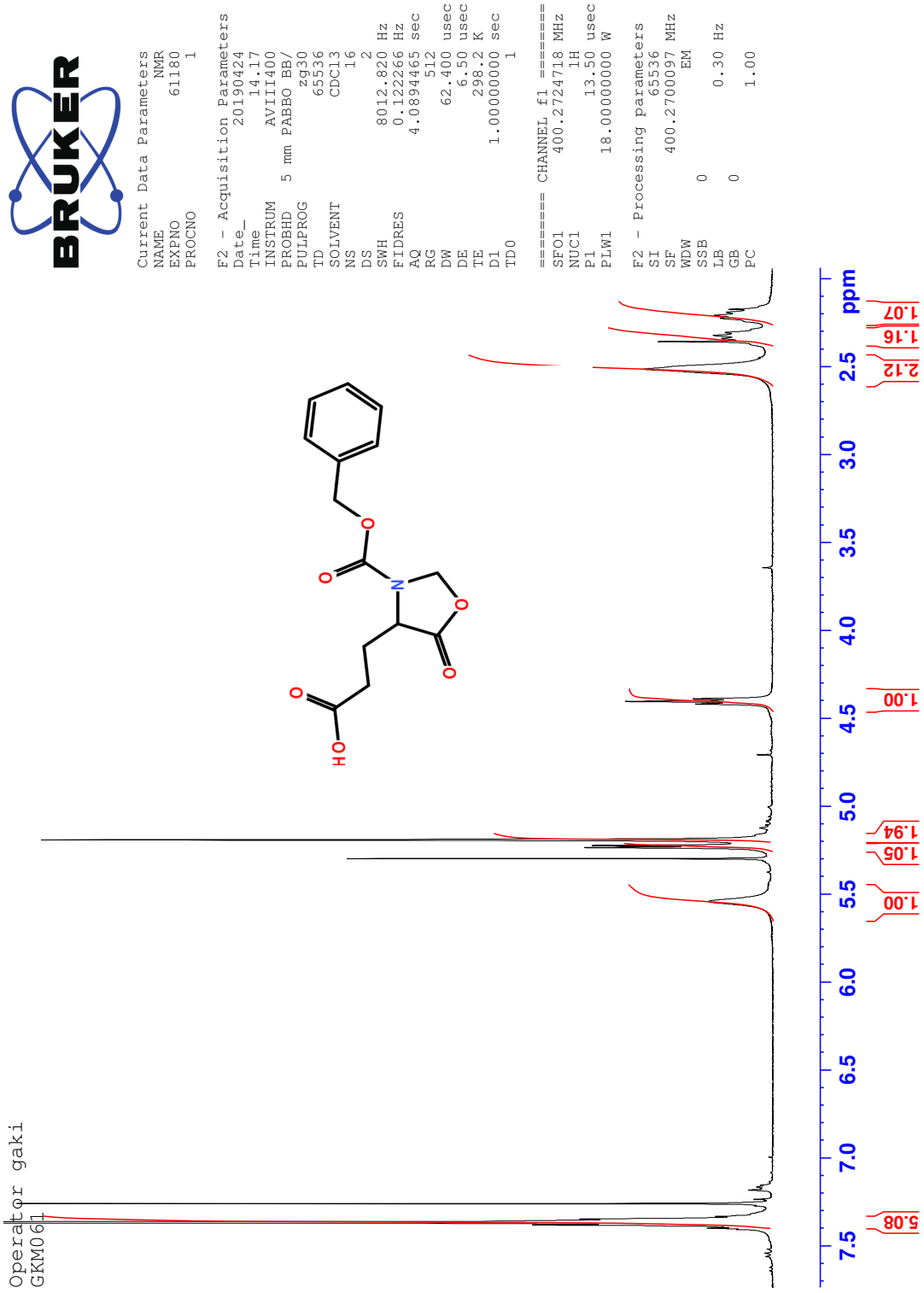

Figure 24: NMR of 3-(3-((benzyloxy)carbonyl)-5-oxooxazolidin-4-yl)propanoic acid **12**

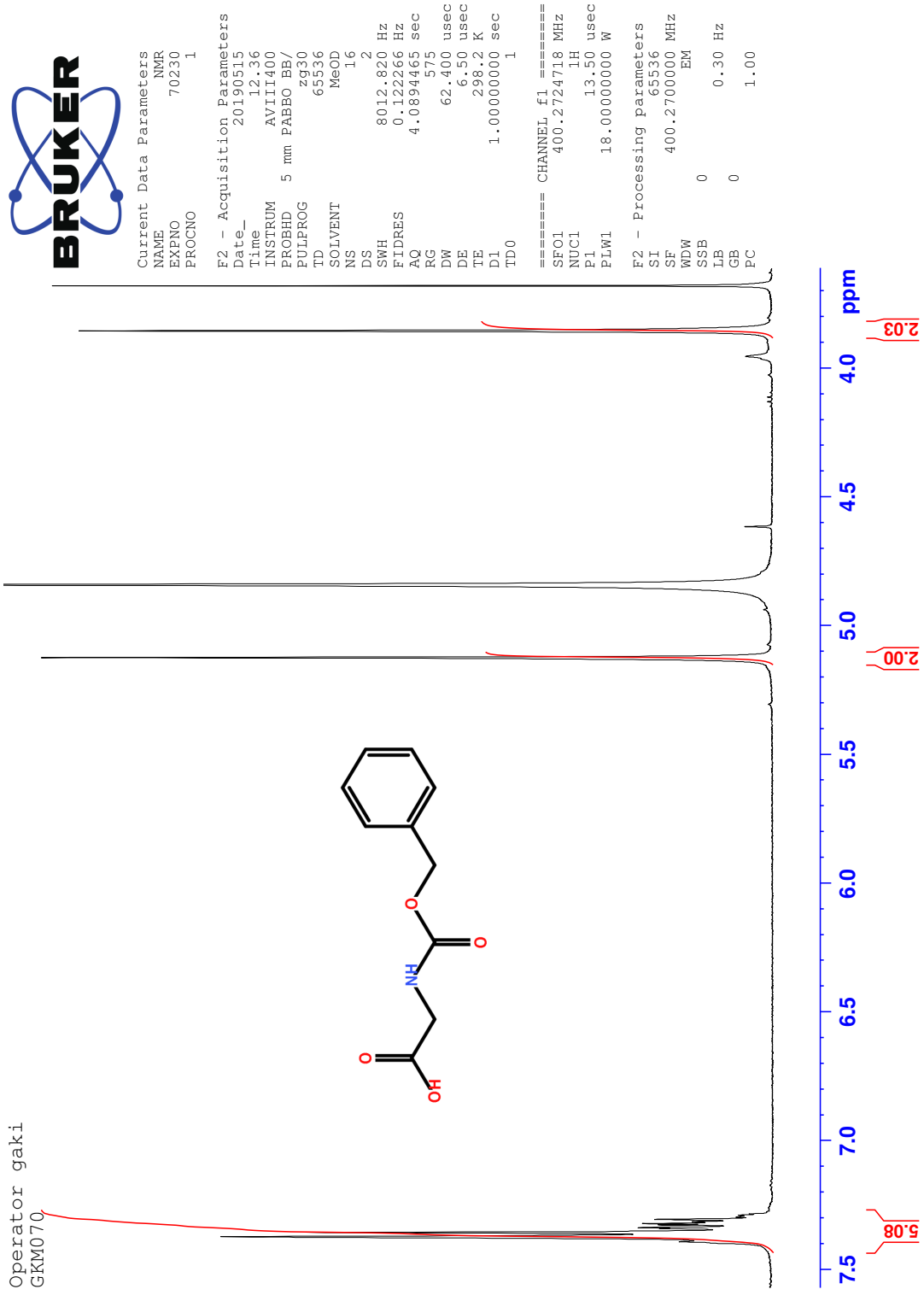

Figure 25: NMR of ((benzyloxy)carbonyl)glycine **22**

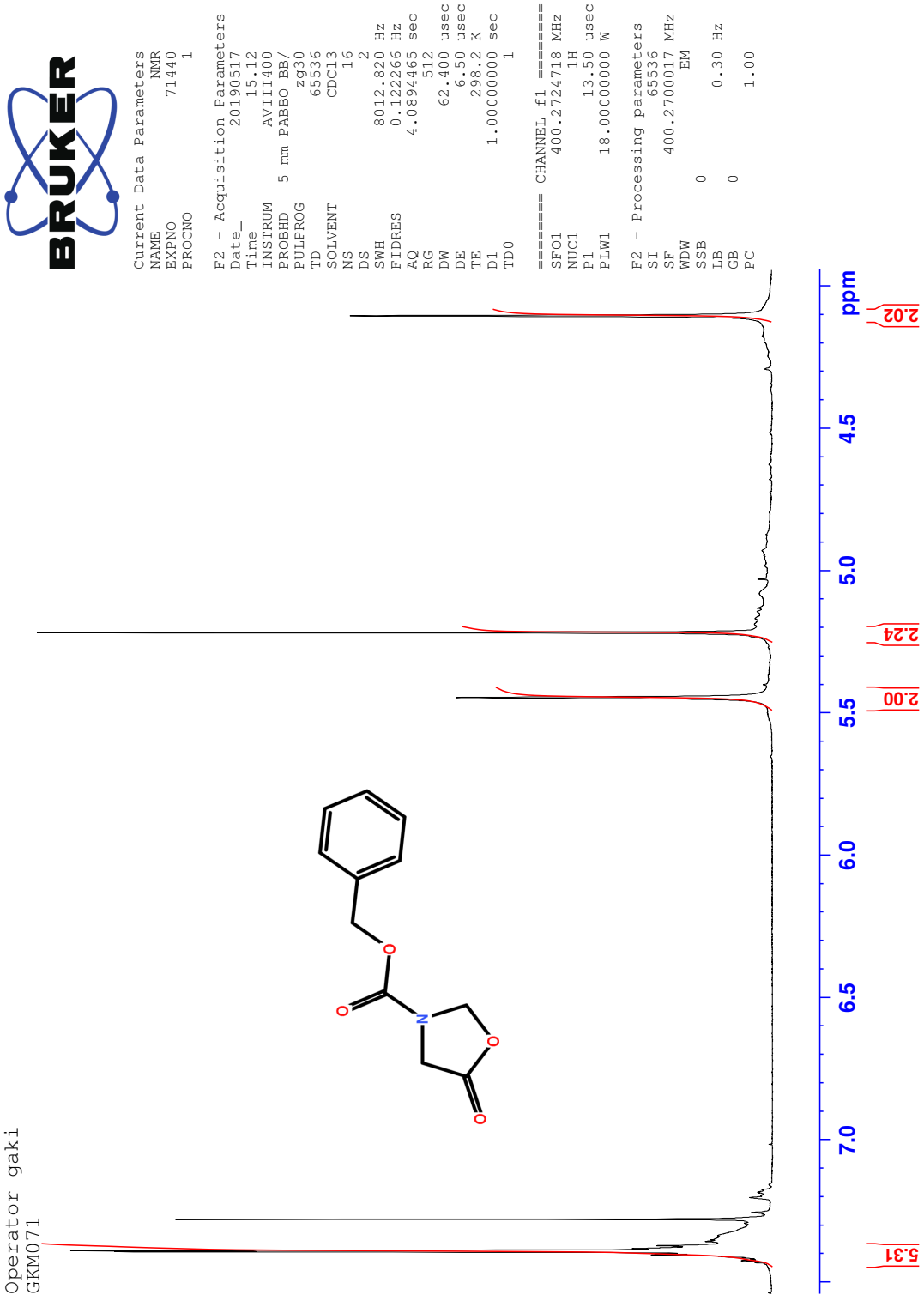

Figure 26: NMR of benzyl 5-oxooxazolidine-3-carboxylate **23**

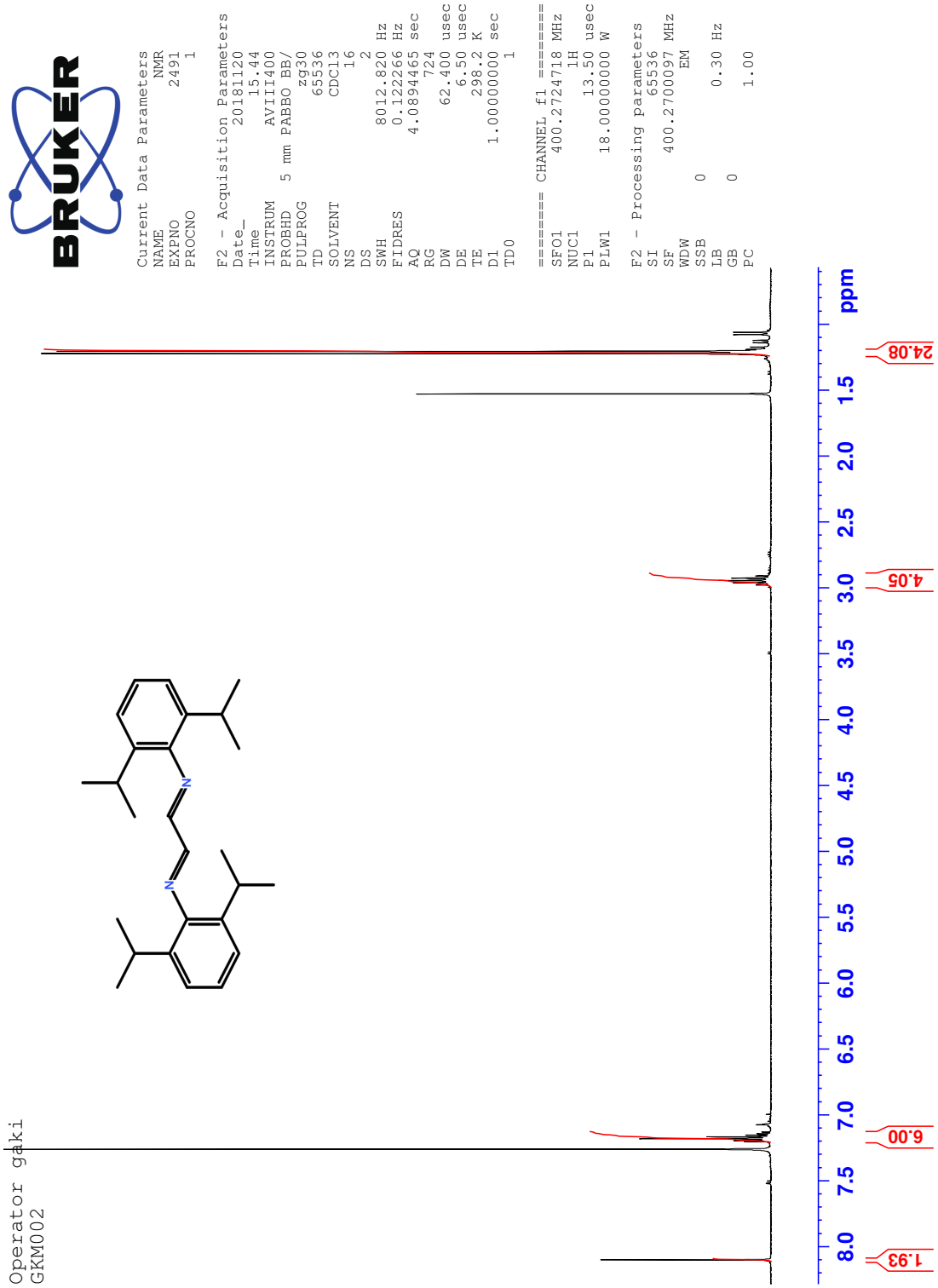

Figure 27: NMR of (1*E*,2*E*)-N^1,N^2-bis(2,6-diisopropylphenyl)ethane-1,2-diimine **37**

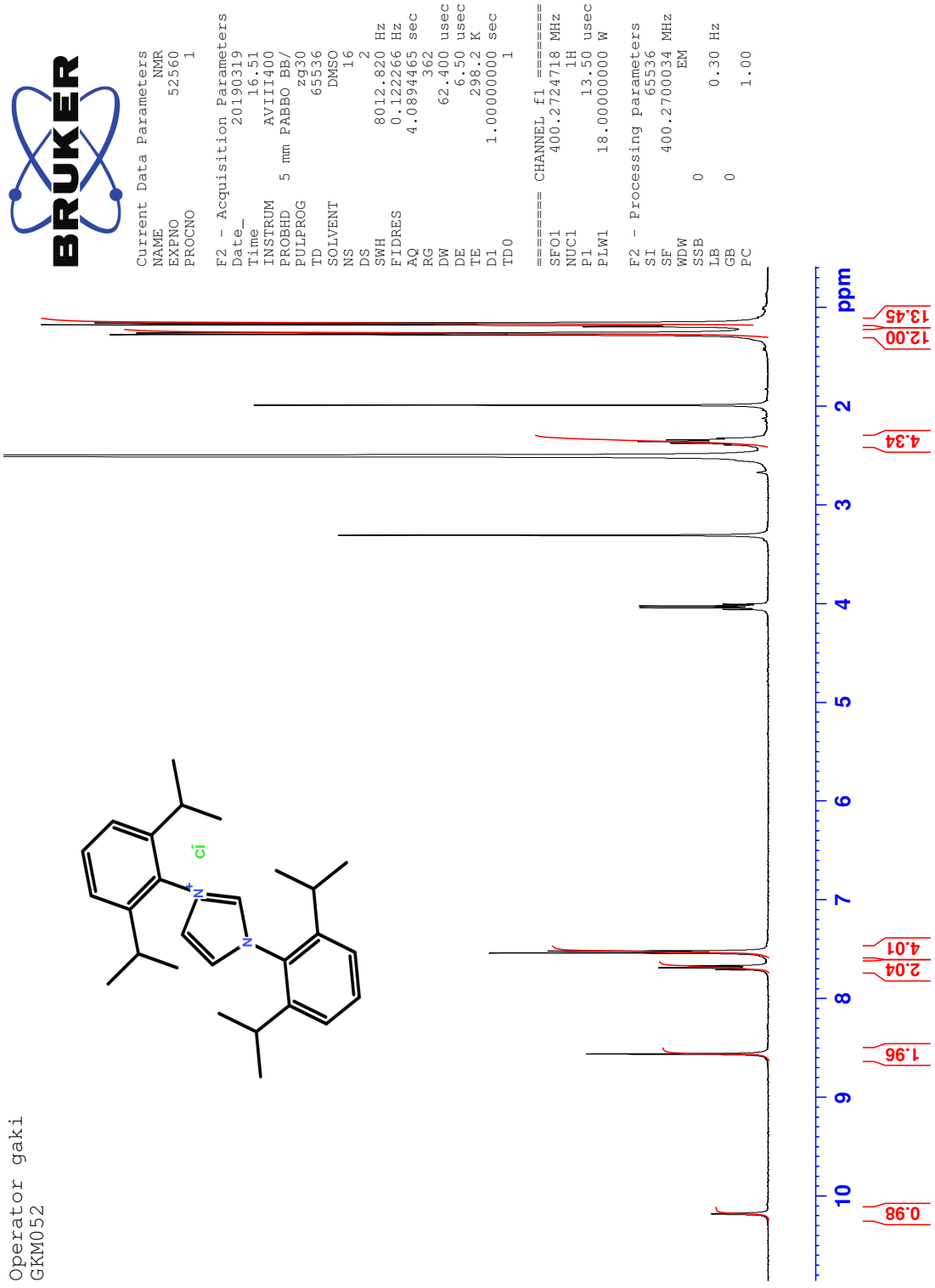

Figure 28: NMR of 1,3-bis(2,6-diisopropylphenyl)-1*H*-imidazol-3-ium chloride **39**

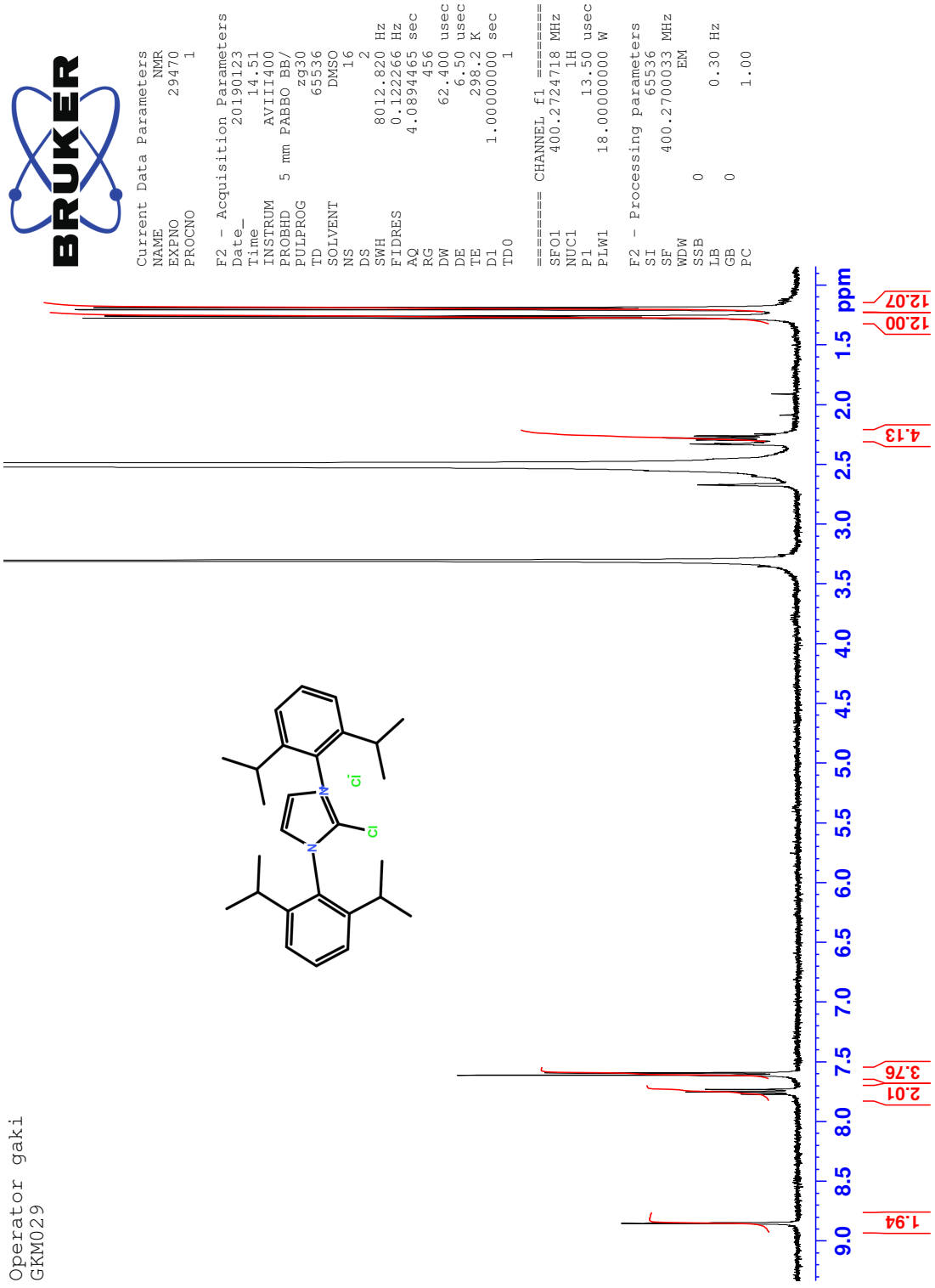

Figure 29: NMR of 2-chloro-1,3-bis(2,6-diisopropylphenyl)-1*H*-imidazol-3-ium chloride **34**

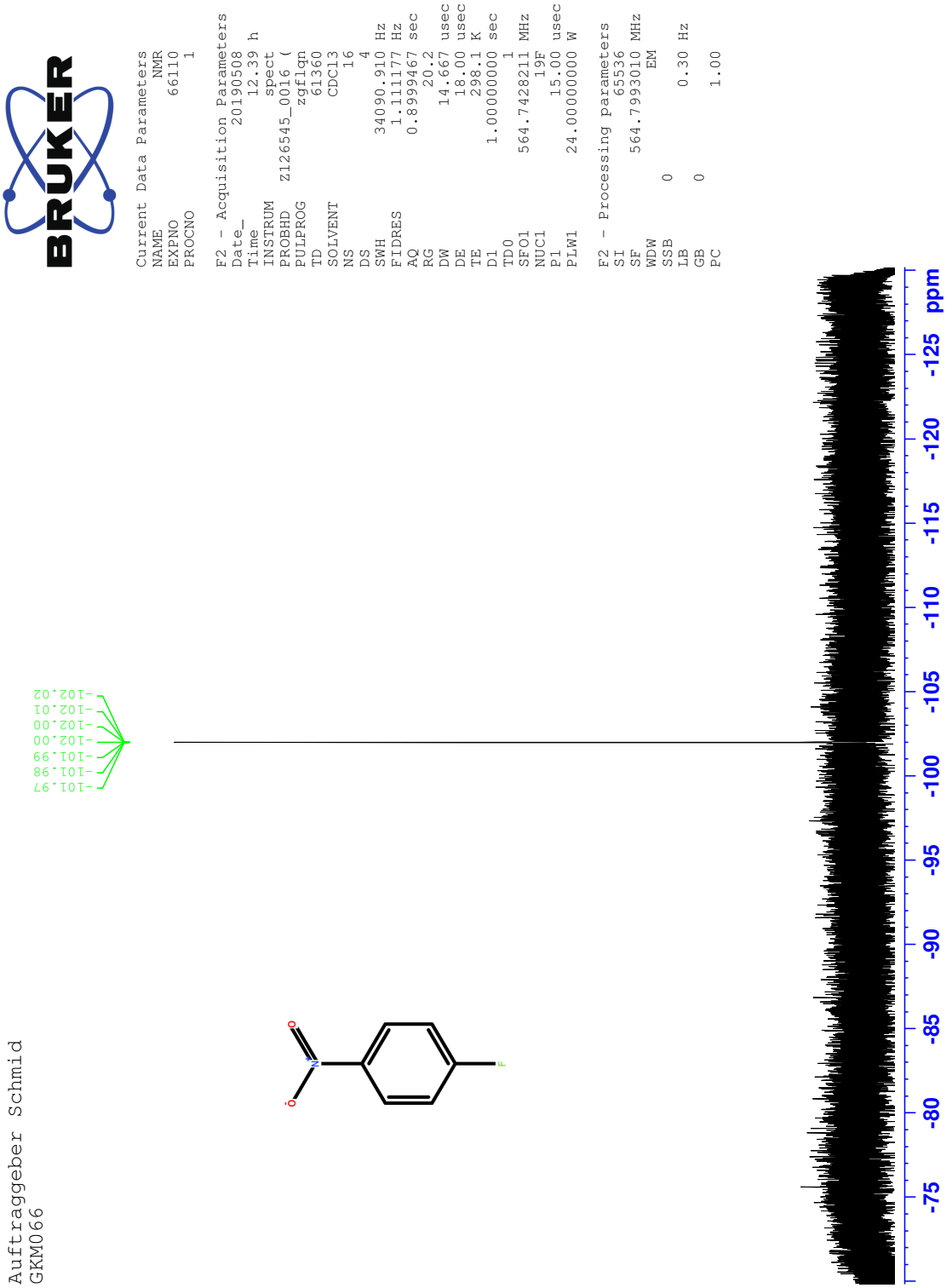

Figure 30: NMR of 1-fluoro-4-nitrobenzene **42b**

Generic Display Report

Analysis Info

Analysis Name	D:\DATA\MS_Service_MSC\61283_GKM012_hct.d	Acquisition Date	10.12.2018 14:05:29
Method	Direct_Infusion_routine-method.m	Operator	MSC
Sample Name	56283_GKM012_hct	Instrument	HCTplus
Comment	Kiesenhofer/Schmid ACN/MeOH + 1% H2O		

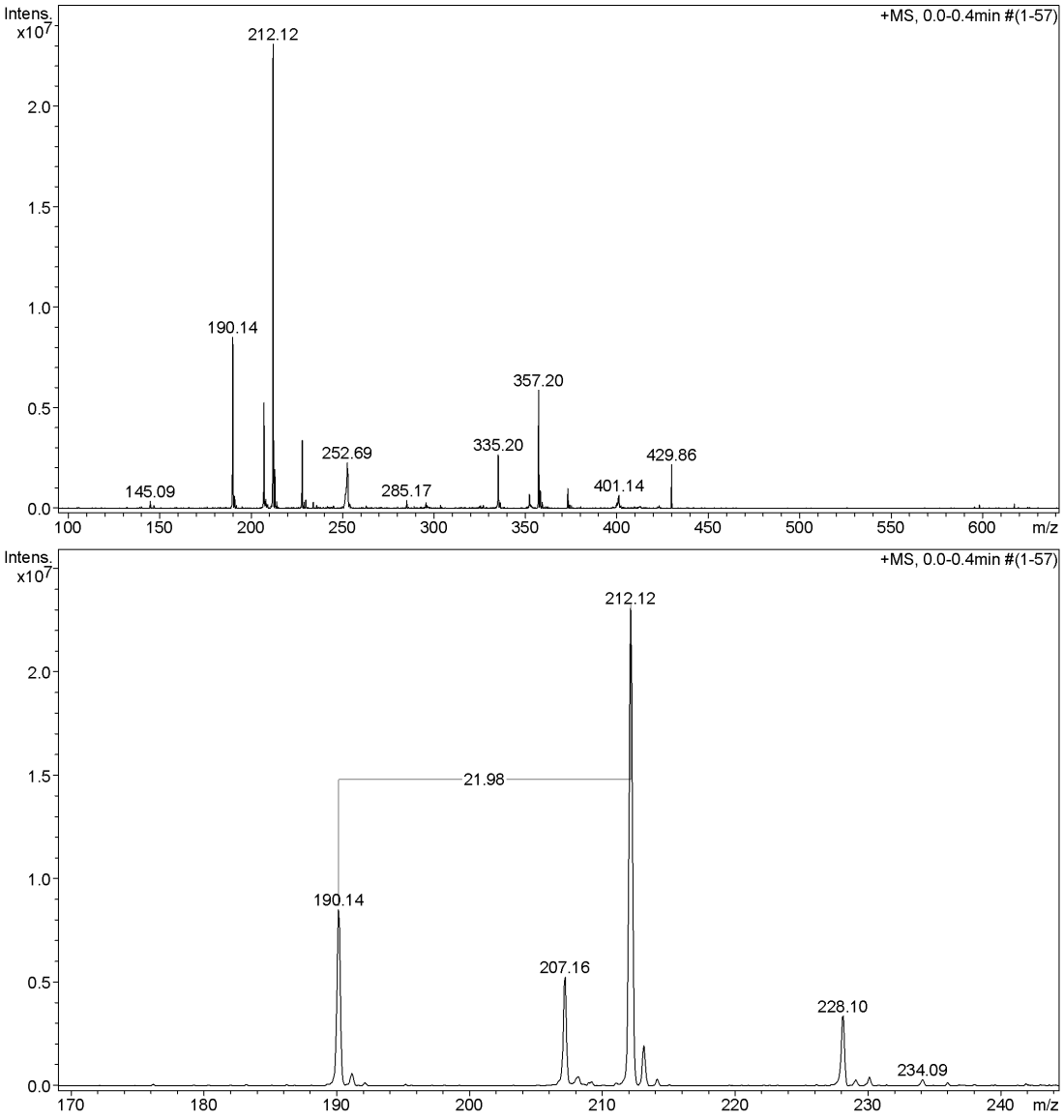

Bruker Daltonics DataAnalysis 3.3 printed: 10.12.2018 14:16:32 Page 1 of 1

Figure 31: MS of diethyl 2-aminomalonate **3**

Generic Display Report

Analysis Info

Acquisition Date	11.01.2019 10:54:29		
Analysis Name	D:\Data\MS_MessService\61628_GK11021_amazon.d		
Method	MSC-Service_direct-injection.m	Operator	MSC
Sample Name	61628_GK11021_amazon	Instrument	amaZon speed ETD
Comment	Kiesenhofer / Schmid / Org.Chem. ACN / MeOH + 1% H2O		

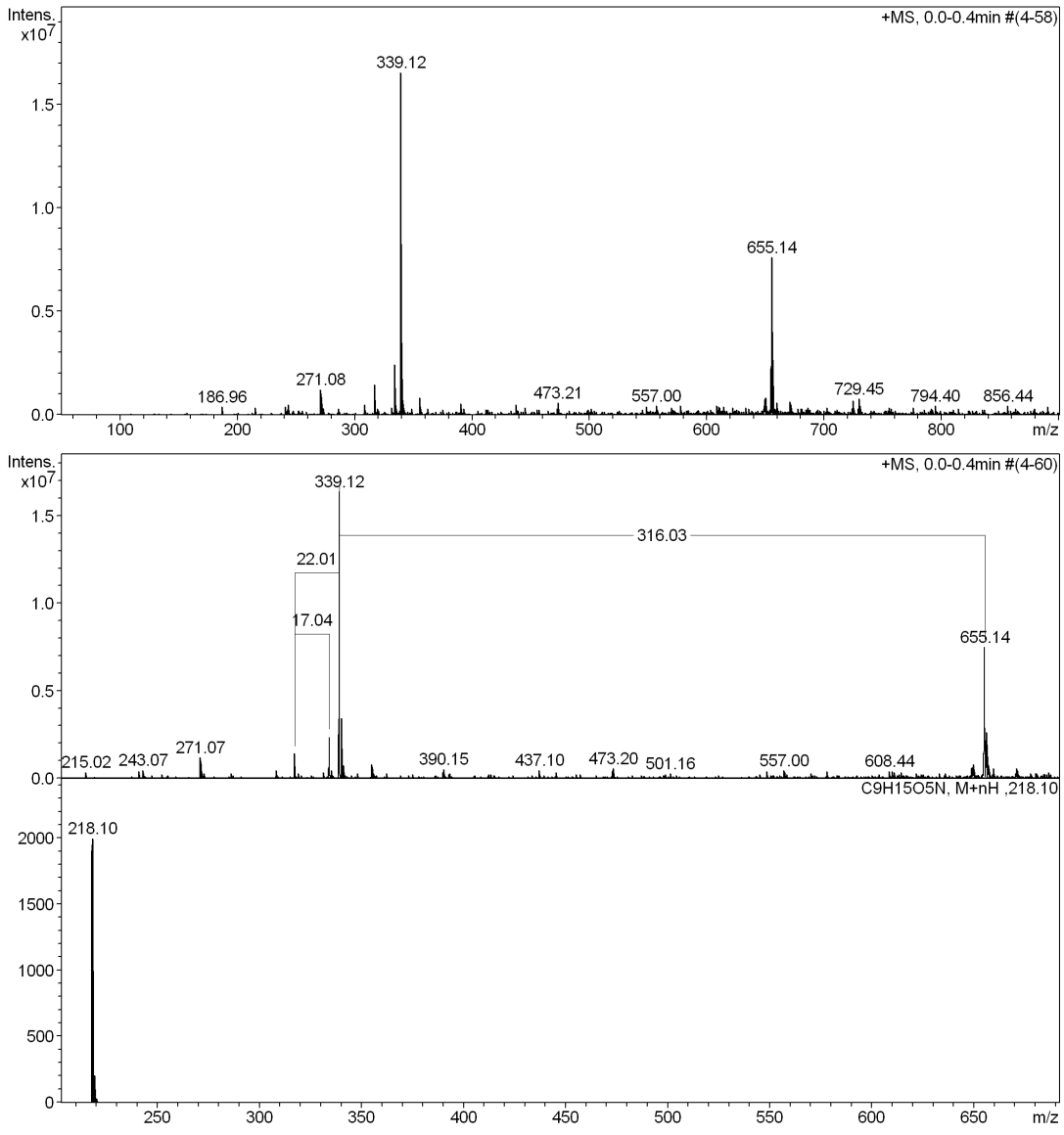

Bruker Compass DataAnalysis 4.0 printed: 11.01.2019 11:00:24 Page 1 of 1

Figure 32: MS of diethyl 2-acetamidomalonate **4**

Generic Display Report

Analysis Info

Analysis Name	D:\Data\MS_MessService\63817_GKM065_amazon.d	Acquisition Date	08.05.2019 11:19:09
Method	MSC-Service_direct-injection.m	Operator	MSC
Sample Name	63817_GKM065_amazon	Instrument	amaZon speed ETD
Comment	Kiesenhofer / Anorg.Chem. ACN / MeOH + 1% H2O		

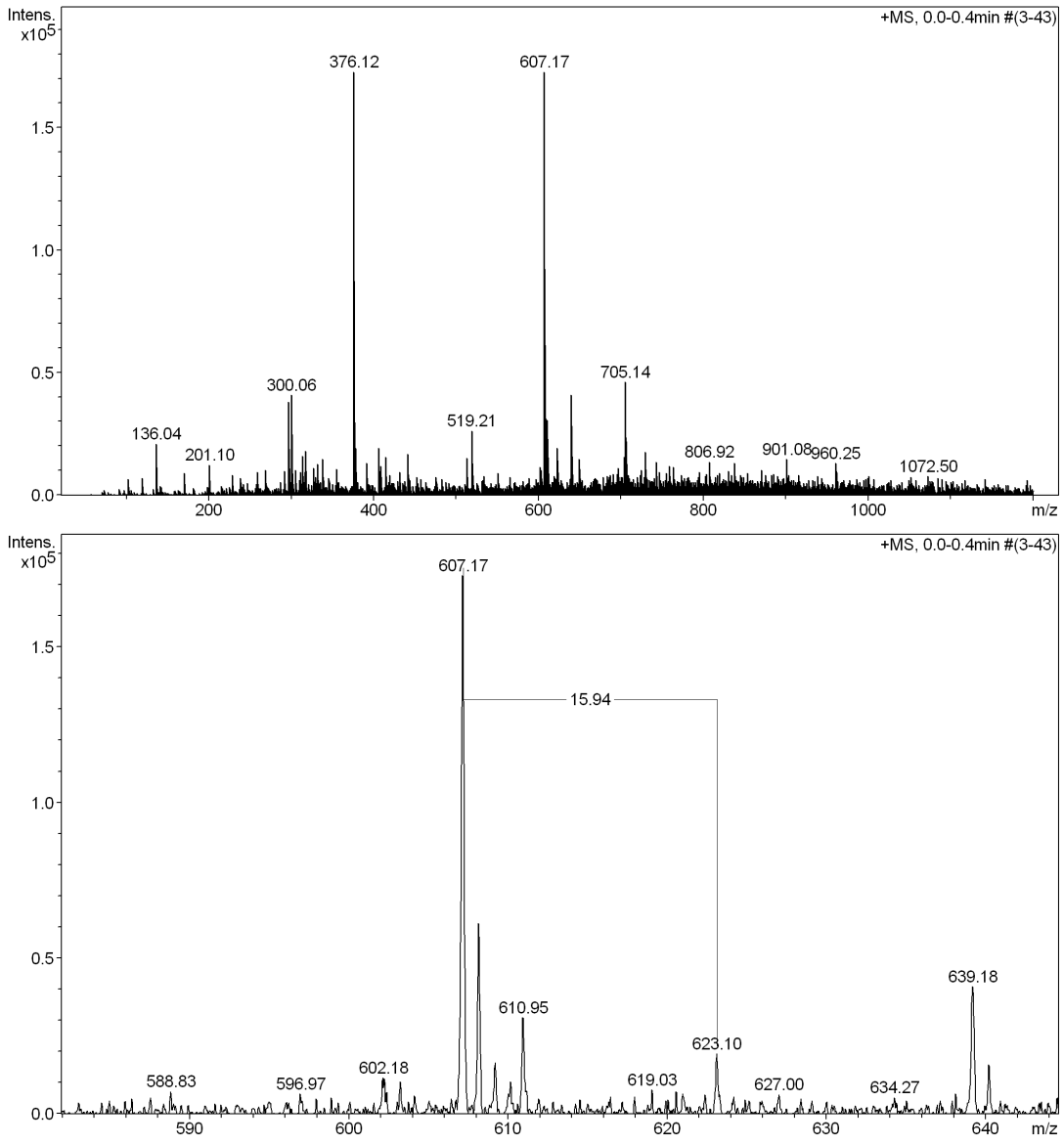

Bruker Compass DataAnalysis 4.0 printed: 08.05.2019 11:23:06 Page 1 of 1

Figure 33: MS of 3-(3-((benzyloxy)carbonyl)-5-oxooxazolidin-4-yl)propanoic peroxyanhydride **14**

Abstract

Proteins and peptides play a major role in every part of the human body as well as in other organisms, ranging from structural elements to signal molecules and enzymes that take care of compounds which require processing in order to e.g. render them harmless. For proteins to fulfill their duty it is necessary that their amino acid sequence is organized into a three-dimensional structure called the secondary structure. Failure of the folding process leads to misfolded peptides that are either non-functional or, in the worst case, pathogenic. To obtain insights on protein structures scientists can resort either to X-ray crystallography as the standard method or to NMR spectroscopy. While X-ray crystallography does not have size limitations and yields fast results with high resolution, it comes at the drawback of the sample protein being required in crystallized form. Hence, this technique fails for proteins that cannot be crystallized. NMR is a complementary approach which is independent from crystallization yet suffers from size limitations. Increasing size leads to bad spectral quality as well as signal overlaps. Strategies have therefore been evolved to cope with this challenges. Site specific isotope labeling is used to remove irrelevant peaks from the spectrum or amplify those of interest. Furthermore, multidimensional spectroscopy has alleviated the assignment of signals a lot. To be able to apply these strategies it is necessary to derive synthetic routes that allow for site specifically labeled amino acids respectively their precursors. Several routes towards the amino acid proline, starting from different compounds, have been explored in this thesis since proline is of central interest concerning conformational changes within a protein.

Fluorine NMR adds another approach to gain information on peptide structures. Albeit poorly suitable as a stand-alone method due to short relaxation times, it unfolds its power in combination with other nuclei: two-dimensional $^{19}F-^{13}C$ TROSY experiments yield sharper carbon peaks compared to $^{1}H-^{13}C$, $^{15}N-^{19}F$ HSQC of the peptide backbone takes only minutes instead of hours for $^{15}N-^{1}H$. Introducing fluorine into organic molecules poses a much greater challenge compared to other halogens, even more so when dealing with costly labeled compounds when high yields are desired also from an economic point of view. Apart from less important approaches such as fluorine containing tags or radical mechanisms, both nucleophilic and electrophilic substitution can be applied. A large array of reactions with different functionalities to start from has been hitherto reported, yet in the case of aromatic targets problems occur due to poor regioselectivity, low yields or a required functionality that is non-existent in natural amino acids. These challenges have been overcome when PhenoFluor and PhenoFluorMix were reported as fluorination agents that can be used to convert phenolic derivatives to the corresponding fluorocompounds, at the same time tolerating a large variety of other functional groups. Although fluorine has about the same van der Waal's radius as hydrogen, it is nevertheless likely to alter the properties of the protein due to great differences in its electronic traits. The aim of this thesis was to synthesize the mentioned fluorinating agents and explore their applicability on different molecules.

Zusammenfassung

Proteine und Peptide stellen ein zentrales Element des menschlichen wie auch jedes anderen Organismus dar. Ihre Aufgaben umfassen das Aufrechterhalten von Strukturen, die Funktion als Signalmoleküle wie auch als Enzyme die Verstoffwechslung von z.B. potentiell schädlichen Stoffen. Um ihre Funktion zu erfüllen, müssen Proteine eine bestimmte dreidimensionale Struktur aufweisen, die Sekundärstruktur. Fehler im Faltungsvorgang führen zu Sekundärstrukturen, die keine Funktion erfüllen oder aber im schlimmsten Fall Krankheiten verursachen. Um die Sekundärstruktur eines Proteins zu bestimmen, stehen im Wesentlichen zwei Methoden zur Verfügung. Als klassische Methode kann die Röntgenstrukturanalyse bezeichnet werden, während NMR Spektroskopie als neuere Technik gilt. Die Röntgenstrukturanalyse erlaubt die Untersuchung von Proteinen beliebiger Größe mit großer Genauigkeit und wenig Zeitaufwand unter der Bedingung, dass Kristalle gebildet werden können. NMR Spektroskopie dagegen ermöglicht auch die Analyse von Proteinen in Lösung, jedoch um den Preis, dass mit zunehmender Größe des Proteins die Qualität der Spektren sinkt und Überlappungen die Auswertung erschweren. Um diesen Einschränkungen zu begegnen, werden Isotopenmarkierungen eingeführt, die Signale entfernen oder verstärken können, oder, im Fall von mehrdimensionalen Experimenten, die Zuordnung um vieles erleichtern. Es bedarf neuer synthetischer Methoden, um gezielt markierte Aminosäuren bzw. deren Vorstufen herstellen zu können. Teil dieser Arbeit war die Untersuchung verschiedener Syntheserouten von Prolin, einer Aminosäure, die stark mit Konformationsänderungen in Proteinen in Verbindung gebracht wird.

Fluor NMR Spektroskopie stellt eine weitere Möglichkeit dar, Proteinstrukturen zu untersuchen. Kurze Relaxationszeiten schränken ihren Einsatz als eigenständiges Experiment ein, jedoch ergibt die Kombination mit anderen Kernen große Vorteile. In zweidimensionalen TROSY Experimenten liegt die Signalbreite der Kohlenstoffe bei $^{19}F-^{13}C$ Paaren unter denjenigen bei $^{1}H-^{13}C$ Einheiten. Auch liegen die Aufnahmezeiten von HSQC Spektren eines $^{19}F-^{15}N$ markierten Proteinrückgrates weit unter denen von unmarkierten $^{1}H-^{15}N$ Strängen. Die Einführung von Fluor in organische Moleküle ist anders als bei anderen Halogenen vergleichsweise schwierig. Umso mehr bei kostspielig isotopenmarkierten Verbindungen, wo auch unter einem wirtschaftlichen Gesichtspunkt hohe Ausbeuten erwünscht sind. Neben weniger oft angewandten Methoden wie flourierte Veresterungen/Ether oder Radikalreaktionen, können nucleophile und electrophile Substitutionsreaktionen eingesetzt werden. Viele verschiedene Ansätze, die von den unterschiedlichsten Startfunktionalitäten ausgehen, wurden publiziert, Regioselektivität, geringe Ausbeuten oder der Einsatz von funktionellen Gruppen, die in natürlichen Proteinen nicht vorkommen, verhinderten den effizienten Einsatz dieser Methoden. PhenoFluor und PhenoFluorMix hingegen bedienen sich phenolischer Funktionalitäten und überführen diese ungeachtet anderer funktioneller Gruppen in die entsprechenden organischen Fluoride. Obwohl Fluor einen ähnlichen van der Waals Radius besitzt, wie Wasserstoff, sind die elektronischen Unterschiede beträchtlich. Es ist daher zu erwarten, dass eine Substitution mit Fluor eine Änderung der Proteineigenschaften mit sich bringt. Ziel dieser Arbeit war die Synthese der erwähnten Fluorierungsreagenzien und ihr Einsatz auf verschiedene Phenolderivate.

Part VI

Bibliography and lists

List of Schemes

List of Figures

Bibliography

[1] K. U. Linderstrøm-Lang, *Lane Medical Lectures: Proteins and Enzymes*, Stanford University Press, **1952**, p. 115.

[2] `https://www.khanacademy.org/science/biology/macromolecules/proteins-and-amino-acids/a/orders-of-protein-structure` (visited on 10/28/2019).

[3] J. C. Kendrew, G. Bodo, H. M. Dintzis, R. G. Parrish, H. Wyckoff, D. C. Phillips, *Nature* **1958**, *181*, 662–666.

[4] `http://www.rcsb.org/pdb/results/results.do?tabtoshow=Current&qrid=708EAD4A` (visited on 10/28/2019).

[5] M. Saunders, A. Wishnia, J. G. Kirkwood, *Journal of the American Chemical Society* **1957**, *79*, 3289–3290.

[6] C. I. D., *Biomedical Spectroscopy and Imaging* **2013**, *2*, 245–264.

[7] M. P. Williamson, T. F. Havel, K. Wüthrich, *Journal of Molecular Biology* **1985**, *182*, 295–315.

[8] L. Banci, I. Bertini, C. Luchinat, M. Mori, *Progress in Nuclear Magnetic Resonance Spectroscopy* **2010**, *56*, 247–266.

[9] D. H. Meadows, O. Jardetzky, R. M. Epand, H. H. Ruterjans, H. A. Scheraga, *Proceedings of the National Academy of Sciences* **1968**, *60*, 766–772.

[10] K. Wüthrich, G. Wider, G. Wagner, W. Braun, *Journal of Molecular Biology* **1982**, *155*, 311–319.

[11] `https://www.protein-nmr.org.uk/general/software/automatic-assignment/` (visited on 10/29/2019).

[12] G. Metz, K. P. Howard, W. B. S. van Liemt, J. H. Prestegard, J. Lugtenburg, S. O. Smith, *Journal of the American Chemical Society* **1995**, *117*, 564–565.

[13] S. M. Douglas, J. J. Chou, W. M. Shih, *Proceedings of the National Academy of Sciences* **2007**, *104*, 6644–6648.

[14] G. M. Clore, M. R. Starich, A. M. Gronenborn, *Journal of the American Chemical Society* **1998**, *120*, 10571–10572.

[15] K. Kuwajima, Y. Goto, F. Hirata, M. Kataoka, M. Terazima, *Water and Biomolecules*, Springer Berlin Heidelberg, **2009**.

[16] M. Allegrozzi, I. Bertini, M. B. L. Janik, Y.-M. Lee, G. Liu, C. Luchinat, *Journal of the American Chemical Society* **2000**, *122*, 4154–4161.

[17] M. Kainosho, P. Güntert, *Quarterly Reviews of Biophysics* **2009**, *42*, 247–300.

[18] M. Markus, K. Dayie, P. Matsudaira, G. Wagner, *Journal of Magnetic Resonance Series B* **1994**, *105*, 192–195.

[19] L.-Y. Lian, D. A. Middleton, *Progress in Nuclear Magnetic Resonance Spectroscopy* **2001**, *39*, 171–190.

[20] D. M. LeMaster, D. M. Kushlan, *Journal of the American Chemical Society* **1996**, *118*, 9255–9264.

[21] A. G. Palmer et al., *Protein NMR Spectroscopy*, Elsevier Academic Press, **2007**.

[22] C. Fernandez, *Current Opinion in Structural Biology* **2003**, *13*, 570–580.

[23] J. Keeler, *Understanding NMR Spectroscopy*, 2nd ed., Wiley, **2010**, pp. 215–219.

[24] A. Bax, *Journal of Magnetic Resonance* **2011**, *213*, 442–445.

[25] `https://www.protein-nmr.org.uk/solution-nmr/assignment-theory/triple-resonance-backbone-assignment/` (visited on 11/07/2019).

[26] S. Grzesiek, A. Bax, *Journal of Magnetic Resonance (1969)* **1992**, *99*, 201–207.

[27] S. M. Mustafi, H. Chen, H. Li, D. M. LeMaster, G. Hernández, *Biochemical Journal* **2013**, *453*, 371–380.

[28] J. Schörghuber, L. Geist, M. Bisaccia, F. Weber, R. Konrat, R. J. Lichtenecker, *Journal of Biomolecular NMR* **2017**, *69*, 13–22.

[29] T. W. Muir, P. E. Dawson, S. B. Kent in *Solid-Phase Peptide Synthesis*, Elsevier, **1997**, pp. 266–298.

[30] B. L. Stoddard, S. Pietrokovski, *Nature Structural Biology* **1998**, *5*, 3–5.

[31] E. L. Lasda, T. Blumenthal, *Wiley Interdisciplinary Reviews: RNA* **2011**, *2*, 417–434.

[32] J. Fiaux, E. B. Bertelsen, A. L. Horwich, K. Wüthrich, *Nature* **2002**, *418*, 207–211.

[33] G. P. Mullen, NMR Structural Biology Facility & Biophysical Core Facility, `https://health.uconn.edu/structural-biology/frequently-asked-questions/` (visited on 11/12/2019).

[34] P. R. L. Markwick, T. Malliavin, M. Nilges, *PLoS Computational Biology* **2008**, *4*, (Ed.: J. McEntyre), e1000168.

[35] G. Ramachandran, A. K. Mitra, *Journal of Molecular Biology* **1976**, *107*, 85–92.

[36] C. Grathwohl, K. Wüthrich, *Biopolymers* **1981**, *20*, 2623–2633.

[37] H. Dyson, M. Rance, R. A. Houghten, R. A. Lerner, P. E. Wright, *Journal of Molecular Biology* **1988**, *201*, 161–200.

[38] P. R. Schimmel, P. J. Flory, *Journal of Molecular Biology* **1968**, *34*, 105–120.

[39] M. W. MacArthur, J. M. Thornton, *Journal of Molecular Biology* **1991**, *218*, 397–412.

[40] A. A. Adzhubei, M. J. Sternberg, A. A. Makarov, *Journal of Molecular Biology* **2013**, *425*, 2100–2132.

[41] A. A. Morgan, E. Rubenstein, *PLoS ONE* **2013**, *8*, (Ed.: D. E. Casarini), e53785.

[42] `https://www.sigmaaldrich.com/catalog/product/aldrich/297038?lang=de&region=AT` (visited on 11/04/2019).

[43] `https://www.sigmaaldrich.com/catalog/product/aldrich/453188?lang=de&region=AT` (visited on 11/04/2019).

[44] E. V. Antina, G. B. Guseva, A. E. Loginova, A. S. Semeikin, A. I. V'yugin, *Russian Journal of General Chemistry* **2010**, *80*, 2374–2381.

[45] P. V. Kattamuri, J. Yin, S. Siriwongsup, D.-H. Kwon, D. H. Ess, Q. Li, G. Li, M. Yousufuddin, P. F. Richardson, S. C. Sutton, L. Kürti, *Journal of the American Chemical Society* **2017**, *139*, 11184–11196.

[46] T. Seitz, J. Baudoux, H. Bekolo, D. Cahard, J.-C. Plaquevent, M.-C. Lasne, J. Rouden, *Tetrahedron* **2006**, *62*, 6155–6165.

[47] X. Liu, Y. Liu, G. Chai, B. Qiao, X. Zhao, Z. Jiang, *Organic Letters* **2018**, *20*, 6298–6301.

[48] W. Kleemiss, G. Köhler, F. Bauer, Pat. Nr. DE 10026108, **2001**.

[49] S. Rama et al., Pat. Nr. 2275/CHE/2013, **2013**.

[50] O. A. Moe, D. T. Warner, *Journal of the American Chemical Society* **1948**, *70*, 2763–2765.

[51] A. Armstrong, T. J. Critchley, M.-E. Gourdel-Martin, R. D. Kelsey, A. A. Mortlock, *Journal of the Chemical Society Perkin Transactions 1* **2002**, 1344–1350.

[52] M. Asemoglu, H. Hellstern, B. Riss, C. Sprecher (NOVARTIS), Pat. Nr. US 2014/0100353 A1, **2014**.

[53] D. D. Young, J. Torres-Kolbus, A. Deiters, *Bioorganic & Medicinal Chemistry Letters* **2008**, *18*, 5478–5480.

[54] H. Vogel, B. Davis, *Journal of the American Chemical Society* **1952**, *74*, 109–112.

[55] L. A. Yanovskaya, V. F. Kucherov, *Bulletin of the Academy of Sciences of the USSR Division of Chemical Science* **1962**, *11*, 616–622.

[56] B. Cai, J. S. Panek, S. Amar, *Journal of Medicinal Chemistry* **2016**, *59*, 6878–6890.

[57] S. P. Singh, A. Michaelides, A. R. Merrill, A. L. Schwan, *The Journal of Organic Chemistry* **2011**, *76*, 6825–6831.

[58] R. Barnett, D. Raszkowski, T. Winckler, P. Stallforth, *Beilstein Journal of Organic Chemistry* **2017**, *13*, 247–250.

[59] W. Bloemhoff, K. E. T. Kerling, *Recueil des Travaux Chimiques des Pays-Bas* **1975**, *94*, 182–185.

[60] Hazardous Substance Fact Sheet: Hydrogen Peroxide, New Jersey Department of Health, **2008**, `https://www.google.at/url?sa=t&rct=j&q=&esrc=s&source=web&cd=27&ved=2ahUKEwj5zva3_bTlAhXHZlAKHRwWA5OQFjAaegQIBBAC&url=https%3A%2F%2Fnj.gov%2Fhealth%2Feoh%2Frtkweb%2Fdocuments%2Ffs%2F1015.pdf&usg=AOvVaw0-7o7WmBC6yZiCJBUKPZhJ` (visited on 11/08/2019).

[61] H.-J. Zeiss, Pat. Nr. EP 530 506 A1, **1993**.

[62] A. G. N. Coxon, R. D. Köhn, *ACS Catalysis* **2016**, *6*, 3008–3016.

[63] M. B. Smith, J. March, *March's Advanced Organic Chemistry: Reactions, Mechanisms, and Structure, 5th Edition*, Wiley-Interscience, **2001**.

[64] H. Stephen, *J. Chem. Soc. Trans.* **1925**, *127*, 1874–1877.

[65] P. Allevi et al., *Tetrahedron Letters* **2001**, *42*, 5319–5321.

[66] M. K. Agrawal et al., Pat. Nr. WO 2017/195147 A1, **2017**.

[67] E. L. Glaisyer, M. S. Watt, K. I. Booker-Milburn, *Organic Letters* **2018**, *20*, 5877–5880.

[68] R. Araújo, F. M. Fernandes, M. F. Proença, C. J. R. Silva, M. C. Paiva, *Journal of Nanoscience and Nanotechnology* **2007**, *7*, 3441–3445.

[69] S. Priestley, C. Decicco, Pat. Nr. WO 01/07407 A1, **2001**.

[70] R. Galán-Fernández, D. Clemente-Tejeda, E. del Ro-Nieto, F. A. Bermejo, *Tetrahedron* **2010**, *66*, 8247–8253.

[71] L. A. Flippin, D. W. Gallagher, K. Jalali-Araghi, *The Journal of Organic Chemistry* **1989**, *54*, 1430–1432.

[72] R. Anbazhagan, A. Vadivelmurugan, H.-C. Tsai, R.-J. Jeng, *Journal of Materials Chemistry C* **2018**, *6*, 1071–1082.

[73] K. Voigt, A. Stolle, J. Salaün, A. de Meijere, *Synlett* **1995**, *1995*, 226–228.

[74] T. Kano, Q. Lan, X. Wang, K. Maruoka, *Advanced Synthesis & Catalysis* **2007**, *349*, 556–560.

[75] J. G. Bundy, E. M. Lenz, D. Osborn, J. M. Weeks, J. C. Lindon, J. K. Nicholson, *Xenobiotica* **2002**, *32*, 479–490.

[76] O. Corcoran, J. C. Lindon, R. Hall, I. M. Ismail, J. K. Nicholson, *The Analyst* **2001**, *126*, 2103–2106.

[77] W. Cui, P. Otten, Y. Li, K. S. Koeneman, J. Yu, R. P. Mason, *Magnetic Resonance in Medicine* **2004**, *51*, 616–620.

[78] Bruker, Almanac, **2011**.

[79] R. E. Hendrick, *Breast Mri: Fundamentals And Technical Aspects*, **2008**, p. 10.

[80] S. L. Cobb, C. D. Murphy, *Journal of Fluorine Chemistry* **2009**, *130*, 132–143.

[81] J. Mason, *Multinuclear NMR*, Springer, **2011**, p. 438.

[82] E. N. G. Marsh, Y. Suzuki, *ACS Chemical Biology* **2014**, *9*, 1242–1250.

[83] J.-x. Yu, V. Kodibagkar, W. Cui, R. Mason, *Current Medicinal Chemistry* **2005**, *12*, 819–848.

[84] J.-X. Yu, W. Cui, D. Zhao, R. P. Mason in *Fluorine and Health*, Elsevier, **2008**, pp. 197–276.

[85] J. L. Kitevski-LeBlanc, R. S. Prosser, *Progress in Nuclear Magnetic Resonance Spectroscopy* **2012**, *62*, 1–33.

[86] A. Boeszoermenyi, S. Chhabra, A. Dubey, D. L. Radeva, N. T. Burdzhiev, C. D. Chanev, O. I. Petrov, V. M. Gelev, M. Zhang, C. Anklin, H. Kovacs, G. Wagner, I. Kuprov, K. Takeuchi, H. Arthanari, *Nature Methods* **2019**, *16*, 333–340.

[87] C. Li, G.-F. Wang, Y. Wang, R. Creager-Allen, E. A. Lutz, H. Scronce, K. M. Slade, R. A. Ruf, R. A. Mehl, G. J. Pielak, *Journal of the American Chemical Society* **2010**, *132*, 321–327.

[88] H. Li, C. Frieden, *Proceedings of the National Academy of Sciences* **2007**, *104*, 11993–11998.

[89] J. G. Bann, J. Pinkner, S. J. Hultgren, C. Frieden, *Proceedings of the National Academy of Sciences* **2002**, *99*, 709–714.

[90] F. Khan, I. Kuprov, T. D. Craggs, P. J. Hore, S. E. Jackson, *Journal of the American Chemical Society* **2006**, *128*, 10729–10737.

[91] T. Didenko, J. J. Liu, R. Horst, R. C. Stevens, K. Wüthrich, *Current Opinion in Structural Biology* **2013**, *23*, 740–747.

[92] J. Feeney, J. E. McCormick, C. J. Bauer, B. Birdsall, C. M. Moody, B. A. Starkmann, D. W. Young, P. Francis, R. H. Havlin, W. D. Arnold, E. Oldfield, *Journal of the American Chemical Society* **1996**, *118*, 8700–8706.

[93] P. Cleve, V. Robinson, H. S. Duewel, J. F. Honek, *Journal of the American Chemical Society* **1999**, *121*, 8475–8478.

[94] D. K. Garner, M. D. Vaughan, H. J. Hwang, M. G. Savelieff, S. M. Berry, J. F. Honek, Y. Lu, *Journal of the American Chemical Society* **2006**, *128*, 15608–15617.

[95] L. A. Luck, C. Johnson, *Protein Science* **2000**, *9*, 2573–2576.

[96] M. Salwiczek, E. K. Nyakatura, U. I. M. Gerling, S. Ye, B. Koksch, *Chem. Soc. Rev.* **2012**, *41*, 2135–2171.

[97] M. Mae, H. Amii, K. Uneyama, *Tetrahedron Letters* **2000**, *41*, 7893–7896.

[98] N. A. Meanwell, *Journal of Medicinal Chemistry* **2011**, *54*, 2529–2591.

[99] G. Bott, L. D. Field, S. Sternhell, *Journal of the American Chemical Society* **1980**, *102*, 5618–5626.

[100] H. Zheng, K. Comeforo, J. Gao, *Journal of the American Chemical Society* **2009**, *131*, 18–19.

[101] T. Arai, T. Imachi, T. Kato, H. I. Ogawa, T. Fujimoto, N. Nishino, *Bulletin of the Chemical Society of Japan* **1996**, *69*, 1383–1389.

[102] L. Wang, J. Xie, P. G. Schultz, *Annual Review of Biophysics and Biomolecular Structure* **2006**, *35*, 225–249.

[103] M. R. Thomas, S. G. Boxer, *Biochemistry* **2001**, *40*, 8588–8596.

[104] J. Klein-Seetharaman, E. V. Getmanova, M. C. Loewen, P. J. Reeves, H. G. Khorana, *Proceedings of the National Academy of Sciences* **1999**, *96*, 13744–13749.

[105] K. D. Dykstra, N. Ichiishi, S. W. Krska, P. F. Richardson in *Fluorine in Life Sciences: Pharmaceuticals, Medicinal Diagnostics, and Agrochemicals*, Elsevier, **2019**, pp. 1–90.

[106] M. B. Nodwell, A. Bagai, S. D. Halperin, R. E. Martin, H. Knust, R. Britton, *Chemical Communications* **2015**, *51*, 11783–11786.

[107] J.-j. Ma, W.-b. Yi, G.-p. Lu, C. Cai, *Organic & Biomolecular Chemistry* **2015**, *13*, 2890–2894.

[108] P. A. Champagne, J. Desroches, J.-D. Hamel, M. Vandamme, J.-F. Paquin, *Chemical Reviews* **2015**, *115*, 9073–9174.

[109] D. J. Adams, J. H. Clark, *Chemical Society Reviews* **1999**, *28*, 225–231.

[110] Y. Ye, S. D. Schimler, P. S. Hanley, M. S. Sanford, *Journal of the American Chemical Society* **2013**, *135*, 16292–16295.

[111] P. S. Fier, J. F. Hartwig, *Science* **2013**, *342*, 956–960.

[112] T. Truong, K. Klimovica, O. Daugulis, *Journal of the American Chemical Society* **2013**, *135*, 9342–9345.

[113] M. Saito, K. Miyamoto, M. Ochiai, *Chemical Communications* **2011**, *47*, 3410.

[114] K. S. L. Chan, M. Wasa, X. Wang, J.-Q. Yu, *Angewandte Chemie International Edition* **2011**, *50*, 9081–9084.

[115] Q. Ding, C. Ye, S. Pu, B. Cao, *Tetrahedron* **2014**, *70*, 409–416.

[116] E. Bellamy, O. Bayh, C. Hoarau, F. Trécourt, G. Quéguiner, F. Marsais, *Chemical Communications* **2010**, *46*, 7043.

[117] H. Hayashi, H. Sonoda, K. Fukumura, T. Nagata, *Chemical Communications* **2002**, 1618–1619.

[118] P. Tang, W. Wang, T. Ritter, *Journal of the American Chemical Society* **2011**, *133*, 11482–11484.

[119] T. Fujimoto, F. Becker, T. Ritter, *Organic Process Research & Development* **2014**, *18*, 1041–1044.

[120] T. Fujimoto, T. Ritter, *Organic Letters* **2015**, *17*, 544–547.

[121] R. J. Lichtenecker, K. Weinhäupl, W. Schmid, R. Konrat, *Journal of Biomolecular NMR* **2013**, *57*, 327–331.

[122] R. J. Lichtenecker, *Org. Biomol. Chem.* **2014**, *12*, 7551–7560.

[123] Winkler AG, `https://www.winkler.eu/produkte/category/pilz-laborheizhauben/` (visited on 11/08/2019).

[124] F. Terrier, *Modern Nucleophilic Aromatic Substitution*, Wiley-VCH, **2013**.

[125] C. N. Neumann, J. M. Hooker, T. Ritter, *Nature* **2016**, *534*, 369–373.

Credits and Acknowledgements

At this point it appears appropriate to express my gratitude to those who made this thesis possible in the first place.

First and foremost to mention is my supervisor Roman who deserves my greatest thanks for accepting me as a master student and contributing to this work with loads of starting literature to introduce me to the topic, theoretical support, a kind atmosphere to work in and the patience he had with me.

A great part of the practical work would have been virtually impossible without the aid of our technician Gerlinde who ever so masterfully reigned over the systematic chaos of the laboratory and always knew where to find what I was looking for. Thank you also for fun conversations at the lunch table.

It takes a lot to organize scatterbrained thoughts into a well-orchestrated final work and my most cordial thanks go to Juliana and Sandra who lectured my rough drafts and ensured coherence and orthography where I failed to maintain them. Ladies, you are precious beyond measure.

There were times during the writing when I felt dispirited and was not so convinced whether I would ever succeed in finishing it. Just then it was wonderful to have friends up my sleeve who are ingenious when it comes to bolstering self-confidence. Here's to you!

Und zu guter Letzt meinen Eltern, die mit unerschöpflicher Geduld und Liebe hinter mir standen und es mir ermöglichten, mir die Zeit zu nehmen, die ich brauchte.

Meinen Eltern,
die mir
Wurzeln und Flügel
gaben.

Created with LaTeX